Browse all Theses and Dissertations

Theses and Dissertations

2006

# Developmental Expression of Calcium-Binding Proteins in the AVCN and MNTB of Normal Hearing and Congenitally Deaf Mice

John L. Roebel
*Wright State University*

Follow this and additional works at: https://corescholar.libraries.wright.edu/etd_all

Part of the Anatomy Commons

DEVELOPMENTAL EXPRESSION OF CALCIUM-BINDING PROTEINS

IN THE AVCN AND MNTB OF NORMAL HEARING

AND CONGENITALLY DEAF MICE

A thesis submitted in partial fulfillment
of the requirements for the degree of
Master of Science (Anatomy)

By

JOHN L. ROEBEL
B.S. Biology, Saint Louis University, 2004

2006
Wright State University

WRIGHT STATE UNIVERSITY

SCHOOL OF GRADUATE STUDIES

June 1, 2006

      I HEREBY RECOMMEND THAT THE THESIS PREPARED UNDER MY SUPERVISION BY John L. Roebel ENTITLED Developmental Expression of Calcium-Binding Proteins in the AVCN and MNTB of Normal Hearing and Congenitally Deaf Mice BE ACCEPTED IN PARTIAL FULFILLMENT OF THE REQUIREMENTS FOR THE DEGREE OF Master of Science (Anatomy).

_____
Robert E.W. Fyffe, Ph.D.
Thesis Director

_____
Timothy C. Cope, Ph.D.
Department Chair

Committee on
Final Examination

_____
Robert E.W. Fyffe, Ph.D.

_____
Larry Ream, Ph.D.

_____
Kathrin Engisch, Ph.D.

_____
Joseph F. Thomas, Jr., Ph.D.
Dean, School of Graduate Studies

# ABSTRACT

Roebel, John L.  M.S. Anatomy, Department of Neuroscience, Cell Biology and Physiology, Wright State University, 2006.  Developmental Expression of Calcium-Binding Proteins in the AVCN and MNTB of Normal Hearing and Congenitally Deaf Mice.

This experiment analyzes synaptic differences in the central auditory pathway between normal hearing and congenitally deaf (*dn/dn*) mice, and provides valuable insight into central changes that correspond with human congenital deafness. Specifically, this experiment analyzes developmental expression of the Calcium ($Ca^{2+}$)-binding proteins Calretinin (CR), Calbindin D-28k (CB) and Parvalbumin (PV) in large excitatory synapses in the anteroventral cochlear nucleus (AVCN) and the medial nucleus of the trapezoid body (MNTB) of normal and *dn/dn* mice.  Immunofluorescence imaging with primary antibodies detecting CR, CB or PV was used to analyze the expression of each at 9 days, 13 days, 20 days, 30 days and 49 days postnatal in normal and *dn/dn* mice.  Results indicated that $Ca^{2+}$-binding expression was similar at each location in normal and *dn/dn* mice at 9 days postnatal, prior to opening of the ear canal and the onset of hearing (which occurs around 11 days postnatal) .  In normal mice, patterns of $Ca^{2+}$-binding protein expression changed progressively after the onset of hearing.  In *dn/dn* mice (which completely lack auditory nerve activity), however, patterns of expression did not change after the onset of hearing, suggesting that patterns of $Ca^{2+}$-binding protein

expression change during development in normal mice in response to evoked auditory nerve activity, and that patterns of $Ca^{2+}$-binding protein expression do not change during development in *dn/dn* mice due to lack of evoked auditory nerve activity.  As a result, $Ca^{2+}$ buffering is impaired in synapses located in the AVCN and MNTB of *dn/dn* mice.

TABLE OF CONTENTS

LIST OF FIGURES

# I. INTRODUCTION

This thesis provides insight into the development of synaptic pathways in the mammalian central nervous system. The aspect of synaptic transmission examined is the developmental expression and localization of the Calcium-binding proteins Calretinin (CR), Calbindin D-28k (CB), and Parvalbumin (PV) in synapses located in the central auditory pathways of normal hearing and congenitally deaf mutant (*dn/dn*) mice. These synapses are the endbulb of Held synapse in the anteroventral cochlear nucleus (AVCN), and the calyx of Held synapse in the medial nucleus of the trapezoid body (MNTB). By comparing developmental expression of these proteins in normal and congenitally deaf mice, one can gain appreciation for the role that spontaneous and/or evoked auditory nerve activity may play in the normal (or abnormal) development of central auditory pathways in general, and in particular, the central auditory pathways in congenitally deaf mammals.

The first hypothesis is that CR, CB and PV expression in the AVCN and MNTB will vary throughout development in normal hearing mice. The expression of each individual $Ca^{2+}$-binding protein will change during development, and, in addition, the patterns of expression of CR, CB and PV will vary with respect to each other. The results will either validate and expand on, or stand in contrast to, the results obtained by Felmy and Schneggenburger (2004) on developmental expression of CR, CB and PV in

1

the MNTB of normal hearing rats and mice. The next hypothesis is that CR, CB and PV will display altered expression patterns during development in the AVCN and MNTB of *dn/dn* mice. Specifically, there will be differences in $Ca^{2+}$-binding protein expression in the AVCN of normal and *dn/dn* mice. This would support a hypothesis proposed by Oleskevich and Walmsley (2002), who believed that the enhanced synaptic transmission they observed in the endbulb of Held synapse in *dn/dn* mice may result from impaired $Ca^{2+}$ buffering in the presynaptic terminal. In addition, there will be topographic gradients of $Ca^{2+}$-binding protein expression in the MNTB of normal hearing mice, and these gradients will be altered or even absent in *dn/dn* mice. These topographic gradients (or lack thereof) of $Ca^{2+}$-binding protein expression may correspond with the established topographic gradients of current and channel expression that underlie the tonotopic organization (or lack thereof) of the MNTB of normal hearing (or *dn/dn*) mice.

## II. SPECIFIC AIMS

The first specific aim was to determine the developmental expression of the Calcium-binding proteins CR, CB, and PV in the endbulb of Held synapse in the AVCN and the calyx of Held synapse in the MNTB of the normal hearing mouse. It was important to determine how the expression of each individual protein varied at given time-points, and to compare the pattern and location of developmental expression of the individual proteins with each other. This aim allowed research by Felmy and Schneggenburger (2004) to be tested and expanded on (see Introduction).

The second specific aim was to examine the developmental expression of CR, CB, and PV in the AVCN and MNTB of congenitally deaf *dn/dn* mice. Again, it was important to determine how expression of each individual $Ca^{2+}$-binding protein varied throughout development, and to also compare the pattern and location of expression of each of these proteins with each other throughout development.

These specific aims allowed comparison of the developmental expression of CR, CB, and PV in the AVCN and MNTB in normal hearing mice with that in *dn/dn* mice. Any significant differences observed would serve as evidence that spontaneous and/or acoustically evoked auditory nerve activity plays a critical role in the normal pattern of $Ca^{2+}$-binding protein expression in the AVCN and MNTB. These aims allowed the hypothesis proposed by Oleskevich and Walmsley (2002) to be tested (see Introduction), and provided insight into the role that the developmental expression of these $Ca^{2+}$-

binding proteins may play in the creation of tonotopic maps in the AVCN and MNTB

(see Introduction).

## III.  BACKGROUND & SIGNIFICANCE

**Overview of the Auditory Pathway**

The central circuitry in the auditory pathway (Fig. 1) is specialized for sound localization, using specialized synaptic structures for precise processing of binaural cues (Walmsley et al. 2006).  Neurons in the superior olivary complex, which includes the medial superior olive (MSO) and lateral superior olive (LSO) nuclei, detect minute differences in the intensity level (in the LSO) and arrival time (in the MSO) of sound in each ear.  The main synaptic specializations that are necessary for the accuracy and precision of these cues are giant calyceal terminals in direct contact with the postsynaptic cell bodies in the pathway.  These large presynaptic specializations ensure rapid, high-fidelity transmission of the auditory signals (Oleskevich, Youssoufian & Walmsley 2004).

Sound is detected by hair cells in the cochlea, which synapse with spiral ganglion cells through ribbon synapses.  Importantly, these ribbon synapses continually release neurotransmitter even in the absence of sound stimulation, which results in spontaneous activity in the auditory nerve fibers (Liberman 1991; see Leao et al. 2006; Walmsley et al. 2006).  This spontaneous activity is present in the auditory nerve even before the opening of the ear canal and the onset of hearing, which in normal mice is around 12 days postnatal (Friauf & Lohmann 1999; Rubel & Fritzsch 2002).  The central projections of
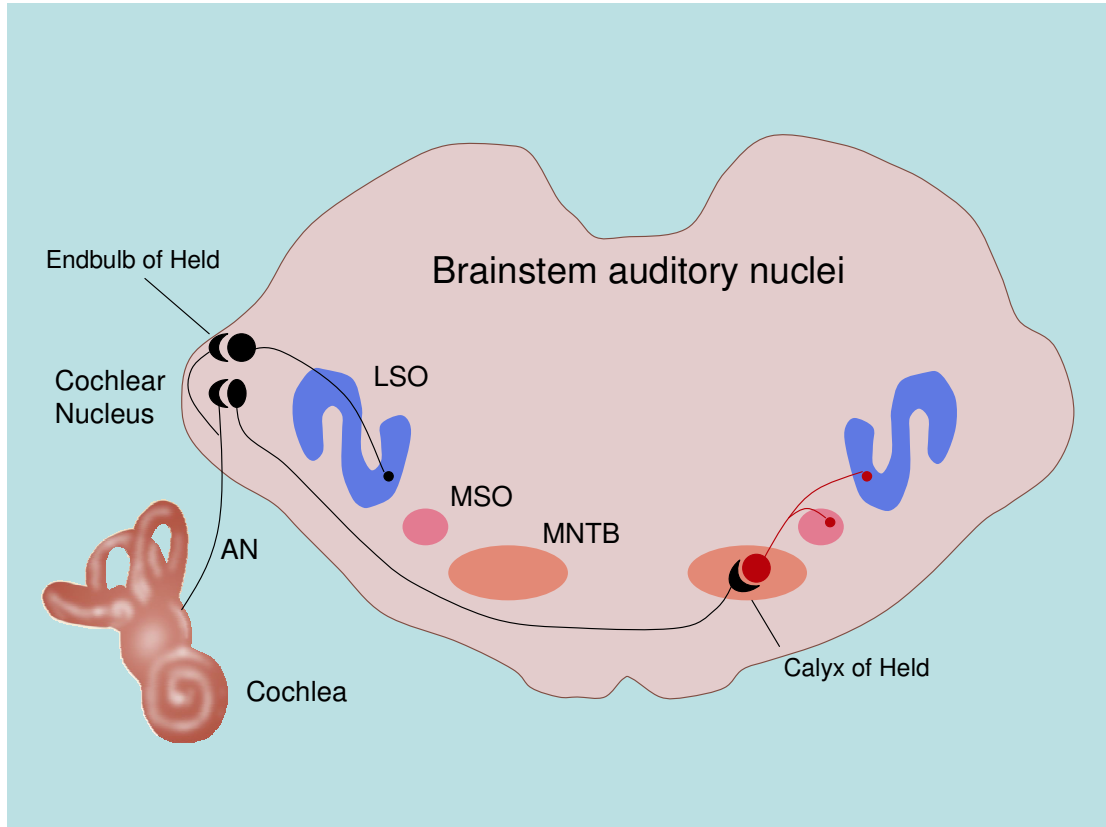
**Figure 1. The auditory pathway in mammals**
This is a simplified schematic diagram showing the cochlear apparatus in the inner ear and the central projections of spiral ganglion cells, the auditory nerve fibers (AN), which form giant calyceal type excitatory synapses, the endbulbs of Held, on bushy cells in the anteroventral cochlear nucleus (AVCN). Spherical bushy cells in the AVCN make ipsilateral contacts with cells in the lateral superior olive (LSO) and bilateral contacts (not illustrated) with cells in the medial superior olive (MSO). Globular bushy cells give rise to axons that form giant calyceal type excitatory synapses, the calyces of Held, with principal cell somata in the contralateral medial nucleus of the trapezoid body (MNTB). The principal cells in the MNTB, in turn, give rise to inhibitory axons which project to the ipsilateral MSO and ipsilateral LSO. Inhibitory glycinergic neurons and synapses are shown in red, while excitatory glutamatergic neurons and synapses are shown in black. (Reprinted, with permission, from Walmsley et al. 2006)

these spiral ganglion cells form the primary auditory nerve fibers which project to the cochlear nucleus in the brainstem (Liberman 1991; see Walmsley et al. 2006).

The cochlear nucleus is divided into two separate nuclei: the dorsal cochlear nucleus (DCN) and the anteroventral cochlear nucleus (AVCN). Spherical and globular bushy cells in the AVCN receive glutamatergic excitatory calyceal-type terminals (Fig. 2) called endbulbs of Held from the auditory nerve fibers (Oleskevich, Youssoufian & Walmsley 2004). The spherical bushy cells give excitatory glutamatergic projections bilaterally to each MSO and ipsilaterally to the LSO. The globular bushy cells give excitatory glutamatergic projections to the principal cells in the contralateral medial nucleus of the trapezoid body (MNTB), which terminate in another calyceal-type terminal (Fig. 2) called the calyx of Held. The MNTB, in turn, gives inhibitory glycinergic axons to both the ipsilateral MSO and the ipsilateral LSO (Spangler, Warr & Henkel 1985; Adams & Mugnaini 1990; see Smith, Owens & Forsythe 2000). Thus, the calyx of Held is viewed as a sign-inverting relay synapse, which converts excitatory glutamatergic input into inhibitory glycinergic output to the MSO and LSO (Smith, Joris & Yin 1998; Futai et al. 2001; Paolini et al. 2001; see Oleskevich, Youssoufian & Walmsley 2004). In addition, there are also various smaller inhibitory synaptic contacts made with the AVCN and MNTB neurons, which are also important in sound localization (Leao et al. 2004b; see Walmsley et al. 2006).

The excitatory synapses in the AVCN between the endbulbs of Held and the bushy cells, and in the MNTB between the calyx of Held and the principal cells, will be the areas of interest in this experiment. Although the surface area of the calyx of Held is greater than the endbulb of Held, the two calyceal-type terminals share morphological

C
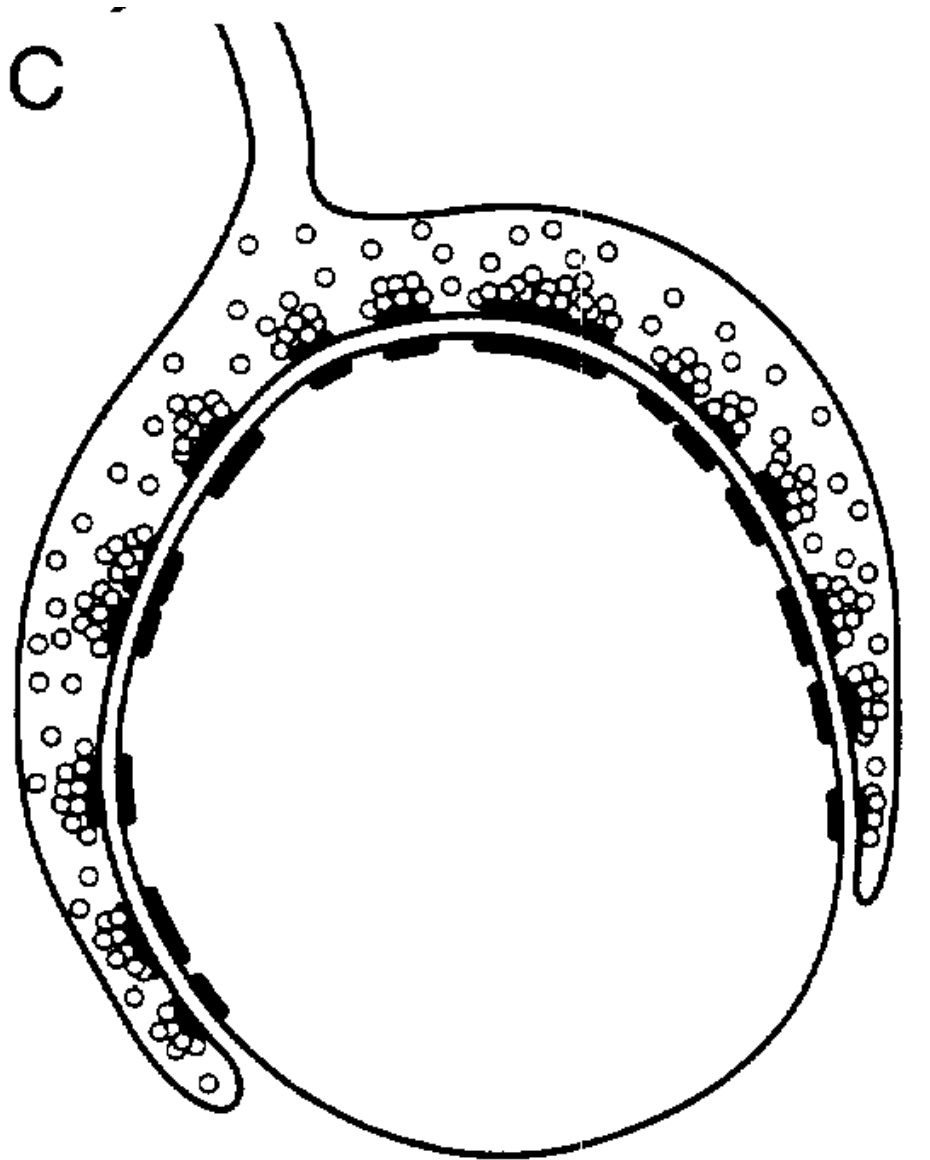


**Figure 2. A calyceal-type terminal**
This is a schematic depicting an example of a calyceal-type terminal, like those found at the Endbulb of Held synapse in the AVCN and the Calyx of Held synapse in the MNTB. (Reprinted, with permission, from Walmsley, Alvarez & Fyffe 1998)

and physiological features (Neises, Mattox & Gulley 1982; Ryugo, Wu & Pongstaporn 1996; Ryugo et al. 1997; Smith, Joris & Yin 1998; Rowland, Irby & Spirou 2000; Nicol & Walmsley 2002; Sätzler et al. 2002; Taschenberger et al. 2002; Lee, Cahill & Ryugo 2003; see Oleskevich, Youssoufian & Walmsley 2004). The calyx of Held has been described as a cup-like structure with finger-like stalks, and it covers about 40% of the principal cell surface area. A single principal cell is contacted by only one calyx of Held (Sätzler et al. 2002). Although many bushy cells in the AVCN receive more than one endbulb of Held (Joris et al. 1994; Nicol & Walmsley 2002), these endbulbs also develop into finger like structures that cover 40-60% of the bushy cell soma (Ryugo & Fekete 1982; Kuwabara, DiCaprio & Zook 1991; Kandler & Friauf 1993; Smith, Joris & Yin 1998; Sätzler et al. 2002; Taschenberger et al. 2002; see Oleskevich, Youssoufian & Walmsley 2004). Both endbulbs and calyces of Held contain hundreds of active zones with clusters of spherical vesicles (Neises, Mattox & Gulley 1982; Ryugo, Wu & Pongstaporn 1996; Ryugo et al. 1997; Smith, Joris & Yin 1998; Rowland, Irby & Spirou 2000; Nicol & Walmsley 2002; Sätzler et al. 2002; Taschenberger et al. 2002; Lee, Cahill & Ryugo 2003; see Oleskevich, Youssoufian & Walmsley 2004). Similar changes also occur at both synapses physiologically, as during development postsynaptic glutamatergic NMDA receptors are replaced by AMPA receptors (Bellingham, Lim & Walmsley 1998; Chuhma & Ohmori 1998; Taschenberger & von Gersdorff 2000; Futai et al. 2001; Joshi & Wang 2002; see Oleskevich, Youssoufian & Walmsley 2004). The AMPA receptors ensure responses that are among the fastest and largest in the central nervous system, which allow presynaptic action potentials to generate postsynaptic responses with very few failures and at very high frequencies (up to 800 Hz) (Wu &

Kelly 1993; Taschenberger & von Gersdorff 2000; Oleskevich & Walmsley 2002; Schneggenburger, Sakaba & Neher 2002; see Oleskevich, Youssoufian & Walmsley 2004). Thus, the shared morphological and physiological characteristics of the endbulb of Held and the calyx of Held play a significant role in ensuring high-fidelity transmission of auditory information in the central auditory pathway. In addition, the large size of these synapses, and the fact that the synaptic contacts are made directly with the cell somata, have made them an ideal target for research on central nervous synapses (Leao et al. 2004b).

**Tonotopic Organization in the Auditory Pathway**

There exists a tonotopic organization of cells within the auditory pathway (Friauf & Lohmann 1999; McAlpine, Jiang & Palmer 2001; Rubel & Fritzsch 2002; Mauk & Buonomano 2004; see Leao et al. 2006). This tonotopic organization begins in the cochlea itself, with the hair cells that respond to high sound frequencies in the basal region of the cochlea, and the hair cells that respond best to low frequencies in the apical region of the cochlea. This arrangement is continued into the brainstem nuclei of the auditory pathway (Walmsley et al. 2006). Leao et al. (2006) reported that in the MNTB of normal hearing mice, cells that respond best to high frequency stimulation are located medially within the nucleus, whereas cells that respond best to low frequency stimulation are located more laterally (Fig. 3). They also showed that there are distinct medio-lateral gradients of voltage-dependent currents and channels types which underlie this tonotopic organization. For example, they found that in normal mice Kv1.1 channels and their low
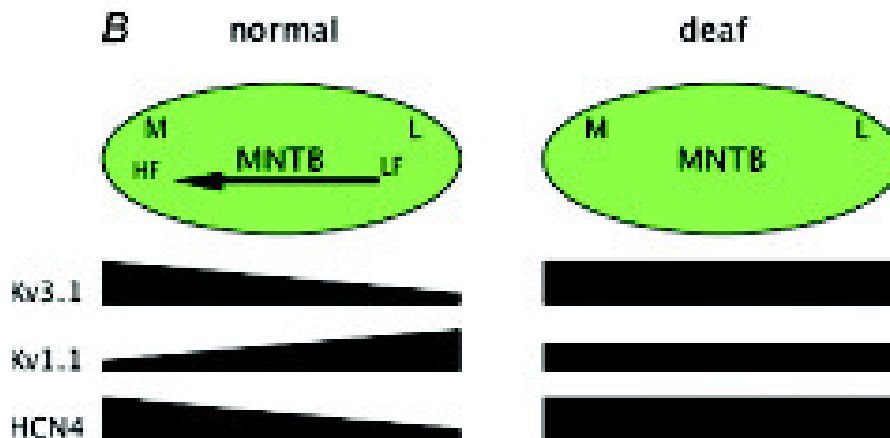
**Figure 3. Tonotopic organization of the MNTB in normal and *dn/dn* mice**
Schematics at the top of the figure represent the medio-lateral tonotopic organization of
the MNTB. Schematic at left illustrates that in normal mice, medially-located principal
cells respond best to high frequency stimulation, and laterally-located principal cells
respond best to low frequency stimulation. Below this schematic, gradients of channel
expression that underlie the tonotopic organization of the MNTB in normal mice are
illustrated. Kv3.1 and HC4 channels are preferentially located in medial principal cells,
while Kv1.1 channels are preferentially located in lateral principal cells. Schematic at
right illustrates that in *dn/dn* mice, no tonotopic organization of cells is observed. Below
this schematic, the lack of gradients of channel expression in the MNTB of *dn/dn* mice is
illustrated. (Reprinted, with permission, from Walmsley et al. 2006)

threshold potassium currents are preferentially located in the more lateral MNTB cells, while Kv3.1 channels with their high threshold potassium currents and HCN4 channels with their hyperpolarization-activated cation currents are preferentially located in the more medial cells (Fig. 3). They proposed that these gradients of membrane and firing properties in the normal mouse MNTB provide a source of time delays, and are thus important in the localization of sound (Leao et al. 2006).

**Congenital Deafness and the Auditory Pathway**

In order to study the effects of auditory dysfunction on the central auditory circuitry, congenitally deaf mutant mice (*dn/dn*) can be used (Bock, Frank & Steel 1982; Keats & Berlin 1999; Oleskevich, Youssoufian & Walmsley 2004; Leao et al. 2004a; b; see Leao et al. 2006). The *dn/dn* mouse is a naturally occurring strain with a recessive mutation of Tmc1 (transmembrane cochlear-expressed gene 1) which results in dysfunctional hair cells in the cochlear apparatus (Leao et al. 2004a). This mutation results in hair cell dysfunction from birth, with no evidence for spontaneous or acoustically evoked auditory nerve activity (Bock, Frank & Steel 1982; Keats & Berlin 1999; Oleskevich, Youssoufian & Walmsley 2004; Leao et al. 2004a; b; see Leao et al. 2006). By comparing properties of the central auditory pathways in *dn/dn* mice and normal mice, researchers have been able to gain valuable insight into congenital deafness and the changes that occur with it centrally (Walmsley et al. 2006).

Resent research has shown that the endbulb of Held synapse between auditory nerve fibers and bushy cells in the AVCN has larger amplitude eEPSCs (evoked

excitatory postsynaptic currents) in *dn/dn* mice compared to CBA mice, due to greater presynaptic release probability, without a change in quantal size (Oleskevich & Walmsley 2002). This result suggests a homeostatic mechanism of altering synaptic strength, as the excitatory release from this neuron is being increased in response to a decrease in firing rate of that neuron in an effort to keep average firing rate near a desired level (Walmsley et al. 2006). In addition, the endbulb synapse of *dn/dn* mice showed greater tetanic depression and frequency of delayed aEPSCs (asynchronous excitatory postsynaptic currents) (Oleskevich & Walmsley 2002).

Research by Ryugo et al. (1996; 1997; 1998) on endbulb structure in the AVCN during development of normal and deaf white cats suggests a correlation between amount of auditory activity and endbulb morphology. They found that in normal cats (with normal developmental auditory nerve fiber activity), there are smaller and more numerous synaptic specializations than in deaf white cats (with altered developmental auditory nerve activity) (Ryugo, Wu & Pongstaporn 1996; Ryugo et al. 1997; Ryugo et al. 1998; see Walmsley et al. 2006). Walmsley et al. (2006) suggest that these results support a theory that during normal development, spontaneous auditory nerve activity causes endbulbs to grow and become specialized, perhaps by a mechanism involving the splitting into many smaller specializations. Postsynaptically, however, bushy cells in the AVCN show no difference in the membrane properties between normal and *dn/dn* mice, even though the bushy cells in *dn/dn* mice have lost their excitatory input (Walmsley et al. 2006).

The excitatory calyx of Held synapse in the MNTB of *dn/dn* mice, on the other hand, showed no change in any of the measured properties of evoked synaptic

transmission and only small changes in spontaneous transmission (Oleskevich,

Youssoufian & Walmsley 2004; Youssoufian, Oleskevich & Walmsley 2005; see

Walmsley et al. 2006). Inhibitory input to the principal cells in the MNTB, however,

shows significant changes between *dn/dn* and normal mice, as glycinergic mIPSCs

(miniature inhibitory postsynaptic currents) are significantly different in amplitude,

duration, and frequency (Leao et al. 2004b). The principal cells in the MNTB also show

altered membrane properties between normal and *dn/dn* mice. In *dn/dn* mice, smaller

low threshold potassium currents in the principal cells results in an increase in their

excitability (Dodson, Barker & Forsythe 2002; Leao et al. 2004a; see Walmsley et al.

2006), and there is also an increase in hyperpolarization activated currents and in high-

threshold potassium currents (Leao et al. 2004a; Leao et al. 2005; see Walmsley et al.

2006). Additionally, numerous changes in channel expression have been found in the

MNTB neurons of normal and *dn/dn* mice. Research by Leao et al. (2005; 2006), has

found in the MNTB of normal mice there are gradients of low-threshold potassium

currents, high-potassium currents, and hyperpolarization-activated cation currents. These

currents correspond with gradients of Kv1.1, Kv3.1, and HCN4 channel expression,

respectively (Fig. 3). In the MNTB of *dn/dn* mice, however, they found that gradients

did not exist for any of these currents or their corresponding channels (Fig. 3), which

serves as evidence that the developmental formation of the tonotopic map in the mouse

MNTB is related to spontaneous auditory nerve activity (Leao et al. 2005; 2006).

**Role of Calcium in Synaptic Transmission and Calcium-binding Proteins**

When a presynaptic action potential reaches a synaptic terminal, it causes voltage-dependent calcium channels to open, and calcium ions rush into the presynaptic terminal due to a large concentration gradient. The increase in intracellular $Ca^{2+}$ concentration triggers fusion of neurotransmitter-containing vesicles with the membrane, and neurotransmitter is released into the synaptic cleft (Katz & Miledi 1965; 1967; 1968; 1970; see Meinrenken, Borst & Sakmann 2002; Felmy, Neher & Schneggenburger 2003). The key to this process is the neuronal maintenance of extremely low intracellular $Ca^{2+}$ concentration through $Ca^{2+}$ extrusion systems (Garcia & Strehler 1999; Kip et al. 2006). $Na^+/Ca^{2+}$ exchangers and a $Ca^{2+}$ ATPase (PMCA) in the plasma membrane force $Ca^{2+}$ out of the cell (Penniston 1983; Carafoli 1987; Strehler 1990; Miller 1991; see Garcia & Strehler 1999; Carafoli et al. 2001), and $Ca^{2+}$ pumps in the endo(sarco)plasmic reticulum (SERCA) and transporters in mitochondrial membranes sequester $Ca^{2+}$ in the endo(sarco)plasmic reticulum and mitochondrial matrices, respectively (Carafoli et al. 2001).

Another important mechanism to maintain the low neuronal cytosolic $Ca^{2+}$ concentration is found in the actions of $Ca^{2+}$-binding proteins. The $Ca^{2+}$-binding proteins Calretinin (CR), Calbindin D-28k (CB), and Parvalbumin (PV) are found in many neurons of the central nervous system (Celio 1990; Arai et al. 1991; Resibois & Rogers 1992; see Felmy & Schneggenburger 2004), and more specifically, in the brainstem auditory nuclei (Arai et al. 1991; Caicedo et al. 1996; Lohmann & Friauf 1996; see Felmy & Schneggenburger 2004). When present in presynaptic terminals, these $Ca^{2+}$-

15

binding proteins reversibly bind $Ca^{2+}$ ions and thus modulate transmitter release and

$Ca^{2+}$-dependent forms of short-term plasticity (Felmy & Schneggenburger 2004).  CR

and CB exhibit rapid $Ca^{2+}$-binding kinetics (Nägerl et al. 2000; see Felmy &

Schneggenburger 2004), and have been shown to reduce peak intracellular $Ca^{2+}$

concentration by binding incoming $Ca^{2+}$ ions before they reach the $Ca^{2+}$ sensor for vesicle

fusion (Edmonds et al. 2000; see Felmy & Schneggenburger 2004).  Thus, CR and CB

can decrease transmitter release probability during basal synaptic transmission (Felmy &

Schneggenburger 2004).  PV, on the other hand, exhibits slow $Ca^{2+}$-binding kinetics

(Lee, Schwaller & Neher 2000; see Felmy & Schneggenburger 2004), in which the

delayed $Ca^{2+}$ binding will accelerate the decay of residual $Ca^{2+}$ ions (Atluri & Regehr

1996; Lee, Schwaller & Neher 2000; see Felmy & Schneggenburger 2004), and results in

suppression of the amount of transmitter release facilitation (Calliard et al. 2000;

Vreugdenhil et al. 2003; see Felmy & Schneggenburger 2004).

Very few projects have examined the subcellular localization and developmental

changes in the expression of $Ca^{2+}$-binding proteins in the AVCN and MNTB.  Felmy &

Schneggenburger (2004) did examine developmental expression of CR, CB, and PV in

the MNTB of normal hearing rats and mice.  Their results indicated that CR is expressed

in some (not all) presynaptic calyces of Held, but not in the postsynaptic principal cells.

They also reported that the number of CR-positive calyces and the density of their

staining increased from 6 days to 31 days postnatal, and that CR-positive calyces in mice

were preferentially located in the lateral portion of the MNTB.  They found that CB was

expressed in all postsynaptic principal cell somata, but not in the presynaptic calyces of

Held.  It had been previously reported that PV was present in the postsynaptic principal

cells in the MNTB (Caicedo et al. 1996; Lohmann & Friauf 1996). Felmy and

Schneggenburger (2004) verified that PV was present in the somata of the principal cells,

but in addition they discovered that PV was present in the presynaptic calyces of Held

and their axons. Again, PV staining in the calyces and principal cell somata increased

with development. Taken together, they concluded that up-regulation of CR and PV in

the calyces of Held leads to increased presynaptic $Ca^{2+}$ buffering strength during

development of normal rats and mice, but that the expression of CR is not uniform in all

calyces of Held (Felmy & Schneggenburger 2004).

To date, there have been no studies analyzing differential expression of $Ca^{2+}$-

binding proteins in the MNTB and AVCN between normal and congenitally deaf mice.

Oleskevich & Walmsley (2002), however, found enhanced synaptic strength in the

endbulb of Held synapse in the AVCN of *dn/dn* mice (aged 11-16 days postnatal) when

compared with normal mice. Their results were based on the finding that transmitter

release probability at this synapse was greater in *dn/dn* mice. They theorized that

auditory nerve activity in normal hearing mice may act to depress release probability,

thus decreasing synaptic depression and improving high-fidelity transmission. In

addition, they found that administration of the membrane permeable calcium buffer

EGTA-AM diminished all observed differences between deaf and normal mice. As a

result, they suggested impaired calcium buffering in the endbulb terminals of deaf mice

may be responsible for the synaptic differences found between the deaf and normal mice

(Oleskevich & Walmsley 2002). We will, therefore, examine $Ca^{2+}$ buffering in the

AVCN of normal and *dn/dn* mice.

# IV. METHODS

## Immunohistochemistry

Normal hearing CBA and congenitally deaf mutant (*dn/dn*) mice from five different developmental time points were used. The normal hearing CBA mice served as the wild-type mice in these experiments. The time points used were: 9 days, 13 days, 20 days, 30 days, and 49 days postnatal. The 9 and 13 days postnatal time points were chosen to represent points immediately before, and immediately after, opening of the ear canal in both *dn/dn* and normal mice, which is around 11 days postnatal (Oleskevich & Walmsley, 2002). The time points 20 and 30 days postnatal represented ages in which the mice were advancing in development. The 49 day postnatal time point was chosen to represent developmentally mature mice.

All mice were anaesthetized intraperitoneally with Nembutal (50 mg/ml) at 100 mg/kg body weight and perfused via the left ventricle with cold vascular rinse, (0.01 M phosphate buffer with 137 mM NaCl, 3.4 mM KCl and 6 mM $NaHCO_3$) followed by fixative (4% paraformaldehyde in 0.1 M phosphate buffer, pH 7.4) for 8-12 minutes. Following perfusion, brains were removed and post-fixed (4% paraformaldehyde in 0.1 M phosphate buffer, pH 7.4) for one hour. Following post-fixation, the brains were transferred into 15% Sucrose (in 0.1 M Phosphate Buffer) solution kept at 4°C until ready for sectioning. Before sectioning, the brainstem/cerebellum was isolated and the rest of

the brain was discarded.  A Microm HM 505E cryostat (Carl Zeiss, Inc., Thornwood,

NY) was used for sectioning.  Tissue was submerged in Cryoprotectant Solution (500 ml

0.1 M Phosphate Buffer pH 7.2, 300 g Sucrose, 10 g Polyvinylpyrrolidone, 300 ml

Ethylene glycol, ~200 ml double distilled $H_2O$) for 5 minutes, OCT (Tissue-Tek #4583)

for 10 minutes, and then frozen in OCT on a stage in the cryostat at -25°C for 30+

minutes.  Transverse sections (10 µm thick) of the brainstem were obtained at the levels

of MNTB and AVCN (Fig. 1) and mounted directly onto slides.  After washing with 0.01

M Phosphate-Buffered Saline with 0.2% Triton X-100 (PBS-T), the sections were

incubated in Normal Horse Serum (1:10 in 0.01 M PBS-T) for one hour.  After removing

the Normal Horse Serum, the sections were incubated overnight at 4°C in a 0.01 M PBS-

T diluted solution containing the following primary antibodies: mouse anti-Calretinin

(Zymed, San Francisco, CA; 1:500 dilution), mouse anti-Calbindin D-28k (Swant,

Bellinzona, Switzerland; 1:1000 dilution), and mouse anti-Parvalbumin (Chemicon,

Temecula, CA; 1:2000 dilution).  Some slides were double-labeled with guinea pig anti-

Vesicular Glutamate Transporter 1 (VGLUT1) (Chemicon, Temecula, CA; 1:1000) in

order to visualize the glutamatergic presynaptic terminals (Fig. 4-5).  The sections were

then washed again with PBS-T, and incubated for three hours in Cy-3-conjugated donkey

anti-mouse IgG (1:50 dilution; Jackson, West Grove, PA) or FITC-conjugated donkey

anti-guinea pig IgG (1:50 dilution; Jackson, West Grove, PA) secondary antibodies in

dark conditions (which were maintained for the duration of the experiments).  The

sections were then washed with 0.01 M Phosphate-Buffered Saline (PBS). Slides that had

been single labeled were incubated with green fluorescent Nissl stain (1:100; Molecular
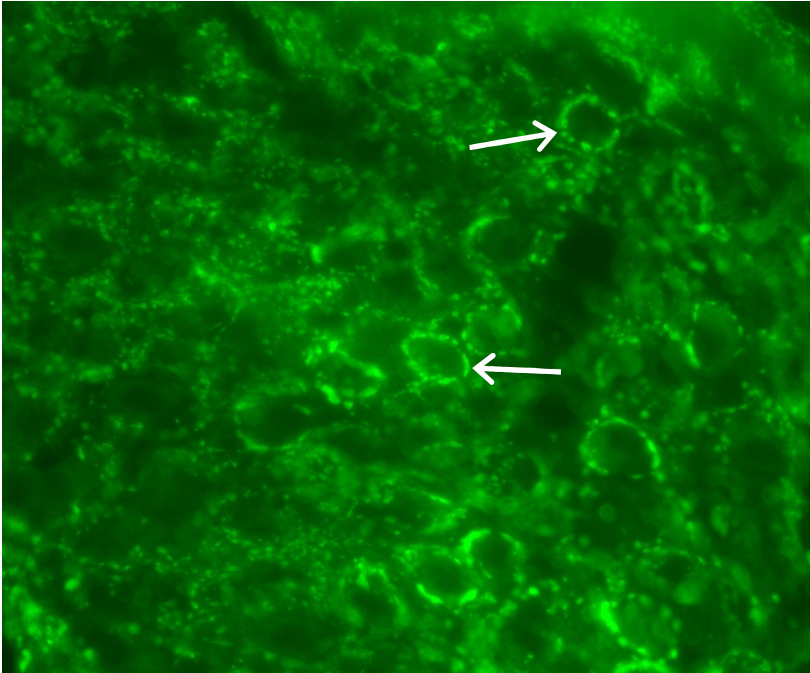
**Figure 4. VGLUT1 expression in the AVCN**
VGLUT1 is expressed in presynaptic endbulb of Held terminals (arrows) in the AVCN.
Fluorescence image taken at 40X magnification.
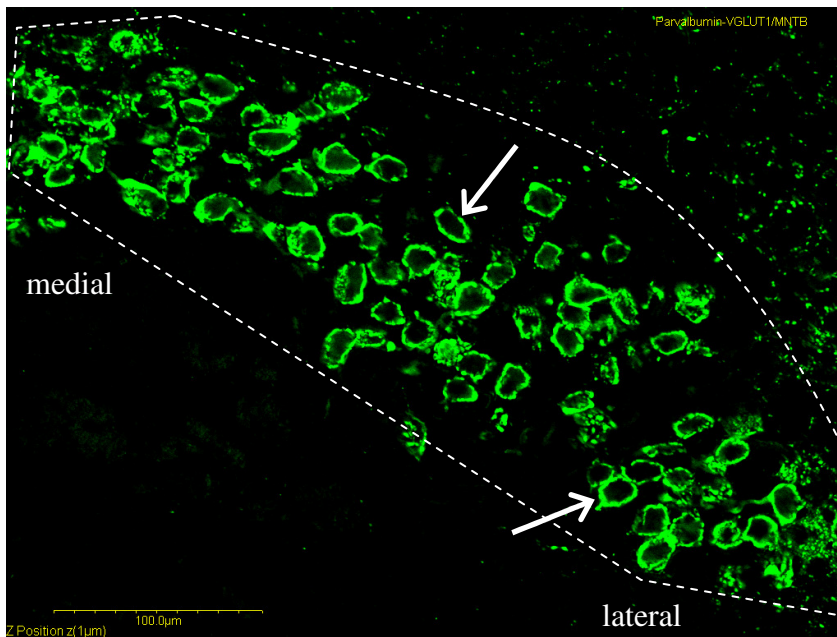


**Figure 5. VGLUT1 expression in the MNTB**
VGLUT1 is expressed in presynaptic calyx of Held terminals (arrows) in the MNTB.
Confocal image obtained with a 20X dry objective. Dashed line indicates area of MNTB.

Probes, Eugene, OR) for 5 minutes in order to visualize postsynaptic cell somata (Fig. 6-7).  These slides were washed again with 0.01 M PBS.  All slides were cover-slipped with fluorescence mounting medium (Vectashield, Vector, Burlingame, CA).

**Specificity of Antibodies**

Mouse anti-Calretinin monoclonal antibody (Zymed, San Francisco, CA) is a mouse IgG that reacts with Calretinin, a protein with a Molecular Weight (M.W.) of 29 kD.  Specificity was proven through immunoblotting followed by two-dimensional gel analysis.  Endogenous expression was shown through microscopy which is standard protocol for Zymed (personal communication).  Mouse anti-Parvalbumin monoclonal antibody (Chemicon, Temecula, CA) is a mouse IgG that has been shown to react with Parvalbumin in human, rat, bovine, porcine, feline, rabbit, canine, frog, fish and goat neural and muscular tissue.  By immunoblot it recognizes a M.W. protein of 12 kD.  The antibody is directed against an epitope at the first $Ca^{2+}$-binding site and specifically stains the $Ca^{2+}$-bound form of Parvalbumin.  Mouse anti-Calbindin D-28k monoclonal antibody (Swant, Bellinzona, Switzerland) is a mouse IgG that reacts with Calbindin D-28k from human, monkey, rabbit, rat, mouse and chicken tissues.  It does not react with other known $Ca^{2+}$-binding proteins, as it specifically stains the $^{45}CA$-binding spot of Calbindin D-28k (MW 28`000, IEP 4.8) in a two-dimensional gel.  In radioimmunoassay it detects Calbindin D-28k with a sensitivity of 10 ng/assay and an affinity of $1.6 \times 10^{12}$ L/M. Guinea Pig anti-Vesicular Glutamate Transporter 1 (VGLUT1) polyclonal antibody (Chemicon, Temecula, CA) reacts with VGLUT1 protein in nerve fibers and terminals

21
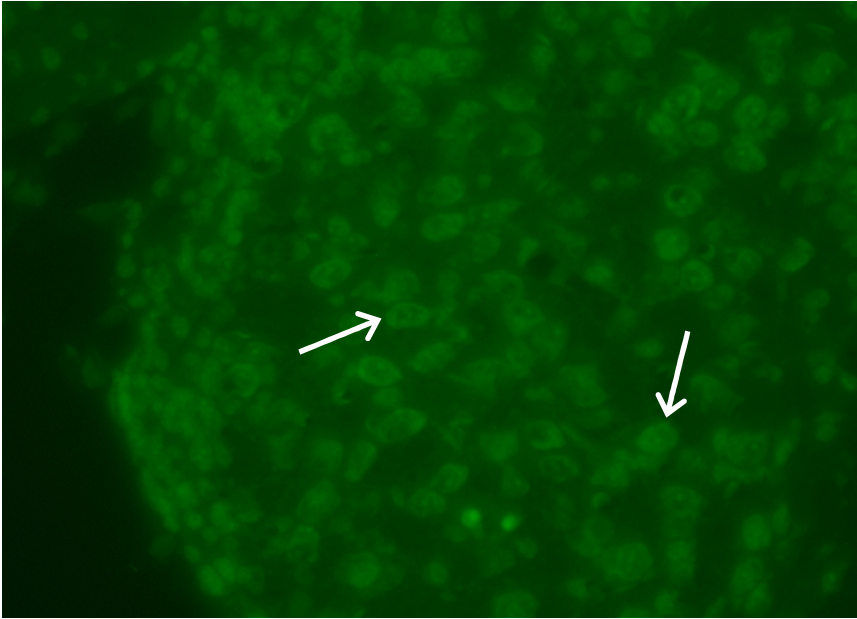
**Figure 6. AVCN – green fluorescent Nissl staining**
Fluorescence image at 20X magnification showing green fluorescent Nissl staining in postsynaptic bushy cell somata (arrows) within the AVCN.
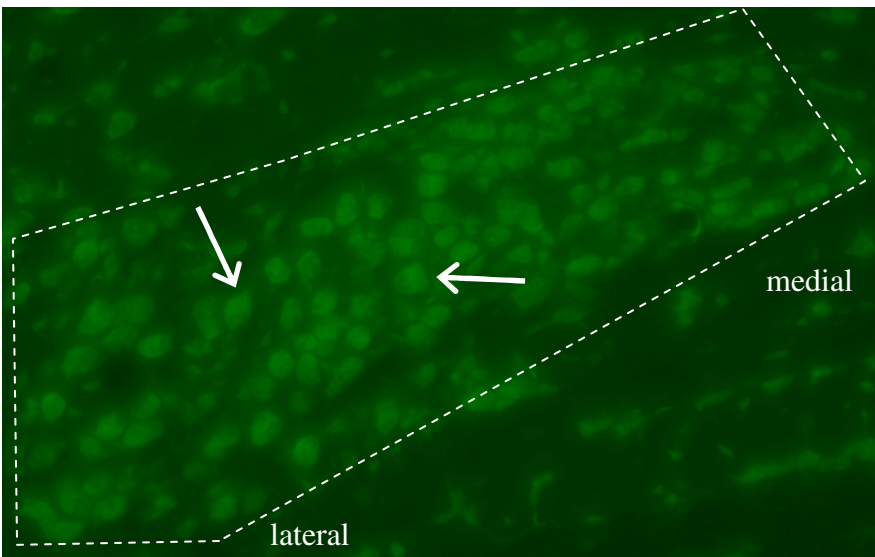


**Figure 7. MNTB – green fluorescent Nissl staining**
Fluorescence image at 20X magnification showing green fluorescent Nissl staining in postsynaptic principal cell somata (arrows) within the MNTB.  Dashed line indicates area of MNTB.

(Fig. 4-5).  Preabsorption of the VGLUT1 antiserum with immunogen peptide eliminates all immunostaining, thus confirming its specificity.  Cy-3-conjugated donkey anti-mouse IgG secondary antibody (Jackson, West Grove, PA) reacts with the heavy chains on mouse IgG and with the light chains common to most mouse immunoglobulins, based on immunoelectrophoresis.  No antibody was detected against non-immunoglobulin serum proteins.  It has been tested by ELISA and/or solid-phase adsorbed to ensure minimal cross-reaction with bovine, chicken, goat, guinea pig, Syrian hamster, horse, human, rabbit, and sheep serum proteins.  FITC-conjugated donkey anti-guinea pig IgG secondary antibody (Jackson, West Grove, PA) reacts with the heavy chains on guinea pig IgG and with the light chains common to most guinea pig immunoglobulins.  No antibody was detected against non-immunoglobulin serum proteins.  It has been tested by ELISA and/or solid-phase adsorbed to ensure minimal cross-reaction with bovine, chicken, guinea pig, Syrian hamster, horse, human, mouse, rabbit, rat, and sheep serum proteins.  Green fluorescent Nissl stain (Molecular Probes, Eugene, OR) binds to Nissl substance, or rough endoplasmic reticulum, within the soma of a neuron (Fig. 6-7).  Specifically, it binds to ribosomal RNA on the surface of endoplasmic reticulum, which is found in abundance in neuronal somata due to their large need for protein synthesis.  The stain is essentially nonfluorescent, except when bound to DNA or RNA.

**Imaging & Data Analysis**

Epi-fluorescence images were collected at 20X and 40X magnifications using an Episcopic-Fluorescence Scope (model optiphot-2, Nikon, Mellville, NY) and a Spot RT

Camera and Software v3.0 (Diagnostic Instruments, Inc., Sterling Height, MI). Confocal images were obtained using a laser scanning confocal microscope (Olympus Fluoview) with 20X or 60X dry objectives, digitally magnified 2-3X at 1024x1024 pixel resolution. Images of $Ca^{2+}$-binding protein expression in the AVCN were taken from the middle (in respect to both the medial-lateral axis and the dorsal-ventral axis) of the nucleus. Images of $Ca^{2+}$-binding protein expression in the MNTB captured the entire nucleus. In order to analyze expression of CR, CB, and PV in the AVCN and MNTB, all images of a respective $Ca^{2+}$-binding protein were taken with the same exact exposure settings for all ages in both normal and dn/dn mice. Images were then compared side by side.

When analyzing expression of CR, CB, and PV in the AVCN and MNTB, it was useful to observe the pattern of expression of each of these proteins in the cerebellum. In the cerebellum, any $Ca2+$-binding protein expression should not be affected by the presence or absence of auditory nerve activity. Thus, the pattern of $Ca2+$-binding protein expression in the cerebellum served as a negative control, and was used to ensure that the staining conditions in the AVCN or MNTB were consistent from animal to animal. In addition, a control experiment, in which the primary antibodies were omitted, was conducted to ensure that the secondary antibodies were only binding to the desired primary antibodies. The results of this experiment showed that the secondary antibodies were not binding to any other antigens.

# V.  RESULTS

<u>AVCN</u>

*Calretinin (CR)*

In the AVCN, CR was expressed in presynaptic nerve fibers and endbulb of Held terminals, but not in postsynaptic bushy cell somata (Fig. 8).  This pattern of expression was confirmed by analyzing sections which were double stained for CR (CY3) and green fluorescent Nissl stain or VGLUT1 (FITC), which stained the postsynaptic bushy cell somata or presynaptic endbulbs of Held, respectively.  In these sections, there was clearly no co-localization of the CR and Nissl stains, thus indicating that CR was not expressed in bushy cell somata (Fig. 9).  Co-localization was observed in the CR and VGLUT1 stains, confirming the presence of CR in the endbulbs of Held (not shown).

The first line to be analyzed was normal hearing mice.  At 9 days postnatal in the normal hearing mouse, CR was expressed in many nerve fibers and a small number of endbulbs of Held (compared to the number observed later in development) (Fig. 10). From 9 days postnatal to 13 days postnatal, the pattern of CR expression began to change.  At 13 days postnatal, CR appeared to be expressed in fewer nerve fibers and in more endbulbs of Held than at 9 days postnatal (Fig. 11).  This pattern of CR being
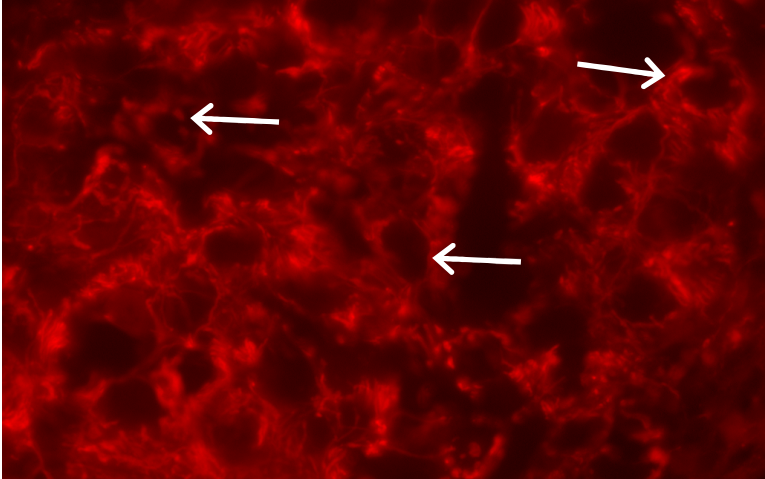
**Figure 8.  Calretinin expression in the AVCN**
CR, shown in red, is localized in nerve fibers and presynaptic endbulbs of Held (arrows), but not in postsynaptic bushy cell somata.  Fluorescence image taken at 20X magnification.
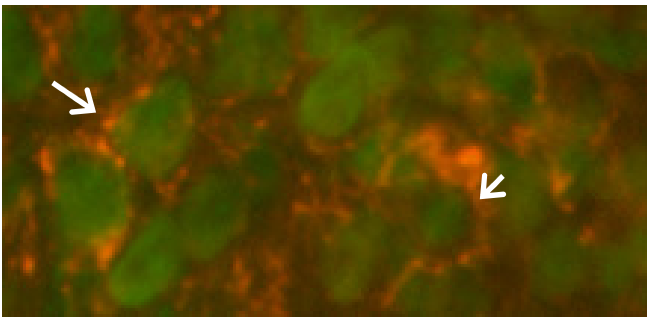


**Figure 9.  Expression of Calretinin and green fluorescent Nissl in the AVCN**
CR, shown in red, is expressed in the endbulbs of Held (arrows), while green fluorescent Nissl (green) is restricted to the bushy cell somata.  No co-localization is observed, confirming that CR is not present in bushy cell somata.  Fluorescence image taken at 20X magnification.
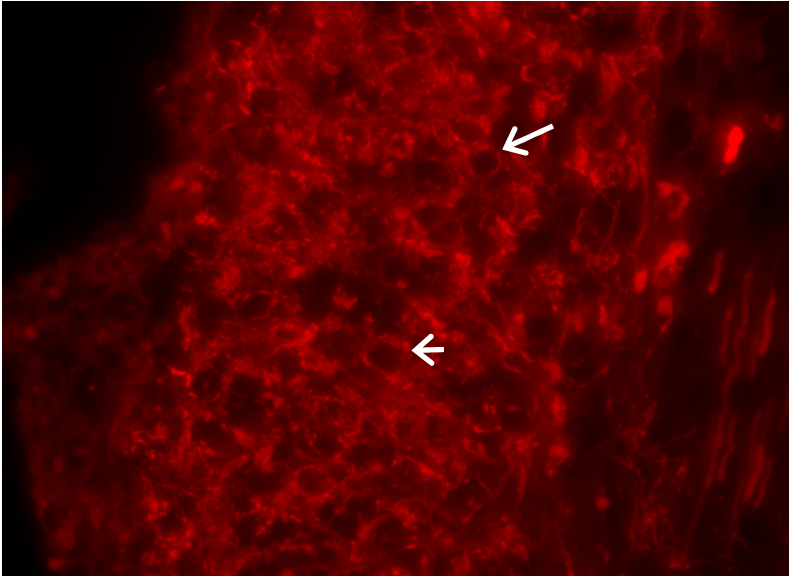
**Figure 10. Calretinin expression in normal mice at 9 days postnatal in the AVCN**
At 9 days postnatal, CR expression in the AVCN of normal mice is relatively diffuse, with CR expressed in many nerve fibers and a small number of endbulb specializations (arrows) (compared to that seen later in development). Endbulbs are relatively large in size (compared to later in development). Fluorescence image obtained at 20X magnification.
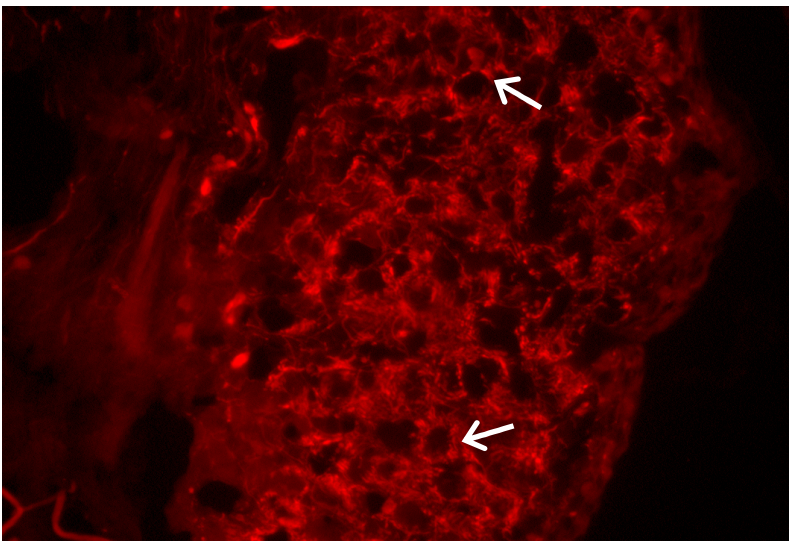


**Figure 11. Calretinin expression in normal mice at 13 days postnatal in the AVCN**
At 13 days postnatal, CR expression in the AVCN of normal mice is seen in fewer nerve fibers and in more endbulb specializations (arrows) than in normal mice at 9 days postnatal. Size of endbulbs appears to have decreased and number of endbulb specializations appears to have increased. Fluorescence image obtained at 20X magnification.

expressed in fewer nerve fibers and more endbulbs of Held continued as development proceeded. In normal hearing mice at 20 days postnatal, CR was expressed in fewer nerve fibers and more endbulbs of Held than in the normal mice at 13 days postnatal, and at 30 days, CR was expressed in fewer nerve fibers and more endbulbs of Held than in the normal mice at 20 days postnatal (Fig. 12-13). Finally, at 49 days postnatal CR was expressed in very few nerve fibers and in numerous endbulbs of Held (not shown). Hence, the overall pattern of the developmental expression in normal hearing mice was for young mice to express CR in many nerve fibers and few endbulbs of Held, and for more mature mice to express CR in progressively fewer nerve fibers and progressively more endbulbs of Held. Interestingly, the size of the endbulb of Held terminals appeared to decrease throughout development, but the amount of endbulb terminals appeared to increase (Fig. 14-15).

At 9 days postnatal in *dn/dn* mice, CR was expressed in many nerve fibers and a small number of endbulbs of Held (Fig. 16). This pattern was very similar to that which was observed in the normal hearing mouse at 9 days postnatal. As development proceeded in *dn/dn* mice, however, the pattern of CR expression did not appear to change from that observed in the 9 day mice. Thus, at 13 days, 20 days, 30 days, and even 49 days postnatal in *dn/dn* mice, CR still appeared to be expressed in many nerve fibers and a small number of endbulbs of Held (Fig. 17-19; *dn/dn* 49 day not shown). Also, the number and size of the endbulb terminals appeared to stay the same as the *dn/dn* mice aged from 9 days through 49 days postnatal (Fig. 20-21).

Thus, vast differences were observed in the developmental expression of CR in the AVCN between normal hearing and congenitally deaf mice. At 9 days

**Figure 12. Calretinin expression in normal mice at 20 days postnatal in the AVCN**
At 20 days postnatal, CR expression in the AVCN of normal mice is seen in fewer nerve fibers and in more endbulbs specializations (arrows) than in normal mice at 13 days postnatal. Size of endbulbs appears to have decreased and number of endbulb specializations appears to have increased. Fluorescence image obtained at 40X magnification.
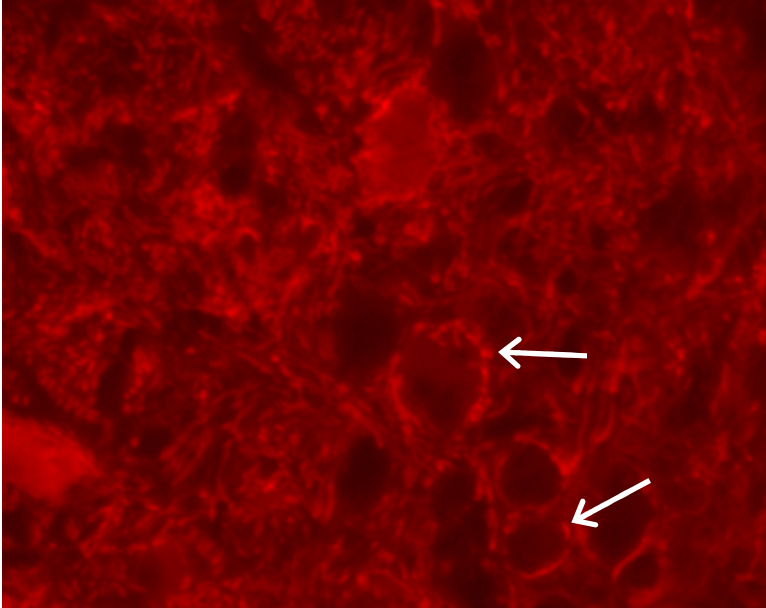


**Figure 13. Calretinin expression in normal mice at 30 days postnatal in the AVCN**
At 30 days postnatal, CR expression in the AVCN of normal mice is seen in fewer nerve fibers and in more endbulb specializations (arrows) than in normal mice at 20 days postnatal. Size of endbulbs appears to have decreased and number of endbulb specializations appears to have increased. Fluorescence image obtained at 20X magnification.
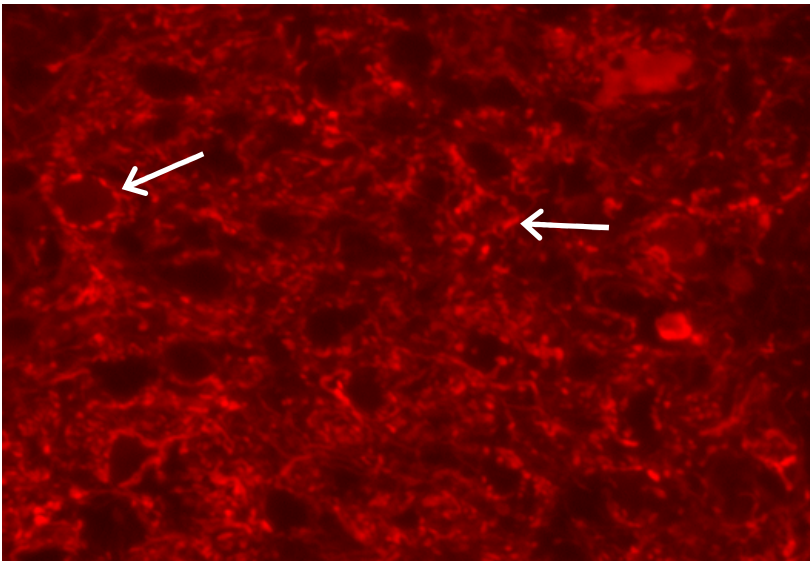
**Figure 14. Calretinin expression in the AVCN of 13 day postnatal normal mice showing endbulb morphology**
The endbulb morphology at 13 days postnatal in normal mice, here visualized by CR staining, shows relatively large synaptic specializations (arrows).  Confocal image taken with 60X dry objective.



**Figure 15. Calretinin expression in the AVCN of 30 day postnatal normal mice showing altered endbulb morphology**
The endbulb morphology (arrows) at 30 days postnatal in normal mice, again visualized by CR staining, shows a decrease in endbulb size and an increase in number of specializations as compared to normal mice at 13 days postnatal.  Confocal image taken with 60X dry objective.

**Figure 16. Calretinin expression in *dn/dn* mice at 9 days postnatal in the AVCN**
At 9 days postnatal, CR expression in the AVCN of *dn/dn* mice is relatively diffuse, with expression seen in many nerve fibers and a small number of endbulb specializations (arrow) (compared to that in mature normal mice). Endbulbs are relatively large in size (compared to that in mature normal mice). Fluorescence image obtained at 20X magnification.



**Figure 17. Calretinin expression in *dn/dn* mice at 13 days postnatal in the AVCN**
At 13 days postnatal, CR expression in the AVCN of *dn/dn* mice is diffuse, with expression seen in many nerve fibers and a small number of endbulb specializations (arrow) (compared to that in mature normal mice). Endbulbs are relatively large in size (compared to that in mature normal mice). Thus, in respect to CR expression in the AVCN, *dn/dn* mice at 13 days postnatal resemble both *dn/dn* and normal mice at 9 days postnatal. Fluorescence image obtained at 20X magnification.
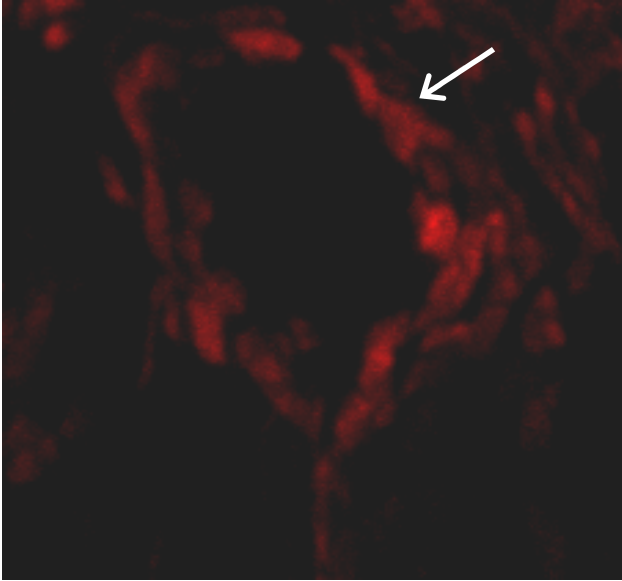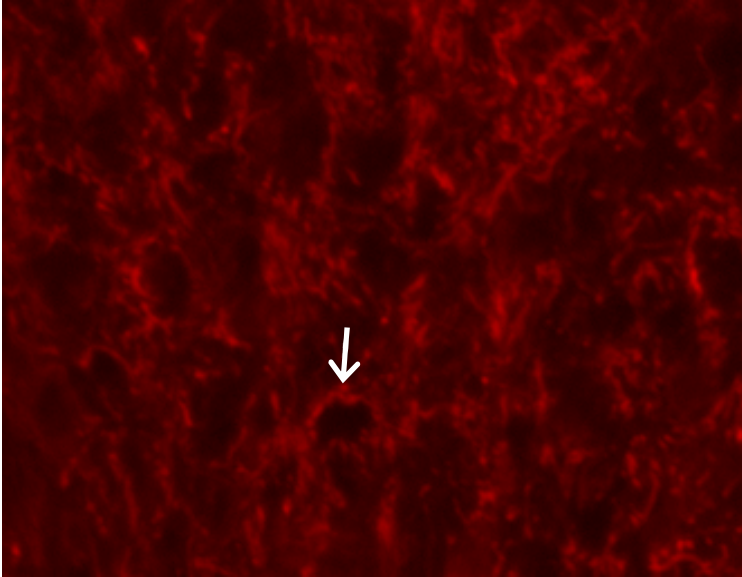
**Figure 18. Calretinin expression in *dn/dn* mice at 20 days postnatal in the AVCN**
At 20 days postnatal, CR expression in the AVCN of *dn/dn* mice is diffuse, with CR seen in many nerve fibers and a small number of endbulb specializations (arrow) (compared to that in mature normal mice). Endbulbs are relatively large in size (compared to that in mature normal mice). Thus, in respect to CR expression in the AVCN, *dn/dn* mice at 20 days postnatal resemble *dn/dn* mice at 13 days and both *dn/dn* and normal mice at 9 days postnatal. Fluorescence image obtained at 20X magnification.
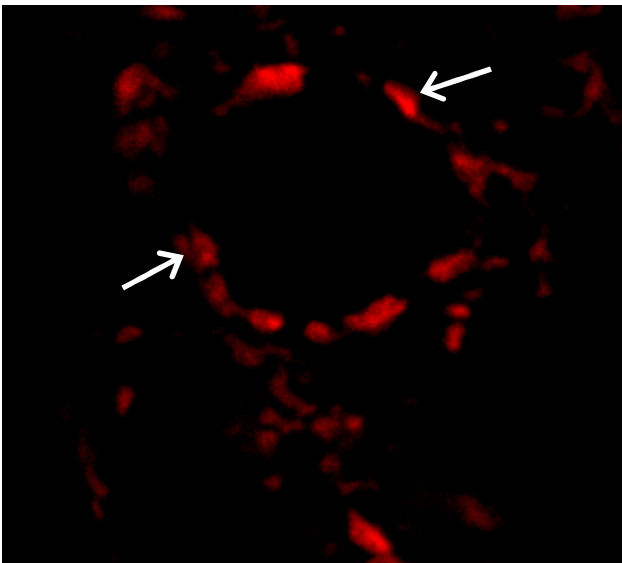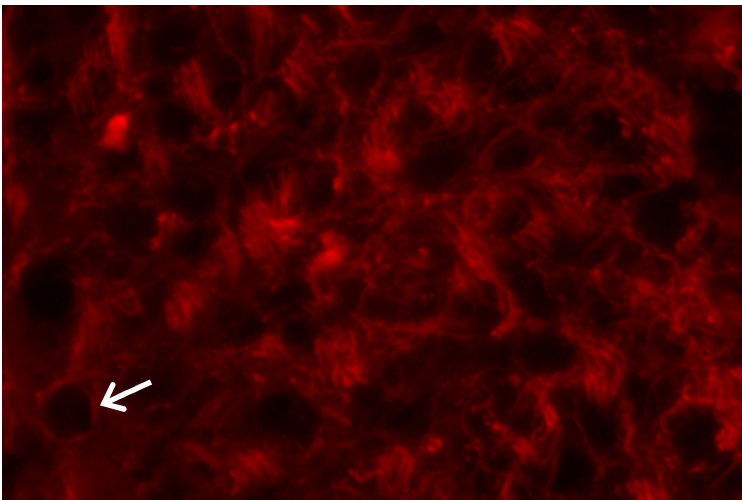


**Figure 19. Calretinin expression in *dn/dn* mice at 30 days postnatal in the AVCN**
At 30 days postnatal, CR expression in the AVCN of *dn/dn* mice is diffuse, with CR seen in many nerve fibers and a small number of endbulb specializations (arrow) (compared to that in mature normal mice). Endbulbs are relatively large in size (compared to that in mature normal mice). Thus, in respect to CR expression in the AVCN, *dn/dn* mice at 30 days postnatal resemble *dn/dn* mice at 9, 13 and 20 days postnatal and normal mice at 9 days postnatal. Fluorescence image obtained at 20X magnification.
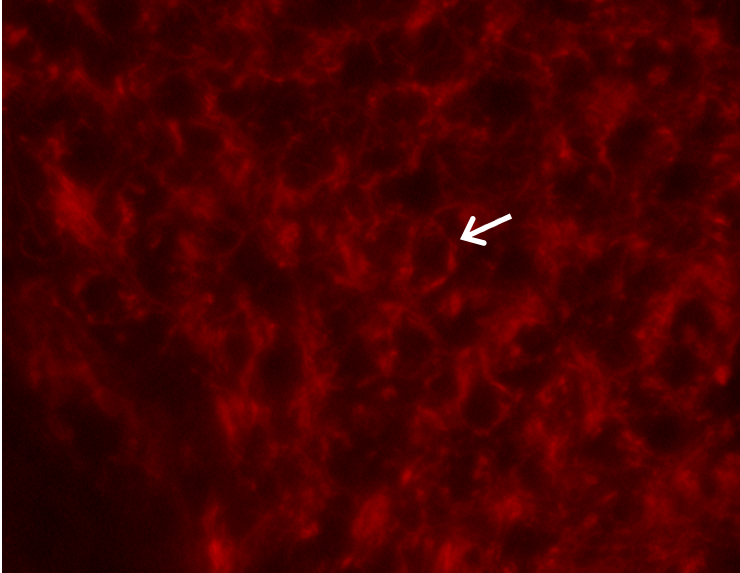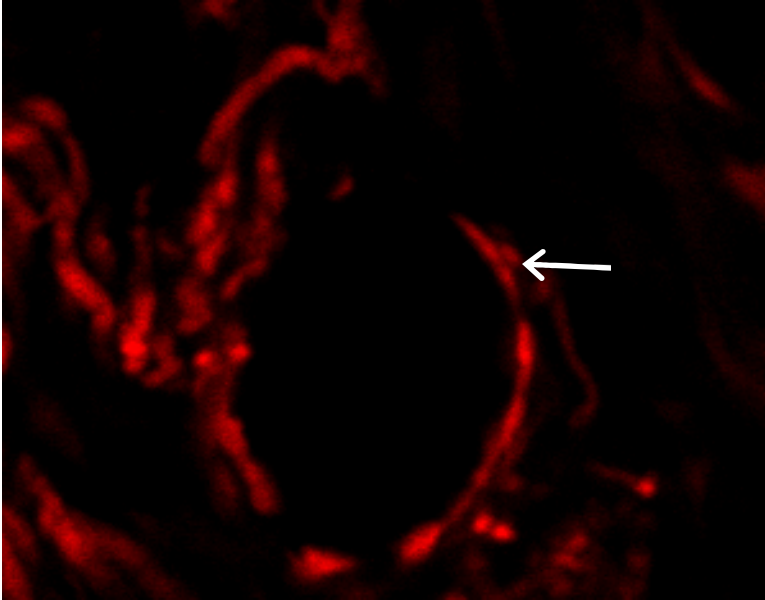
**Figure 20. Calretinin expression in the AVCN of 13 day postnatal *dn/dn* mice showing endbulb morphology**
The endbulb morphology (arrow) at 13 days postnatal in *dn/dn* mice, here visualized by CR staining, shows relatively large synaptic specializations, and resembles that in normal mice at 13 days postnatal.  Confocal image taken with 60X dry objective.
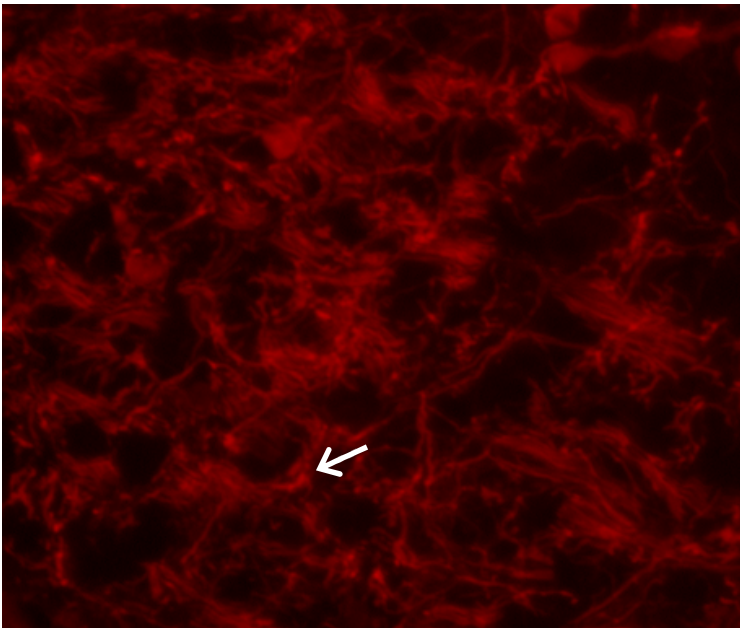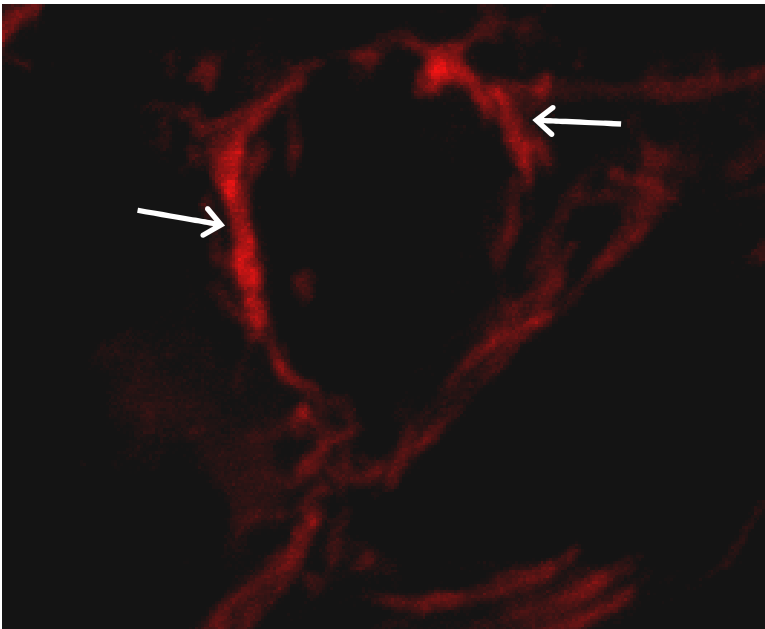


**Figure 21. Calretinin expression in the AVCN of 30 day postnatal *dn/dn* mice showing endbulb morphology**
The endbulb morphology (arrows) at 30 days postnatal in *dn/dn* mice, here visualized by CR staining, shows relatively large synaptic specializations, and resembles that in both *dn/dn* and normal mice at 13 days postnatal.  Confocal image taken with 60X dry objective.

postnatal in both normal and *dn/dn* mice, CR was expressed in many nerve fibers and relatively few endbulb of Held terminals (Fig. 10, Fig. 16). In normal hearing mice, however, CR expression changed throughout development, as it was expressed in progressively fewer nerve fibers and progressively more endbulb of Held terminals (Fig. 11-15). In *dn/dn* mice, on the other hand, there appeared to be no change in CR expression as development proceeded. The pattern of CR expression in the 9 day postnatal *dn/dn* mice was the same as was observed in the 13 day, 20 day, 30 day, and 49 day postnatal *dn/dn* mice (Fig. 17-21). Because the pattern of CR expression in 9 day normal and 9 day *dn/dn* mice was the same, it appeared that CR expression at every age in *dn/dn* mice resembled that which was observed in 9 day normal hearing mice. In addition, the size and number of endbulb of Held terminals were different between normal and *dn/dn* mice. In normal mice, endbulb terminals appeared to be large in size and few in number early in development, and became progressively smaller and more numerous as development proceeded (Fig. 14-15). In *dn/dn* mice, endbulb terminals also appeared to be large in size and few in number early in development. As development proceeded in the *dn/dn* mice, however, there was no observed change in the size and number of endbulb of Held terminals, as mature mice also appeared to have endbulb terminals that were large in size and few in number (Fig. 20-21).

*Calbindin D-28k (CB)*

In the AVCN, Calbindin D-28k was only expressed in postsynaptic bushy cell somata (Fig. 22). This pattern of CB expression was confirmed by double labeling with CB (CY3) and green fluorescent Nissl stain or VGLUT1 (FITC). In sections receiving CB and VGLUT1, no co-localization was observed, confirming that CB was not expressed in endbulbs of Held (Fig. 23). In sections receiving CB and Nissl, co-localization was observed, confirming the presence of CB in some bushy cell somata (Fig. 24). Interestingly, CB was not expressed in all bushy cell somata. In fact, CB was expressed in very few bushy cells (Fig. 23, 24). The amount of CB expression in the AVCN was far less than was observed for CR and PV. These results applied to both the normal hearing and congenitally deaf mice.

At 9 days postnatal in normal mice, CB appeared to be expressed weakly in just a few bushy cell somata (Fig. 25). At 13 days postnatal, CB expression began to change, as there was an increase in both the number of bushy cell somata expressing CB and in the intensity of CB staining (Fig. 26). This pattern of CB expression continued as development proceeded, as the 20 day, 30 day, and 49 day normal mice all showed an increase in the number of bushy cell somata expressing CB and in the intensity of CB staining (Fig. 27-28; normal 49 day not shown).

In *dn/dn* mice, CB expression began as it did in the normal mice, with CB being expressed weakly in just a few bushy cell somata (Fig. 29). As development proceeded in *dn/dn* mice, however, the number of bushy cells expressing CB and the intensity of CB staining remained the same (Fig. 30-32). Thus, in *dn/dn* mice, 9 day, 13 day, 20 day, 30

35
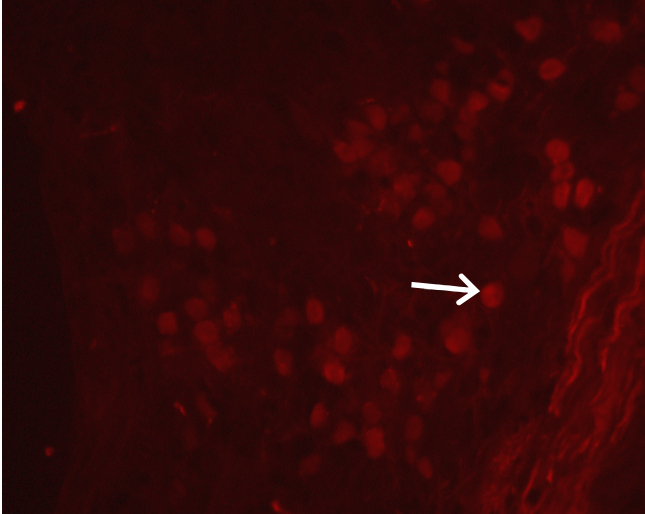
**Figure 22. Calbindin D-28k expression in the AVCN**
CB, shown in red, is localized in postsynaptic bushy cell somata (arrow), but not in nerve fibers or presynaptic endbulbs of Held.  Fluorescence image taken at 20X magnification.
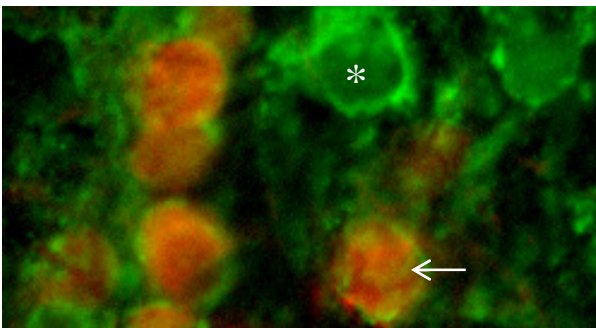


**Figure 23. Expression of Calbindin D-28k and VGLUT1 in the AVCN**
CB, shown in red, is localized in some bushy cell somata.  * indicates bushy cell not expressing CB.  VGLUT1, shown in green, is localized in endbulbs of Held (arrow).  No co-localization is observed, confirming that CB is not present in the endbulbs of Held. Fluorescence image taken at 40X magnification.
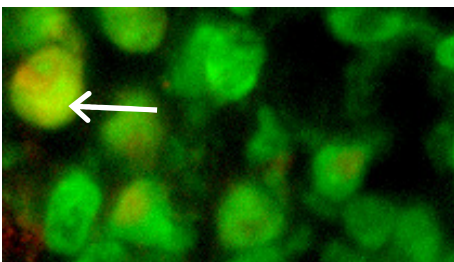


**Figure 24. Expression of Calbindin D-28k and green fluorescent Nissl in the AVCN**
CB, shown in red, and green fluorescent Nissl, shown in green, are both localized in bushy cell somata.  Only one bushy cell, at the top left colored yellow (arrow), is positive for co-localization, yet this confirms the presence of CB in the bushy cell somata. Fluorescence image taken at 40X magnification.
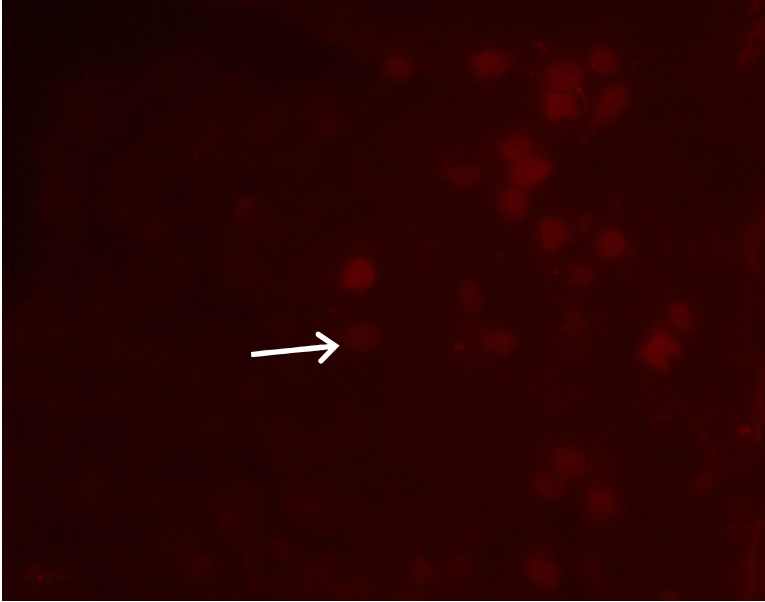
**Figure 25. Calbindin D-28k expression in normal mice at 9 days postnatal in the AVCN**

At 9 days postnatal in normal mice, CB appeared to be expressed weakly in only a few postsynaptic bushy cell somata (arrow). Fluorescence image obtained at 20X magnification.
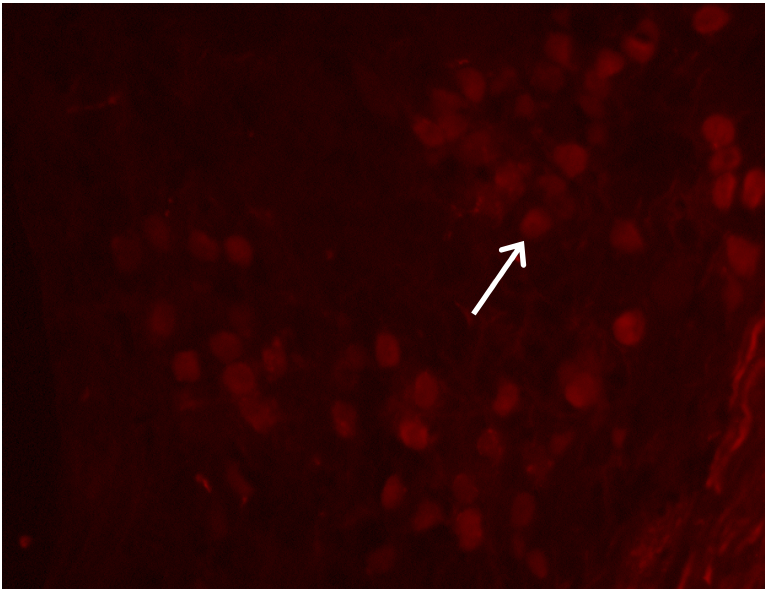


**Figure 26. Calbindin D-28k expression in normal mice at 13 days postnatal in the AVCN**

At 13 days postnatal in normal mice, CB was expressed in more bushy cell somata (arrow) and stained with greater intensity than in normal mice at 9 days postnatal. Fluorescence image obtained at 20X magnification.
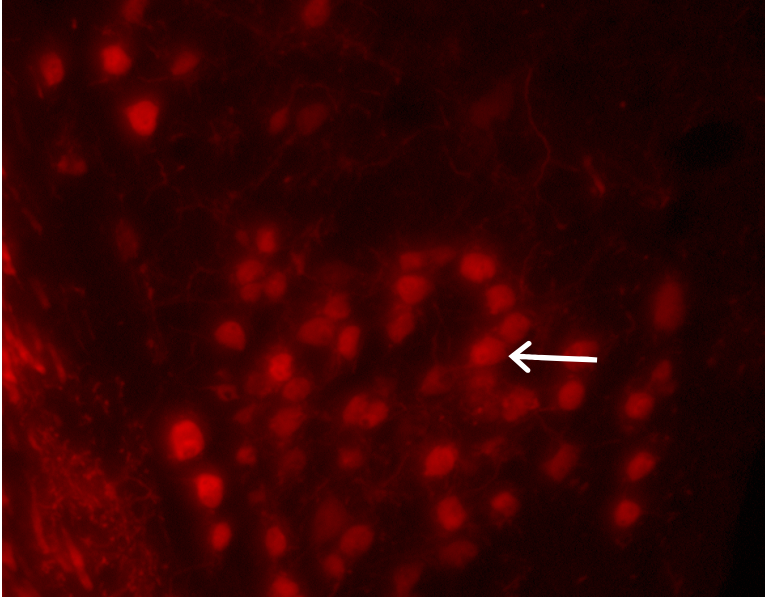
**Figure 27. Calbindin D-28k expression in normal mice at 20 days postnatal in the AVCN**
At 20 days postnatal in normal mice, CB was expressed in more bushy cell somata (arrow) and stained with greater intensity than in normal mice at 13 and 9 days postnatal. Fluorescence image obtained at 20X magnification.
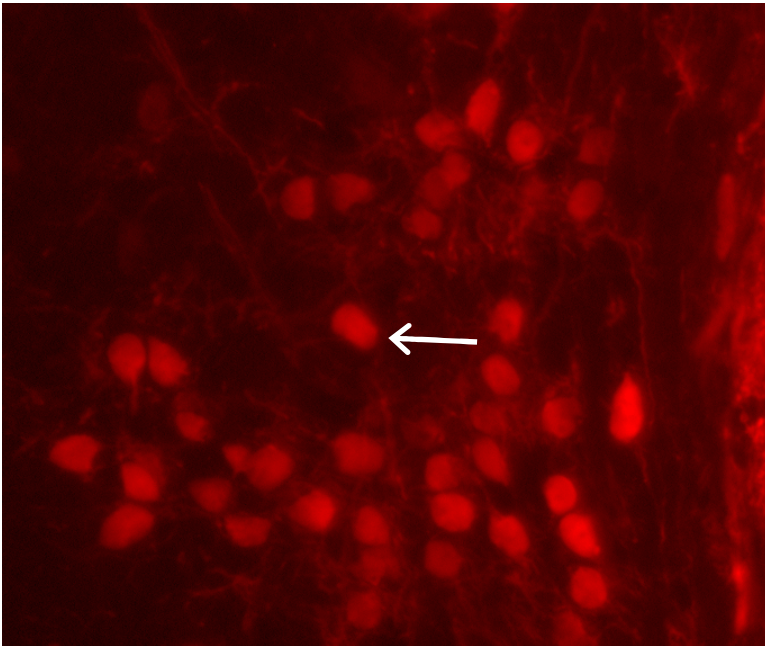


**Figure 28. Calbindin D-28k expression in normal mice at 30 days postnatal in the AVCN**
At 30 days postnatal in normal mice, CB was expressed in more bushy cell somata (arrow) and stained with greater intensity than in normal mice at 20, 13 and 9 days postnatal.  Fluorescence image obtained at 20X magnification.
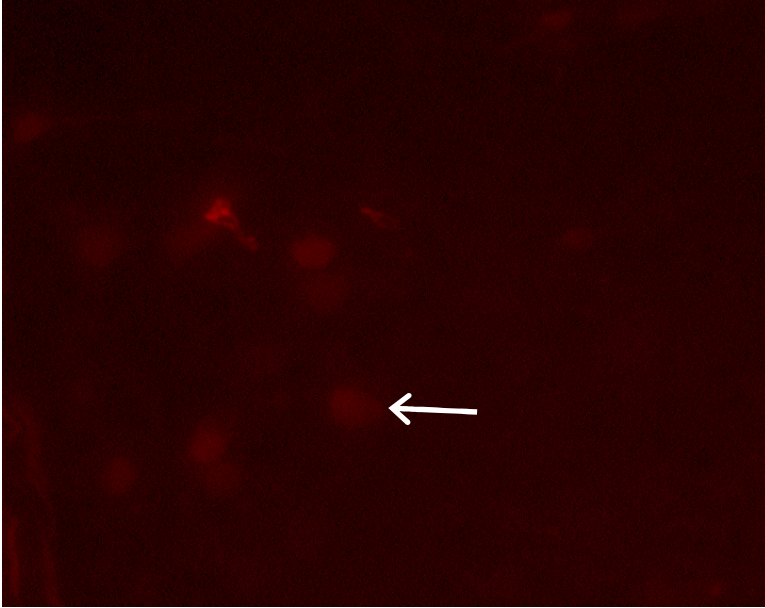
**Figure 29. Calbindin D-28k expression in *dn/dn* mice at 9 days postnatal in the AVCN**

At 9 days postnatal in *dn/dn* mice, CB appeared to be expressed weakly in only a few postsynaptic bushy cell somata (arrow), and resembled that in normal mice at 9 days postnatal. Fluorescence image obtained at 20X magnification.
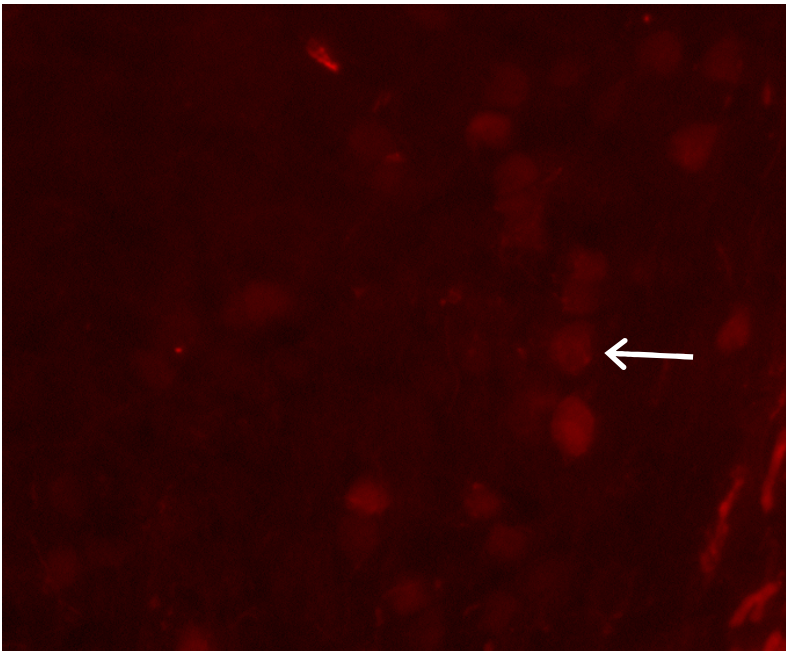


**Figure 30. Calbindin D-28k expression in *dn/dn* mice at 13 days postnatal in the AVCN**

At 13 days postnatal in *dn/dn* mice, CB again appeared to be expressed weakly in only a few postsynaptic bushy cell somata (arrow), and resembled that in both *dn/dn* and normal mice at 9 days postnatal. Fluorescence image obtained at 20X magnification.
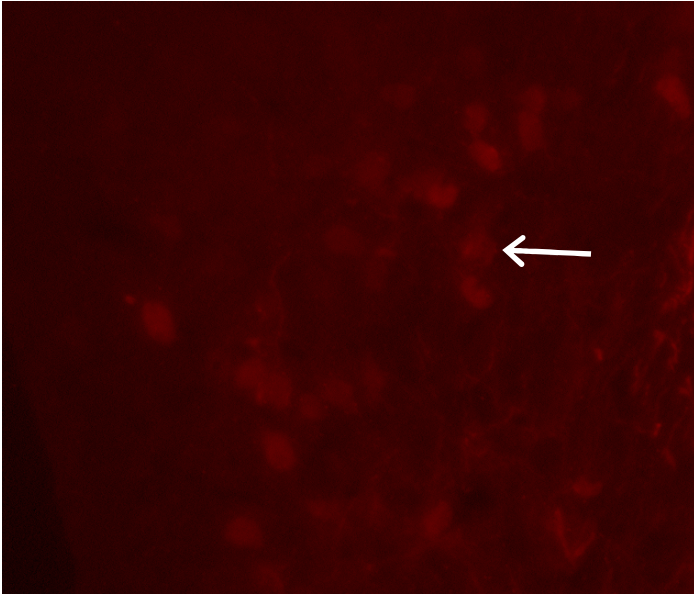
**Figure 31. Calbindin D-28k expression in *dn/dn* mice at 20 days postnatal in the AVCN**

At 20 days postnatal in *dn/dn* mice, CB again appeared to be expressed weakly in only a few postsynaptic bushy cell somata (arrow), and resembled that in *dn/dn* mice at 9 and 13 days postnatal and normal mice at 9 days postnatal. Fluorescence image obtained at 20X magnification.
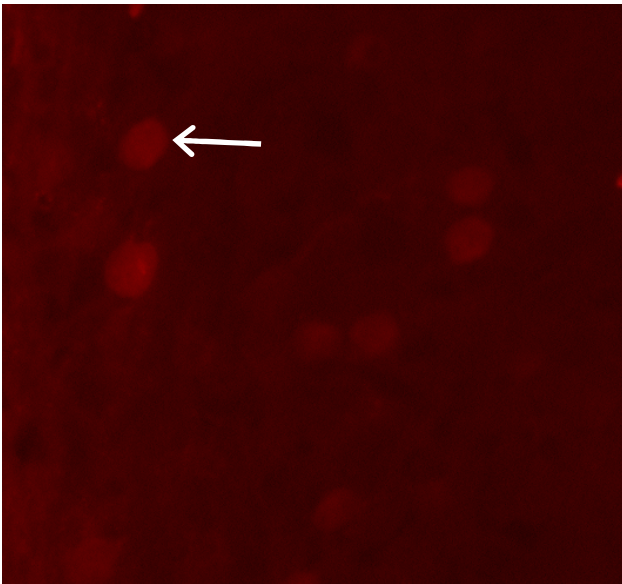


**Figure 32. Calbindin D-28k expression in *dn/dn* mice at 30 days postnatal in the AVCN**

At 30 days postnatal in *dn/dn* mice, CB again appeared to be expressed weakly in only a few postsynaptic bushy cell somata (arrow), and resembled that in *dn/dn* mice at 9, 13 and 20 days postnatal and normal mice at 9 days postnatal. Fluorescence image obtained at 20X magnification.

day and 49 day postnatal mice all exhibited similar CB expression, with CB being weakly expressed in very few bushy cell somata (Fig. 29-32; *dn/dn* 49 day not shown).

Thus, differences were observed in the developmental expression of CB in the AVCN of normal hearing and congenitally deaf mice. 9 day postnatal normal and *dn/dn* mice both expressed CB weakly in only a few bushy cell somata (Fig. 25, 29). In *dn/dn* mice, this pattern of CB expression did not change during development, so CB expression at all ages in the AVCN of *dn/dn* mice resembled that which was observed in 9 day postnatal normal hearing mice (Fig. 29-32). Normal hearing mice, however, exhibited a developmental change in CB expression, as progressively more bushy cell somata exhibited CB expression, and the intensity of CB staining increased (Fig. 25-28).

*Parvalbumin (PV)*

In the AVCN, PV was expressed in nerve fibers and both presynaptically, in endbulbs of Held, and postsynaptically, in the bushy cell somata (Fig. 33). PV appeared to be expressed in all endbulbs and all bushy cells in the AVCN. These results were confirmed by utilizing double-labeling experiments with PV (CY3) and green fluorescent Nissl stain or VGLUT1 (FITC). Sections stained with PV and Nissl showed co-localization, confirming the presence of PV in the postsynaptic bushy cell somata (not shown). Sections stained with PV and VGLUT1 also showed co-localization, confirming the presence of PV in the presynaptic endbulbs of Held (not shown).

Normal hearing mice at 9 days postnatal expressed PV presynaptically in nerve fibers and endbulb of Held terminals, and also postsynaptically in bushy cell somata

41
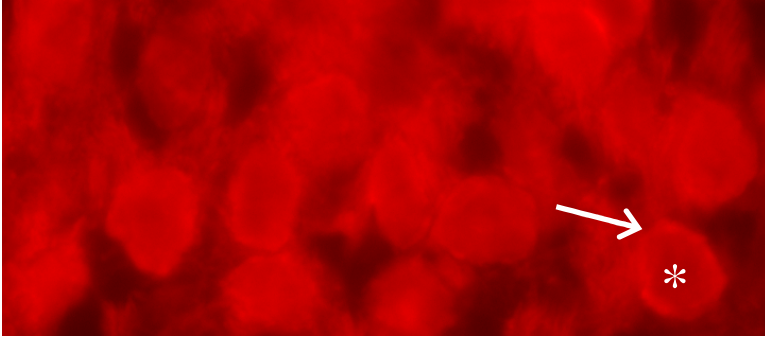
**Figure 33. Parvalbumin expression in the AVCN**
PV, seen in red, is localized in presynaptic endbulbs of Held (arrow) and in postsynaptic bushy cell somata (*).  Fluorescence image obtained at 40X magnification.

(not shown).  At this stage of development, the intensity of PV staining in the endbulbs of

Held was far greater than the staining intensity in the bushy cell somata.  Thus, at 9 days,

PV was expressed at a higher level presynaptically than postsynaptically in normal

hearing mice.  As development proceeded, the level of PV expression in the postsynaptic

bushy cells increased progressively (Fig. 34, 35).  In 30 day postnatal normal mice, the

strength of PV intensity was so strong postsynaptically that it was not possible to

distinguish PV staining in the bushy cells from that in the endbulbs of Held, mainly

because of the close opposition of the endbulbs with the bushy cell somata (Fig. 36).  As

a result, it was not clear what was happening with PV expression in the endbulbs of Held

during development.  One possibility was that PV expression in the endbulbs of Held

stayed the same throughout development.  Another possibility, however, was that PV

expression in the endbulbs was decreasing throughout development, and was being

masked by the PV expression increase in the bushy cells.  A final possibility was that PV

expression did increase in the endbulbs, but that this increase was being masked by the

large increase in PV expression in the bushy cell somata.

At 9 days postnatal in *dn/dn* mice, PV was also present in the presynaptic nerve

fibers and endbulb of Held terminals and postsynaptically in bushy cell somata (Fig. 37).

At this stage, PV staining was again stronger in the endbulbs of Held than in the bushy

cell somata.  As development proceeded in *dn/dn* mice, no change in PV expression was

observed (Fig. 38-40).  All ages of *dn/dn* mice showed the same pattern of PV expression

that was observed in the 9 day postnatal *dn/dn* mice, with PV staining stronger in the

presynaptic endbulbs of Held than in the postsynaptic bushy cell somata.
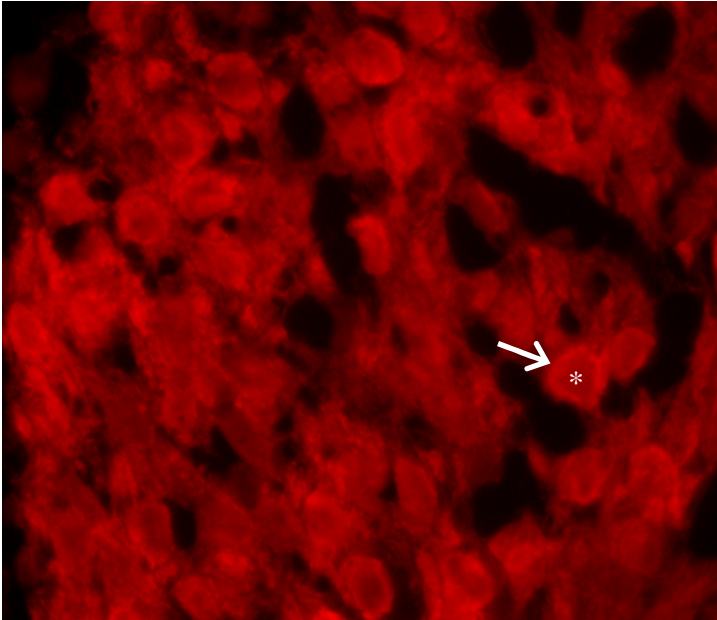
**Figure 34. Parvalbumin expression in normal mice at 13 days postnatal in the AVCN**

At 13 days postnatal in the AVCN, PV staining is slightly stronger in the postsynaptic bushy cell somata (*) than was seen at 9 days postnatal.  PV expression in the endbulbs of Held (arrows) appears to be about the same in 13 day as in 9 day postnatal normal mice.  Fluorescence image obtained at 20X magnification.
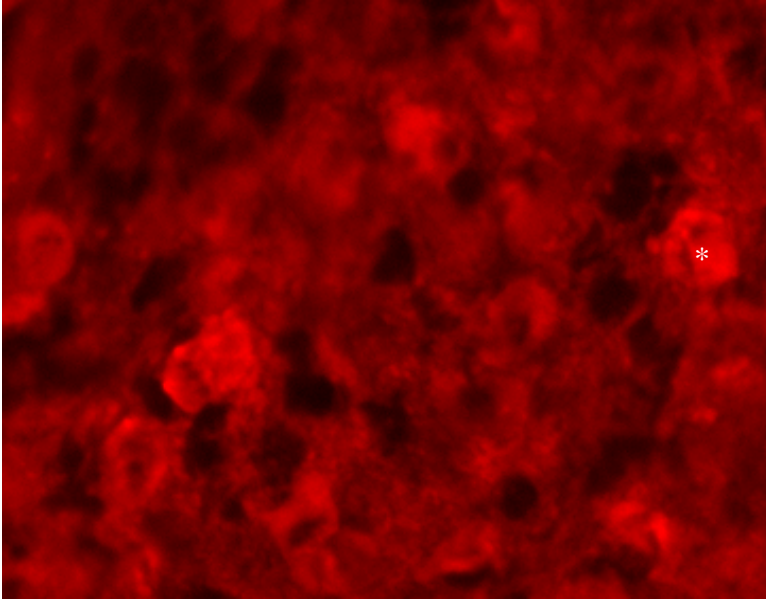
**Figure 35. Parvalbumin expression in normal mice at 20 days postnatal in the AVCN**

At 20 days postnatal in the AVCN, PV staining is slightly stronger in the postsynaptic bushy cell somata (*) than was seen at 13 days postnatal.  PV expression in the endbulbs of Held appears to be about the same in 20 day as in 13 day and 9 day postnatal normal mice.  Fluorescence image obtained at 20X magnification.
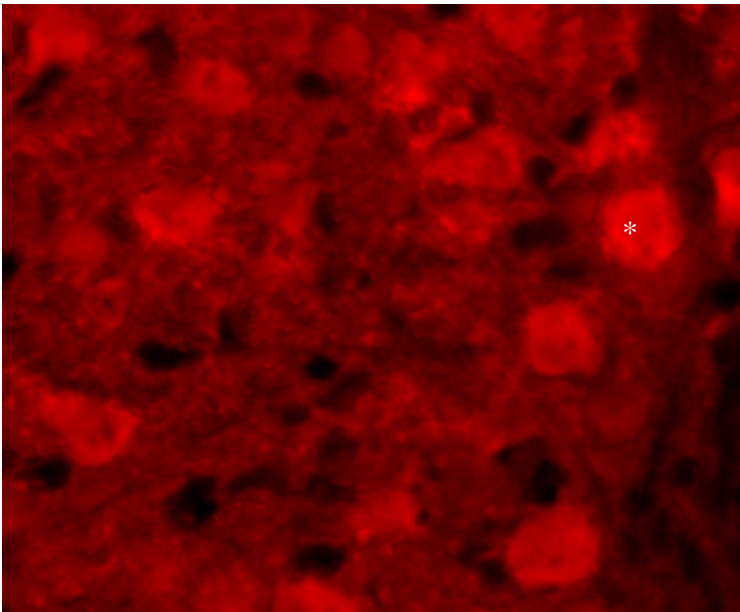


**Figure 36. Parvalbumin expression in normal mice at 30 days postnatal in the AVCN**

At 30 days postnatal in the AVCN, PV staining is stronger in the postsynaptic bushy cell somata (*) than was seen at 20 days postnatal.  PV expression in the endbulbs of Held appears to be about the same in 30 day as in 20, 13 and 9 day postnatal normal mice.  Fluorescence image obtained at 20X magnification.
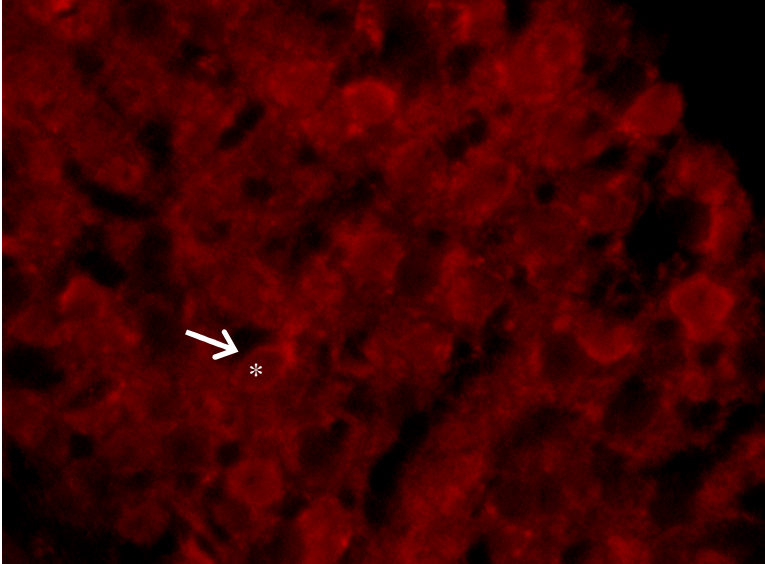
**Figure 37. Parvalbumin expression in *dn/dn* mice at 9 days postnatal in the AVCN**
At 9 days postnatal, PV expression in the AVCN of *dn/dn* mice is seen in presynaptic endbulbs of Held and in postsynaptic bushy cell somata. At 9 days in *dn/dn* mice, staining is stronger in the endbulbs (arrow) than in the bushy cell somata (*), and resembles that seen in 9 day postnatal normal mice. Fluorescence image obtained at 20X magnification.
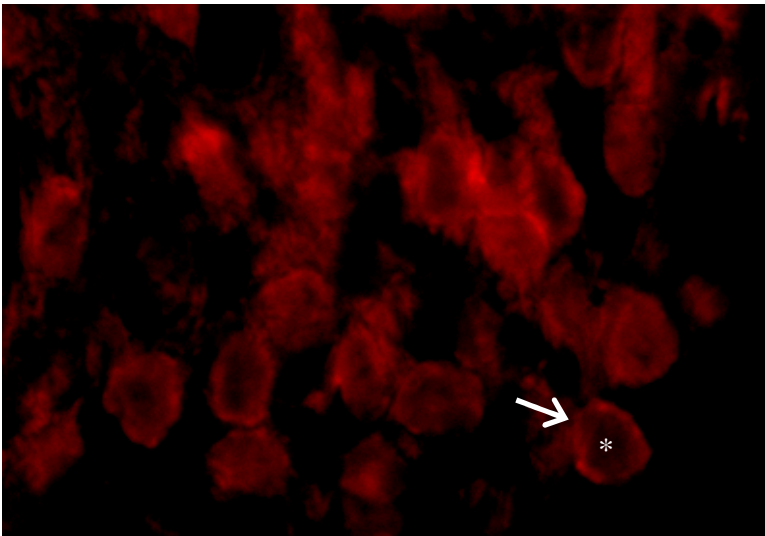


**Figure 38. Parvalbumin expression in *dn/dn* mice at 13 days postnatal in the AVCN**
At 13 days postnatal, PV expression in the AVCN of *dn/dn* mice is seen in presynaptic endbulbs of Held and in postsynaptic bushy cell somata. At 13 days in *dn/dn* mice, staining is stronger in the endbulbs (arrow) than in the bushy cell somata (*), and resembles that seen in 9 day postnatal *dn/dn* mice and 9 day postnatal normal mice. Fluorescence image obtained at 20X magnification.
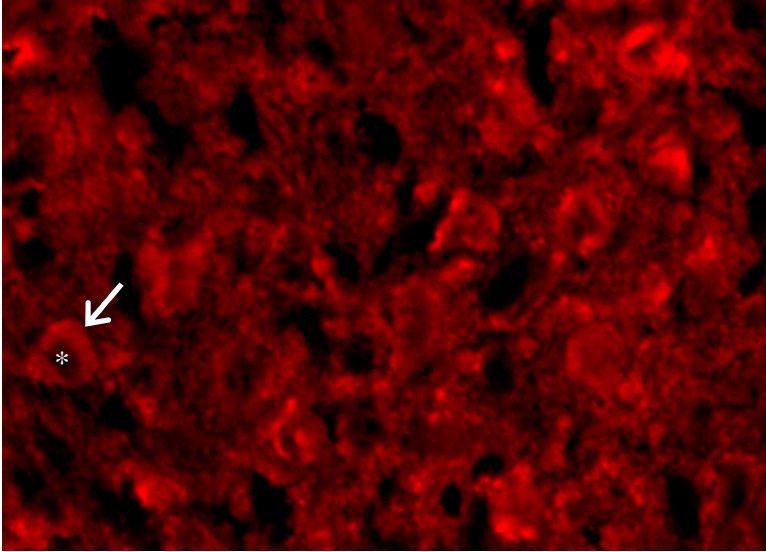
**Figure 39. Parvalbumin expression in *dn/dn* mice at 20 days postnatal in the AVCN**
At 20 days postnatal, PV expression in the AVCN of *dn/dn* mice is seen in presynaptic endbulbs of Held and in postsynaptic bushy cell somata. At 20 days in *dn/dn* mice, staining is stronger in the endbulbs (arrow) than in the bushy cell somata (*), and resembles that seen in 9 and 13 day postnatal *dn/dn* mice and 9 day postnatal normal mice. Fluorescence image obtained at 20X magnification.
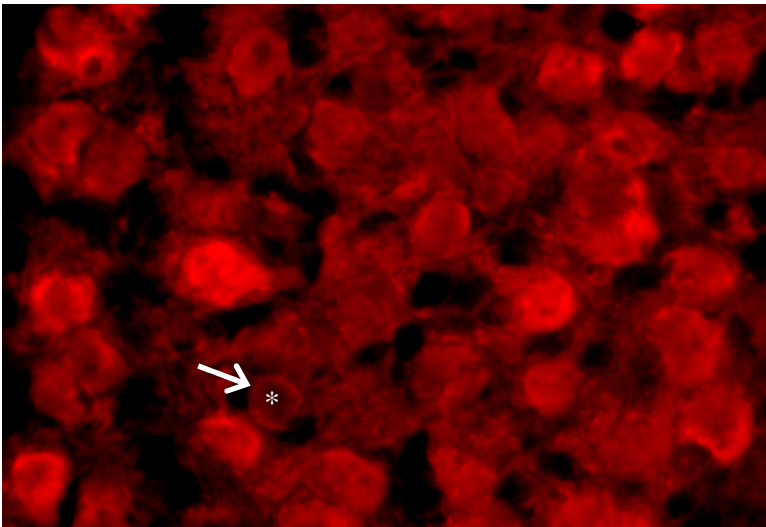


**Figure 40. Parvalbumin expression in *dn/dn* mice at 30 days postnatal in the AVCN**
At 30 days postnatal, PV expression in the AVCN of *dn/dn* mice is seen in presynaptic endbulbs of Held and in postsynaptic bushy cell somata. At 30 days in *dn/dn* mice, staining is stronger in the endbulbs (arrow) than in the bushy cell somata (*), and resembles that seen in 9, 13 and 20 day postnatal *dn/dn* mice and 9 day postnatal normal mice. Fluorescence image obtained at 20X magnification.

Thus, differences in the developmental expression of PV were observed in the AVCN of normal hearing and congenitally deaf mice.  In both normal and *dn/dn* mice, PV expression at 9 days postnatal was far greater in the presynaptic endbulbs of Held than in the postsynaptic bushy cell somata (Fig. 34, 37).  This pattern of PV expression in *dn/dn* mice did not change during development, so at all ages PV expression in the AVCN of *dn/dn* mice resembles that which was observed in 9 day postnatal normal hearing mice (Fig. 37-40).  In normal hearing mice, however, PV expression did change during development, as PV staining intensity in the postsynaptic bushy cell somata increased progressively as development proceeded (Fig. 34-36).  Again, it was not clear if PV expression in the presynaptic endbulbs of Held changed during development or, if it did, whether that change was an increase or decrease in PV expression.

MNTB

*Calretinin (CR)*

In the MNTB, Calretinin was observed in nerve fibers and presynaptic calyx of Held terminals, as well as in postsynaptic principal cell somata (Fig. 41).  CR was not expressed in all calyces of Held, and was also not expressed in all principal cell somata. In addition, a topographic pattern of CR expression was observed with respect to the medio-lateral organization of the MNTB (see below).  These results were confirmed
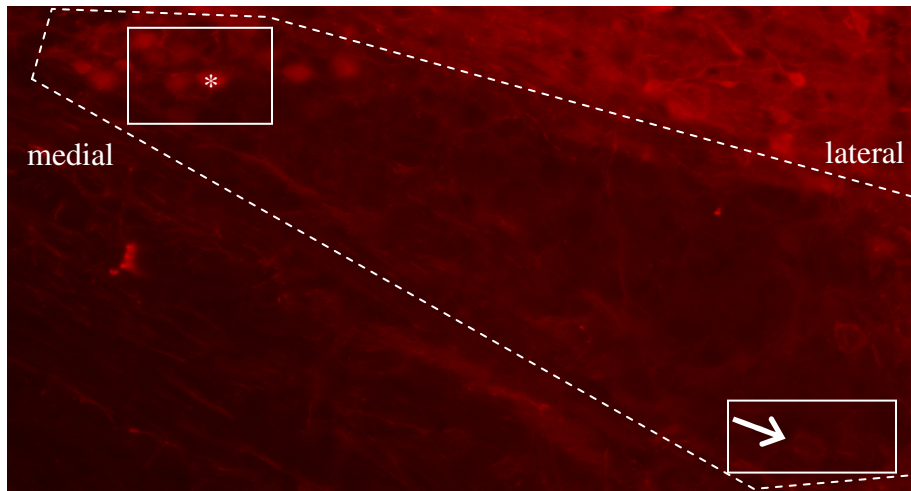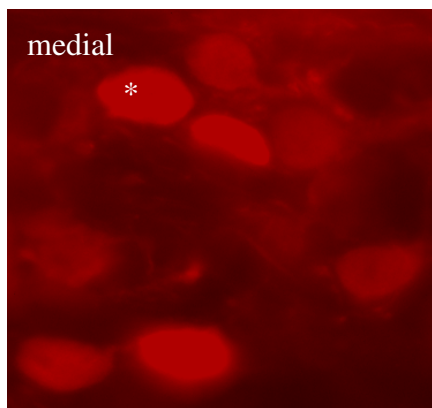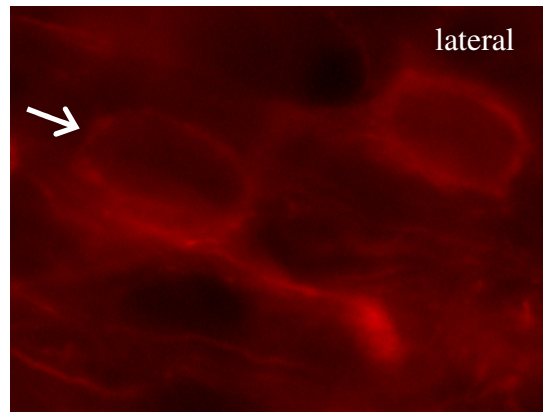
**Figure 41. Calretinin expression in the MNTB**
**A.** CR, seen in red, is localized in presynaptic calyces of Held (arrow) and postsynaptic principal cell somata (*) in the MNTB. Fluorescence image obtained at 20X magnification. Dashed line indicates area of MNTB. Note, in the lower left corner of the image, the fibers of the trapezoid body, which carry axons from the contralateral AVCN, and were used to positively identify the location of the MNTB. **B.** Image obtained at 40X showing principal cell somata (*) from the medial MNTB expressing CR. **C.** Image obtained at 40X showing calyces of Held (arrow) from the lateral MNTB expressing CR.

using double labeling experiments with CR (CY3) and green fluorescent Nissl stain or VGLUT1 (FITC). Sections stained with CR and Nissl showed some co-localization, confirming the presence of CR in some principal cell somata (Fig. 42). Sections stained with CR and VGLUT1 also showed some co-localization, indicating the presence of CR in some calyces of Held (Fig. 43).

Normal hearing mice at 9 days postnatal expressed CR mainly in principal cell somata preferentially located in the medial portion of the MNTB (Fig. 44). At this age, CR was expressed in very few calyces of Held. CR expression in normal mice began to change at 13 days postnatal. At this age, CR was still expressed mainly in principal cell somata medially, but CR also began to be expressed in a few calyces of Held preferentially located in the lateral MNTB (Fig. 45). At 20 and 30 days postnatal, CR was expressed in progressively fewer principal cell somata medially, and progressively more calyces of Held laterally (Fig. 46, 47). By the time normal mice reached 49 days postnatal, CR was expressed mainly in calyces of Held throughout the MNTB (even though most were still laterally located), with only an occasional medially-located principal cell soma expressing CR (not shown). Thus, a topographic gradient of CR expression was observed in the MNTB. This topographic gradient changed during development of the normal hearing mice. Early in development, CR was expressed mainly in principal cell somata in the medial MNTB. As development proceeded, CR was expressed in progressively fewer principal cell somata medially, and progressively more calyces of Held laterally. In mature normal hearing mice, CR was expressed in very few principal cell somata medially, and very many calyces of Held throughout the MNTB, with most still being located laterally.
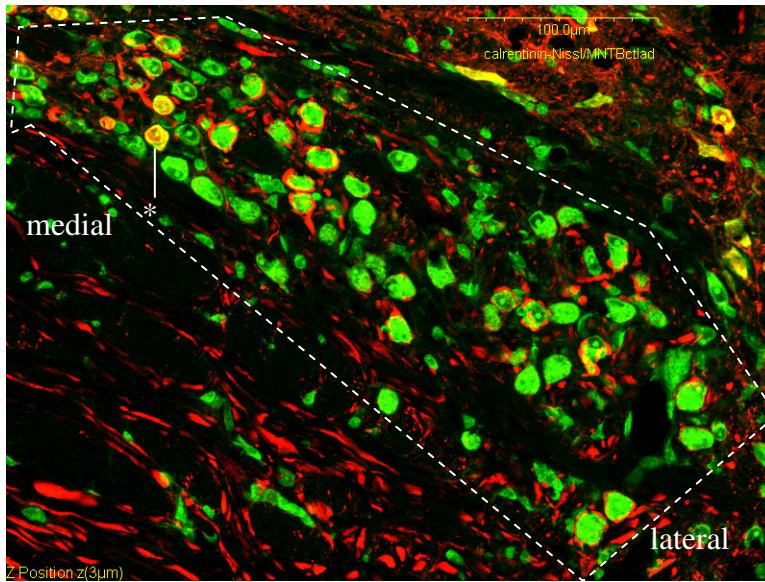
**Figure 42. Expression of Calretinin and green fluorescent Nissl in the MNTB**
This is a 20X dry objective confocal image showing CR (red) and green fluorescent Nissl (green) expression in the MNTB. Areas of co-localization appear yellow (*), and confirm the presence of CR in principal cell somata. Dashed line indicates area of MNTB.
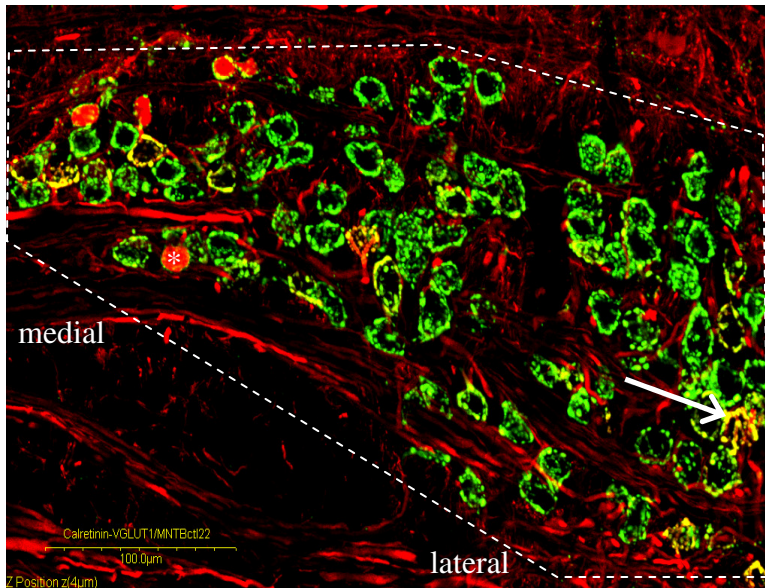


**Figure 43. Expression of Calretinin and VGLUT1 in the MNTB**
This is a 20X dry objective confocal image showing CR (red) and VGLUT1 (green) expression in the MNTB. Areas of co-localization appear yellow, and confirm the presence of CR in calyces of Held (arrow) and in principal cell somata (*). Dashed line indicates area of MNTB.
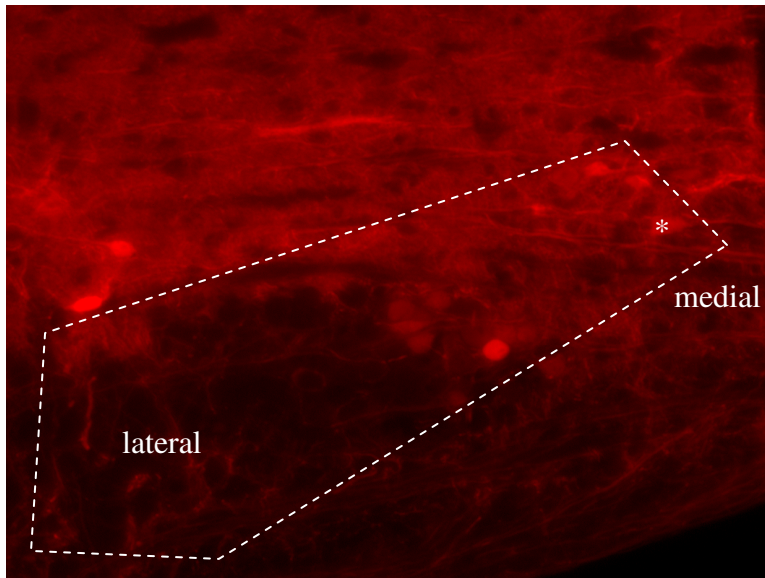
**A.**

**B.**
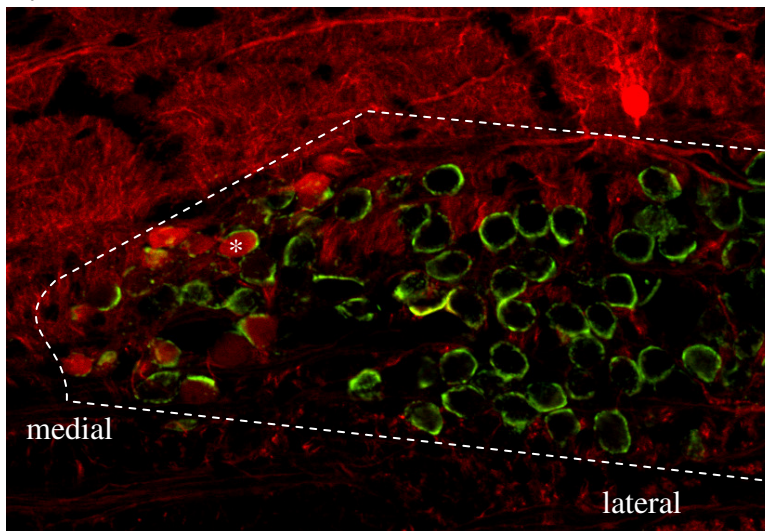
**Figure 44.  Calretinin expression in normal mice at 9 days postnatal in the MNTB**
**A.**  Fluorescence image (20X) of 9 day postnatal normal mouse MNTB, showing CR
expression mainly in principal cell somata (*) in the medial MNTB (to the right), and CR
expression in very few calyces of Held.  Dashed line indicates area of MNTB.  **B.**
Confocal image (20X dry objective) showing CR (red) and VGLUT1 (green) expression
in the MNTB of a normal mouse at 9 days postnatal.  CR is seen mainly in principal cell
somata (*) in the medial MNTB (to the left) and in very few calyces of Held.  Areas of
yellow indicate co-localization.  Dashed line indicates area of MNTB.
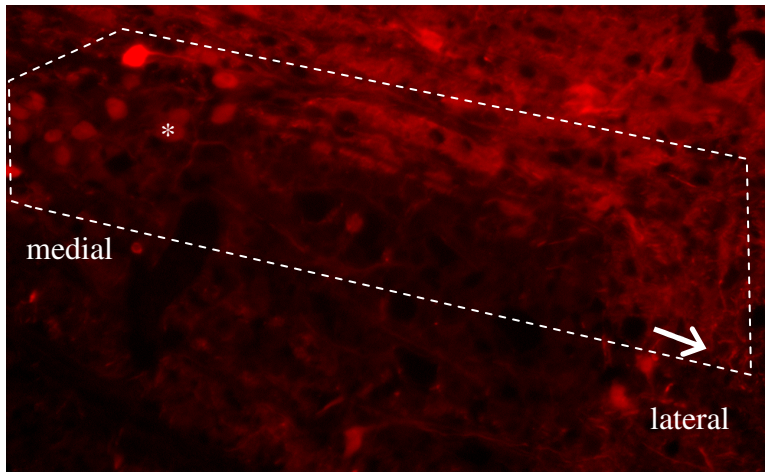
**Figure 45. Calretinin expression in normal mice at 13 days postnatal in the MNTB**
Fluorescence image (20X) showing the MNTB of a normal mouse at 13 days postnatal.
CR (red) is still expressed in a few principal cell somata (*) medially (as in normal mice
at 9 days postnatal), but has begun to be expressed in more calyces of Held (arrow)
laterally than in normal mice at 9 days postnatal. Dashed line indicates area of MNTB.
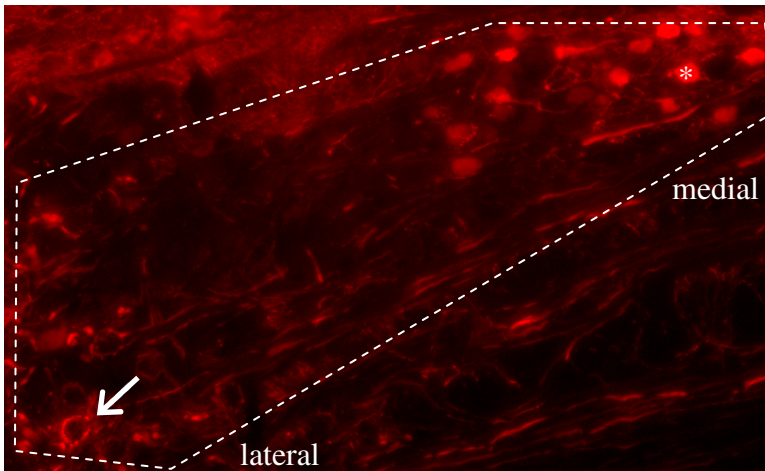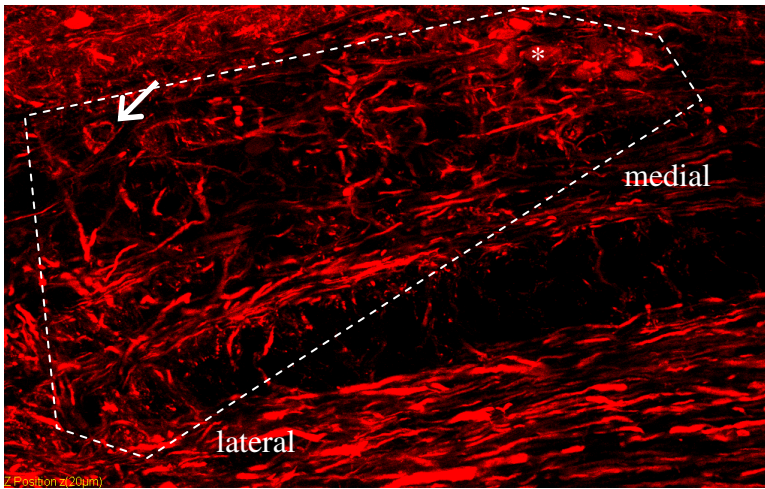
**Figure 46. Calretinin expression in normal mice at 20 days postnatal in the MNTB**
CR (red) is still expressed in a few principal cell somata medially (*) (as in normal mice
at 9 and 13 days postnatal), but is expressed in more calyces of Held (arrow) laterally
than in normal mice at 9 and 13 days postnatal.  Dashed line indicates area of MNTB.  **A.**
Fluorescence image (20X) **B.** Confocal image (20X dry objective).
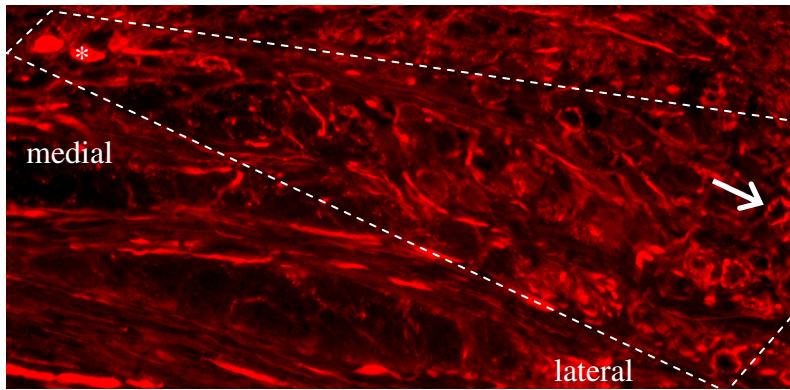
**A.**

**B.**
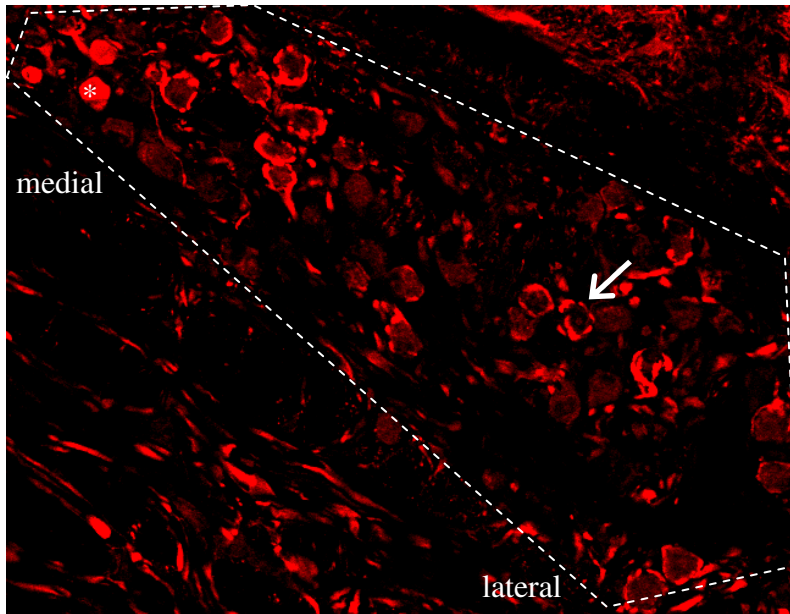
**Figure 47. Calretinin expression in normal mice at 30 days postnatal in the MNTB**
At 30 days postnatal in normal mice, CR (red) is expressed in fewer principal cell somata
(*) in the medial MNTB than at 20, 13 and 9 days postnatal in normal mice. CR is also
expressed in far more calyces of Held (arrow) (particularly in the lateral MNTB) at 30
days postnatal than at 20, 13 and 9 days postnatal in normal mice. Dashed line indicates
area of MNTB. **A.** Fluorescence image (20X). **B.** Confocal image (20X dry objective).

Congenitally deaf mice at 9 days postnatal also expressed CR mainly in principal cell somata preferentially located in the medial portion of the MNTB (Fig. 48). At 9 days CR was again expressed in very few calyces of Held, and if they did express CR, they were located laterally. During development, however, *dn/dn* mice did not exhibit a change in CR expression. All ages of *dn/dn* mice expressed CR in principal cell somata medially, along with an occasional calyx of Held in the lateral MNTB (Fig. 49-51). Thus, a topographic gradient of CR expression existed in *dn/dn* mice, but this topographic gradient did not change during development.

Thus, significant differences were observed in the developmental expression of CR in the MNTB of normal hearing and congenitally deaf mice. At 9 days postnatal, in both normal and *dn/dn* mice, CR was expressed mainly in medially-located principal cell somata, with very few calyces of Held expressing CR laterally (Fig. 44, 48). The pattern of CR expression in *dn/dn* mice did not change during development, so CR expression in all ages of *dn/dn* mice resembled that which was observed in 9 day postnatal normal hearing mice (Fig. 44, 48-51). In normal mice, on the other hand, the pattern of CR expression changed throughout development. CR was expressed in progressively more calyces of Held laterally, and progressively fewer principal cell somata medially, as development proceeded (Fig. 44-47). By 49 days postnatal, normal hearing mice mainly expressed CR in calyces of Held (throughout the MNTB, but most located laterally), with only an occasional medially-located principal cell soma expressing CR (not shown). The topographic pattern of CR expression in *dn/dn* mice remained the same throughout development, while the topographic pattern of CR expression in normal hearing mice changed during development.

56
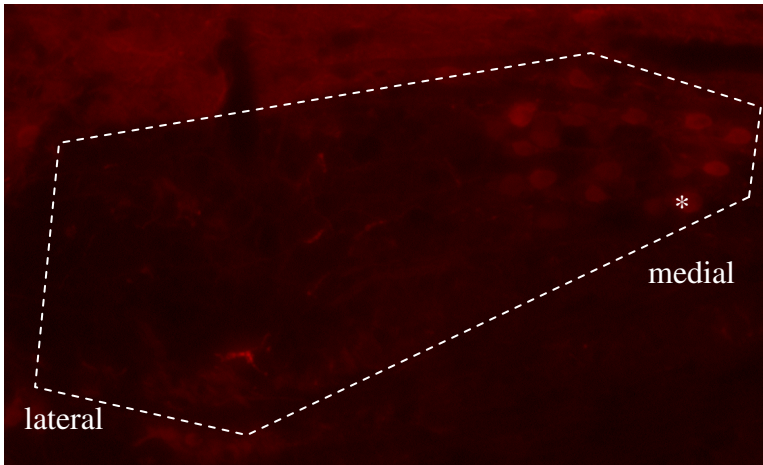
**A.**
**B.**
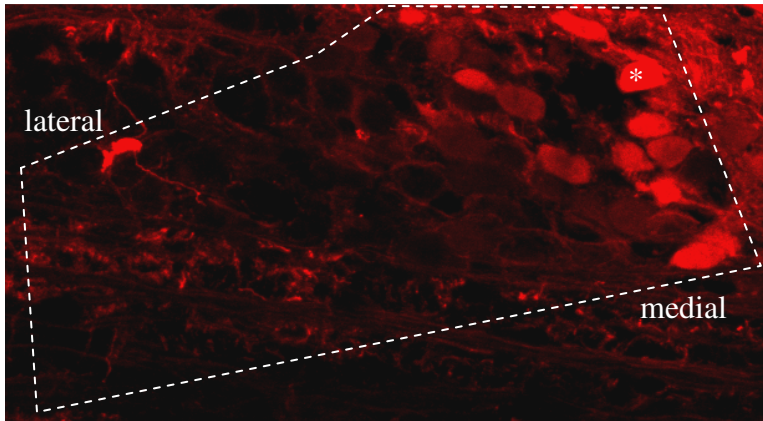


**Figure 48. Calretinin expression at 9 days postnatal in *dn/dn* mice in the MNTB**
At 9 days postnatal in *dn/dn* mice, CR (red) is expressed in principal cell somata (*) in the medial MNTB, and very few calyces of Held. This pattern in 9 day postnatal *dn/dn* mice is very similar to that in 9 day postnatal normal mice. Dashed line indicates area of MNTB. **A.** Fluorescence image (20X). **B.** Confocal image (20X) dry objective.
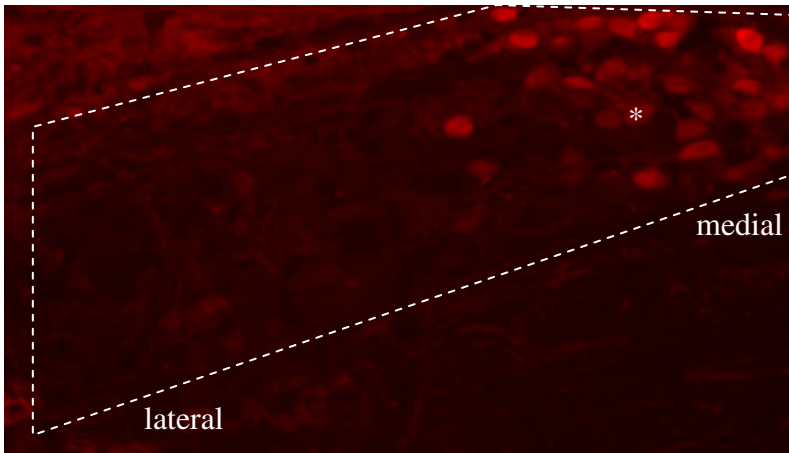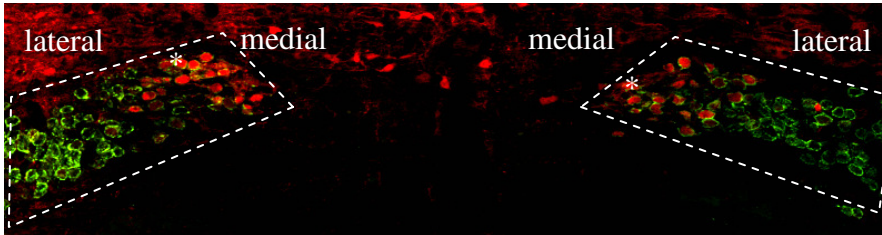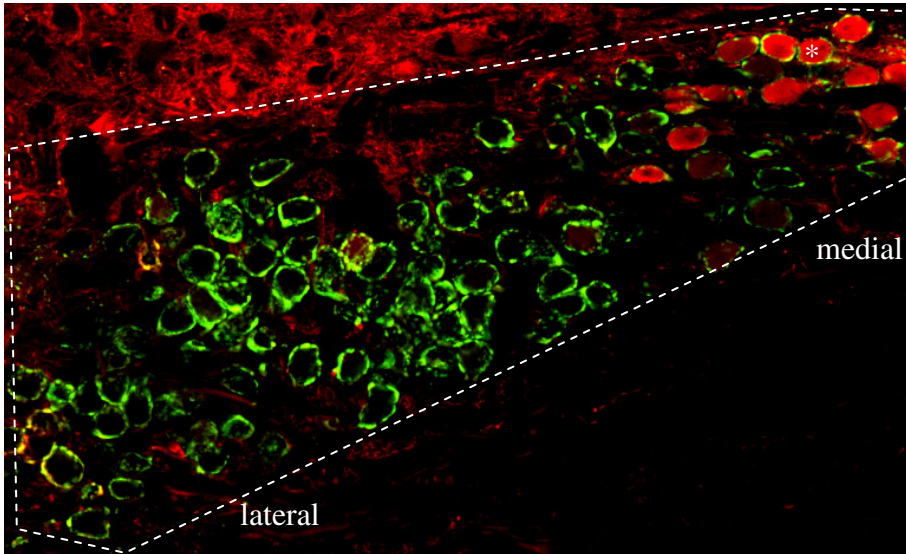
**Figure 49. Calretinin expression at 13 days postnatal in *dn/dn* mice in the MNTB**
At 13 days postnatal in *dn/dn* mice, CR (red) is still expressed mainly in principal cell somata (*) in the medial MNTB, and in very few calyces of Held, a pattern very similar to that in 9 day postnatal *dn/dn* and 9 day postnatal normal mice.  Dashed line indicates area of MNTB.  **A.** Fluorescence image (20X).  **B.** Confocal image, double labeled with VGLUT1 (green), showing both MNTBs (10X dry objective).  **C.** Confocal image, double labeled with VGLUT1 (20X dry objective).
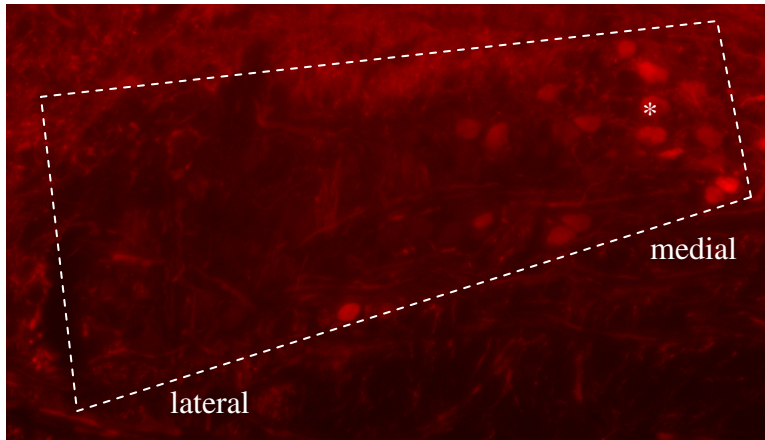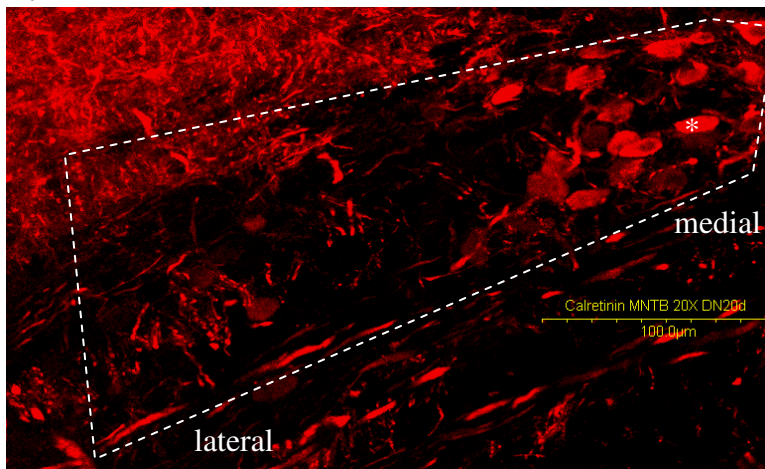
**Figure 50. Calretinin expression at 20 days postnatal in *dn/dn* mice in the MNTB**
At 20 days postnatal in *dn/dn* mice, CR is still expressed mainly in principal cell somata
(*) in the medial MNTB, and in very few calyces of Held.  This pattern of CR expression
is very similar to that in 9 and 13 day postnatal *dn/dn* mice and 9 day postnatal normal
mice.  Dashed line indicates area of MNTB.  **A.** Fluorescence image (20X).  **B.** Confocal
image (20X dry objective).
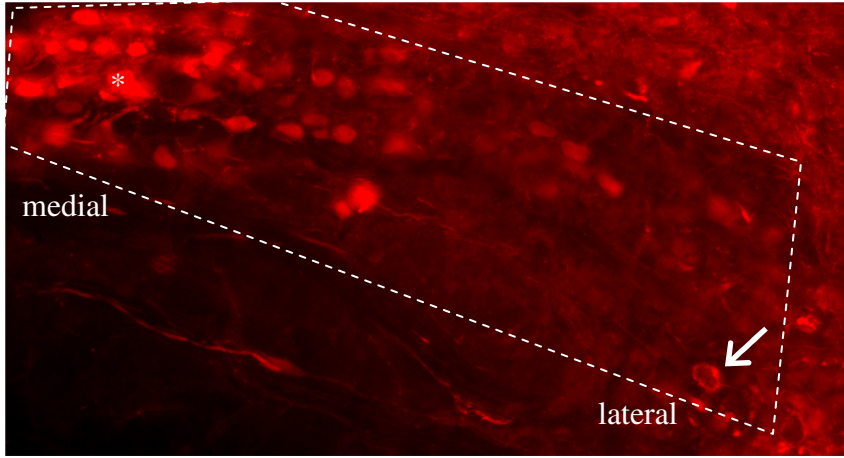
**A.**

**B.**
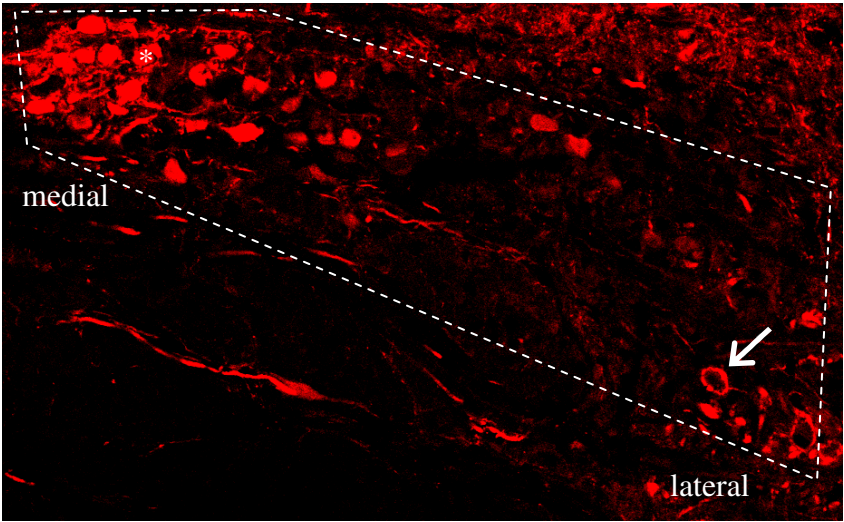


**Figure 51. Calretinin expression at 30 days postnatal in *dn/dn* mice in the MNTB**
At 30 days postnatal in *dn/dn* mice, CR is still expressed mainly in principal cell somata
(*) in the medial MNTB, and in very few calyces of Held (arrow).  This pattern of CR
expression is very similar to that in 9, 13 and 20 day postnatal *dn/dn* mice and 9 day
postnatal normal mice.  Dashed line indicates area of MNTB.  **A.** Fluorescence image
(20X).  **B.** Confocal image (20X dry objective).

*Calbindin D-28k (CB)*

In the MNTB, Calbindin was observed in some nerve fibers and the postsynaptic principal cell somata, but not in the presynaptic calyces of Held (Fig. 52). CB appeared to be present in the somata of all principal cells in the MNTB. These results were confirmed using double-labeling with CB (CY3) and green fluorescent Nissl stain or VGLUT1 (FITC), in order to identify areas of co-localization. Sections receiving CB and Nissl showed co-localization (Fig. 53), confirming the presence of CB in the principal cell somata. Sections receiving CB and VGLUT1 did not show co-localization (Fig. 54), confirming that CB was not present in the presynaptic calyces of Held.

Normal hearing mice at 9 days postnatal expressed CB in all of the postsynaptic principal cell somata. The intensity of CB staining in the principal cells appeared uniform throughout the medio-lateral extent of the MNTB (Fig. 55). During development, the pattern of CB expression in normal mice appeared to change. At 13 days postnatal, the intensity of CB staining in principal cell somata located in the lateral portion of the MNTB appeared to increase slightly (Fig. 56). This gradual increase in CB staining intensity in the lateral MNTB continued throughout development, as CB intensity in the lateral MNTB appeared stronger in the 20 and 30 day postnatal normal mice (Fig. 57, 58). By 49 days postnatal, there appeared to be a distinct medio-lateral gradient of CB expression in the MNTB of normal mice (not shown). The intensity of CB staining in the lateral principal cell somata appeared to be significantly stronger than that in the medial cells. Thus, a topographical gradient of CB expression appeared to occur during development in normal hearing mice.
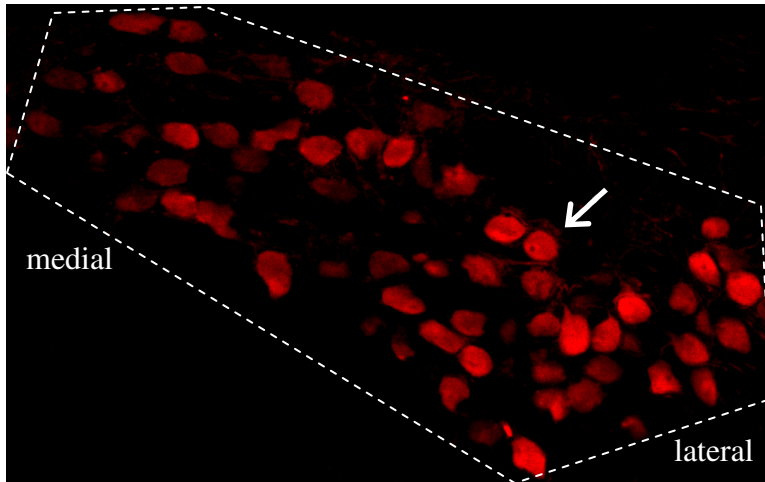
**Figure 52. Calbindin D-28k expression in the MNTB**
CB, seen in red, is localized in principal cell somata (arrow), not in calyces of Held.
Dashed line indicates area of MNTB.  Confocal image taken with 20X dry objective.
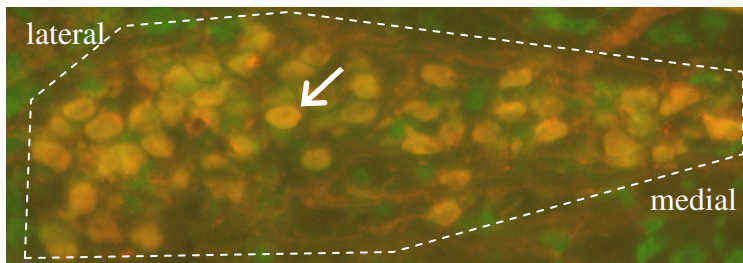


**Figure 53. Expression of Calbindin D-28k and green fluorescent Nissl in the MNTB**
CB (red) and green fluorescent Nissl (green) are both localized in principal cell somata,
but not in the calyces of Held.  Areas of co-localization (arrow) (yellow) confirm the
presence of CB in principal cell somata.  Dashed line indicates area of MNTB.
Fluorescence image taken at 20X.
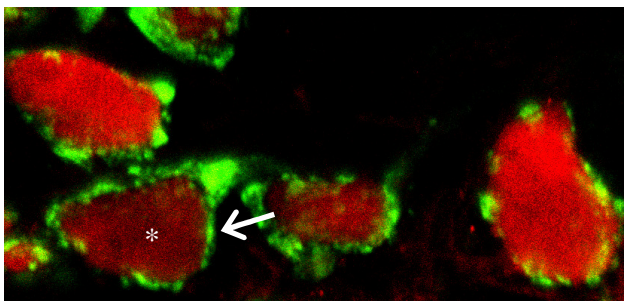


**Figure 54. Expression of Calbindin D-28k and VGLUT1 in the MNTB**
Confocal image, taken with the 60X dry objective, showing double labeling of CB (red)
and VGLUT1 (green) in the MNTB.  CB is observed only in the principal cell somata (*),
and VGLUT1 is observed only calyces of Held (arrow).  Little co-localization was
observed.
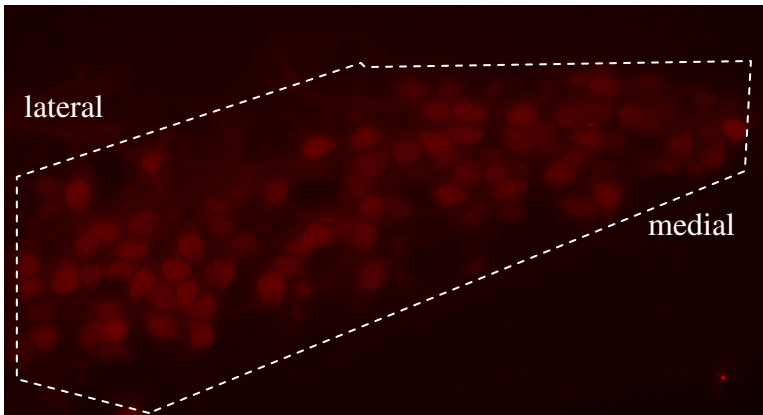
**Figure 55.  Calbindin D-28k expression at 9 days postnatal in normal mice in the MNTB**

At 9 days postnatal, CB expression in normal mice is observed in all postsynaptic principal cell somata in the MNTB.  Staining intensity appears to be about equal throughout the entire medio-lateral extent of the MNTB.  Dashed line indicates area of MNTB.  Fluorescence image at 20X magnification.
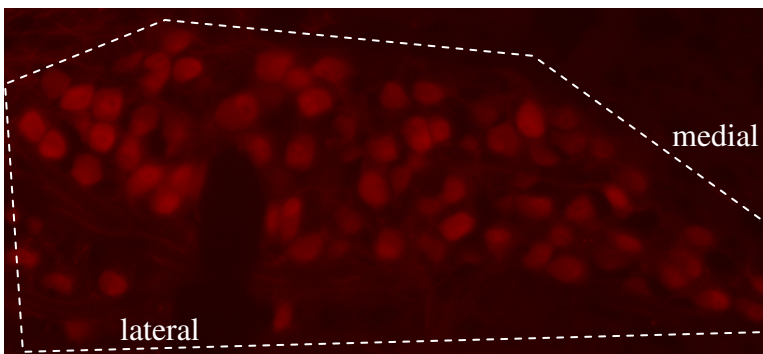


**Figure 56. Calbindin D-28k expression at 13 days postnatal in normal mice in the MNTB**

At 13 days postnatal, CB expression in normal mice is observed in all postsynaptic principal cell somata in the MNTB.  Staining intensity appears to be increasing in cells in the lateral MNTB, and remaining about equal in cells in the medial MNTB (in comparison to staining intensity in normal mice at 9 days postnatal).  Dashed line indicates area of MNTB.  Fluorescence image at 20X magnification.
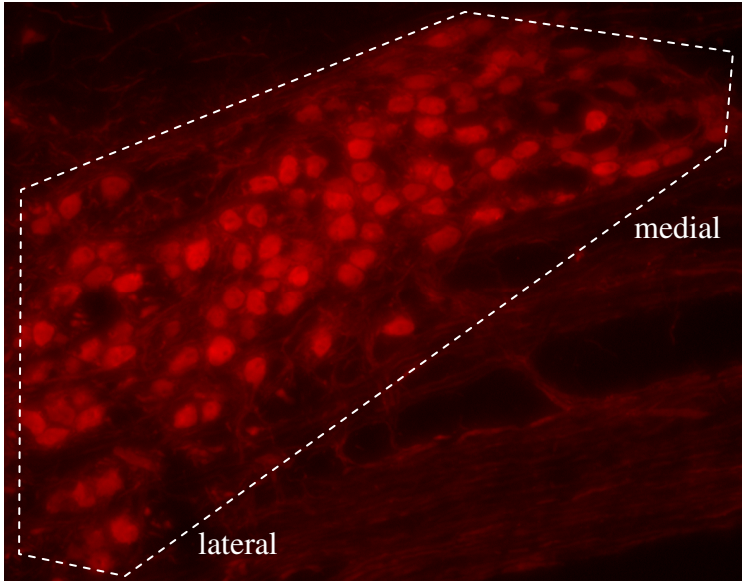
**Figure 57. Calbindin D-28k expression at 20 days postnatal in normal mice in the MNTB**

At 20 days postnatal, CB expression in normal mice is observed in all postsynaptic principal cell somata in the MNTB. Staining intensity appears to be increasing in cells in the lateral MNTB, and remaining about equal in cells in the medial MNTB (in comparison to staining intensity in normal mice at 13 days postnatal). Dashed line indicates area of MNTB. Fluorescence image at 20X magnification.
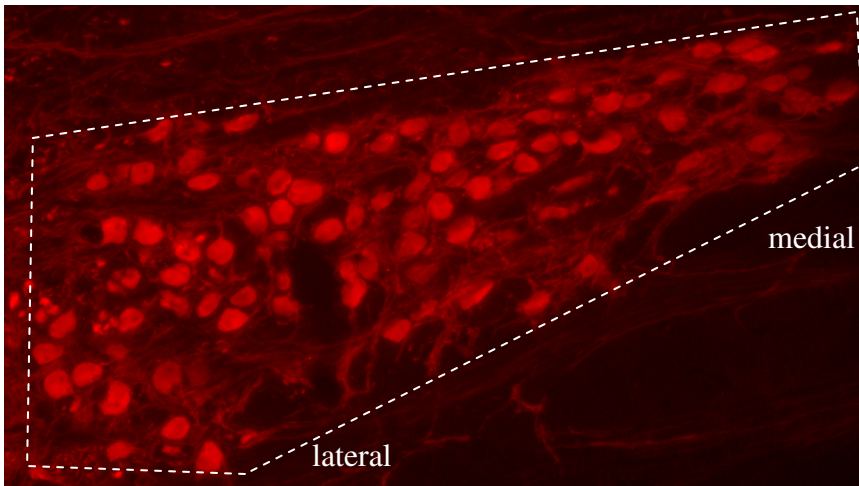


**Figure 58. Calbindin D-28k expression at 30 days postnatal in normal mice in the MNTB**

At 30 days postnatal, CB expression in normal mice is observed in all postsynaptic principal cell somata in the MNTB. Staining intensity at this stage is clearly greater in principal cells in the lateral MNTB than in cells in the medial MNTB. Dashed line indicates area of MNTB. Fluorescence image at 20X magnification.

64

Congenitally deaf mice at 9 days postnatal also expressed CB in all of the postsynaptic principal cell somata.  At this age, the intensity of CB staining in the principal cells appeared uniform throughout the medio-lateral extent of the MNTB (Fig. 59).  During development in *dn/dn* mice, however, no change appeared to occur in the pattern of CB expression.  Thus, in *dn/dn* mice at all observed ages (9, 13, 20, 30 and 49 days postnatal) CB staining intensity appeared uniform throughout the medio-lateral extent of the MNTB (Fig. 59-62; *dn/dn* 49 day not shown).  No topographical gradient of CB expression in the MNTB appeared to occur during development in congenitally deaf mice.

Thus, large differences appeared to occur in the developmental expression of CB in the MNTB of normal hearing and congenitally deaf mice.  In both normal and *dn/dn* mice at 9 days postnatal, CB expression in principal cell somata appeared uniform throughout the medio-lateral extent of the MNTB (Fig. 55, 59).  No change in the developmental expression of CB appeared to occur in *dn/dn* mice, as all subsequent ages appeared to resemble the pattern of expression in both normal and *dn/dn* mice at 9 days postnatal (Fig. 55, 59-62).  There was no apparent topographic gradient of CB expression in the MNTB during development in *dn/dn* mice.  Normal hearing mice, however, did appear to exhibit a developmental change in CB expression, as CB staining intensity appeared to increase in the lateral principal cell somata throughout development (Fig. 55-58).  In the mature normal hearing mice, a distinct topographic gradient of CB expression in the medio-lateral organization of the MNTB was observed (Fig. 57, 58).  Importantly, all observations of CB staining intensity were obtained only from analyzing fluorescence images.  Detailed optical density analysis, through a DAB staining
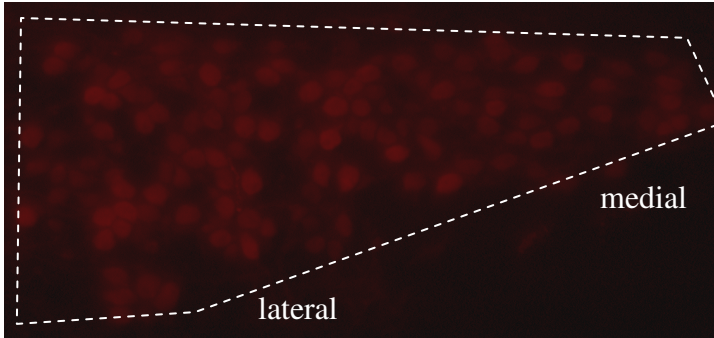
**Figure 59. Calbindin D-28k expression at 9 days postnatal in *dn/dn* mice in the MNTB**

At 9 days postnatal in *dn/dn* mice, CB staining intensity appears to be about equal throughout the medio-lateral extent of the MNTB. This pattern is similar to the one observed in 9 day postnatal normal mice. Dashed line indicates area of MNTB. Fluorescence image at 20X magnification.
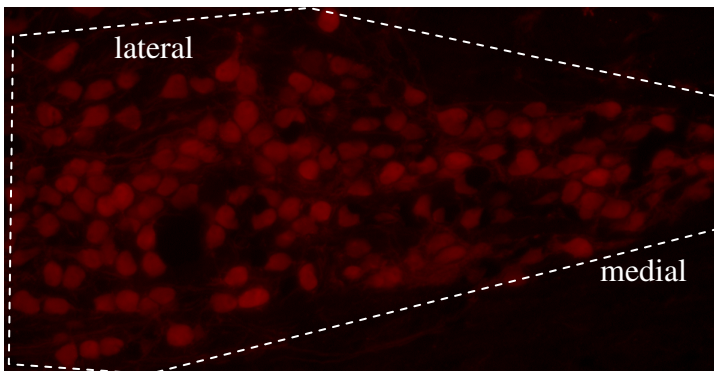


**Figure 60. Calbindin D-28k expression at 13 days postnatal in *dn/dn* mice in the MNTB**

At 13 days postnatal in *dn/dn* mice, CB staining intensity appears to be about equal throughout the medio-lateral extent of the MNTB. This pattern is similar to the one observed in 9 day postnatal *dn/dn* and 9 day postnatal normal mice. Dashed line indicates area of MNTB. Fluorescence image at 20X magnification.
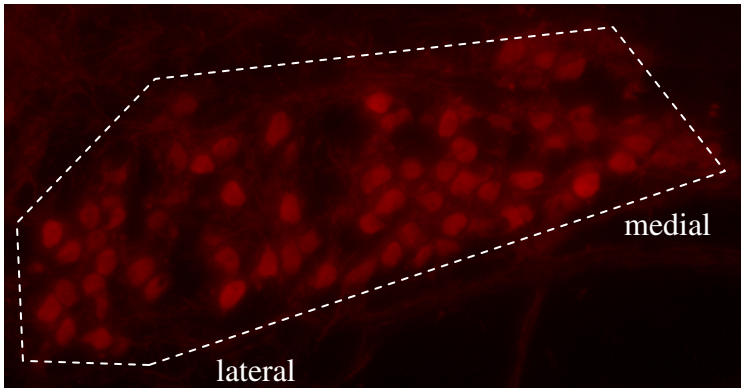
**Figure 61. Calbindin D-28k expression at 20 days postnatal in *dn/dn* mice in the MNTB**

At 20 days postnatal in *dn/dn* mice, CB staining intensity appears to be about equal throughout the medio-lateral extent of the MNTB.  This pattern is similar to the one observed in 9 and 13 day postnatal *dn/dn* and 9 day postnatal normal mice.  Dashed line indicates area of MNTB.  Fluorescence image at 20X magnification.
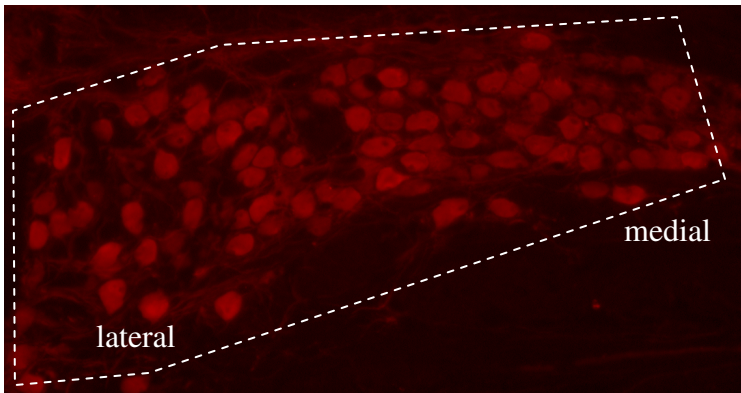


**Figure 62. Calbindin D-28k expression at 30 days postnatal in *dn/dn* mice in the MNTB**

At 30 days postnatal in *dn/dn* mice, CB staining intensity appears to be about equal throughout the medio-lateral extent of the MNTB.  This pattern is similar to the one observed in 9, 13, and 20 day postnatal *dn/dn* and 9 day postnatal normal mice.  Dashed line indicates area of MNTB.  Fluorescence image at 20X magnification.

experiment, is needed to quantify and verify these results.  Such an experiment is currently underway.

*Parvalbumin (PV)*

In the MNTB, Parvalbumin was expressed in nerve fibers and presynaptically in calyces of Held, as well as postsynaptically in principal cell somata (Fig. 63). PV appeared to be expressed in all calyces of Held, as well as all principal cell somata, in the MNTB.  These results were confirmed by again utilizing double-labeling experiments with PV (CY3) and green fluorescent Nissl stain or VGLUT1 (FITC).  Sections stained with PV and Nissl showed co-localization (not shown), confirming the presence of PV in the principal cell somata.  Sections stained with PV and VGLUT1 also showed co-localization (Fig. 64), confirming the presence of PV in the calyces of Held.

Normal hearing mice at 9 days postnatal expressed PV in nerve fibers and presynaptic calyces of Held, and postsynaptically in principal cell somata (Fig. 65).  At this age, the intensity of PV staining appeared to be far greater in the calyces of Held than in the principal cell somata.  As development proceeded in normal mice, the intensity of PV staining in the postsynaptic principal cell somata increased progressively (Fig. 66-68).  By 49 days postnatal, the intensity of PV staining in the principal cells had increased dramatically (not shown).  At this point, it was not possible to distinguish the postsynaptic principal cell somata from the calyces of Held, as both were in close opposition and expressing PV.  As a result, it was impossible to determine if there were developmental changes in PV expression in the presynaptic calyces of Held.  It is

**Figure 63. Parvalbumin expression in the MNTB**
In the MNTB, PV is expressed in both presynaptic calyces of Held and postsynaptic principal cell somata (*).  Fluorescence image taken at 20X magnification.
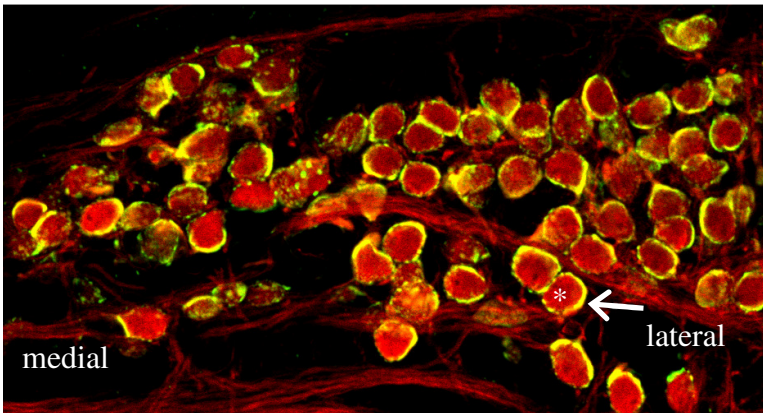


**Figure 64. Expression of Parvalbumin and VGLUT1 in the MNTB**
Confocal image (20X dry objective) showing dual labeling of PV (red) and VGLUT1 (green).  Areas of co-localization appear yellow, and indicate that PV is present in the presynaptic calyces of Held (arrow).  PV is also present in the principal cell somata (*).
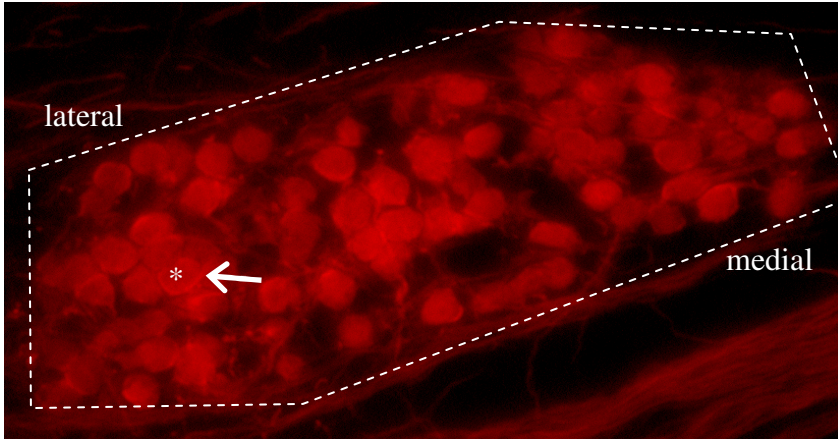
**Figure 65. Parvalbumin expression at 9 days postnatal in normal mice in the MNTB**

At 9 days postnatal in normal mice, PV staining intensity is stronger in the presynaptic calyces of Held (arrow) than in the postsynaptic principal cell somata (*). Dashed line indicates area of MNTB. Fluorescence image taken at 20X magnification.
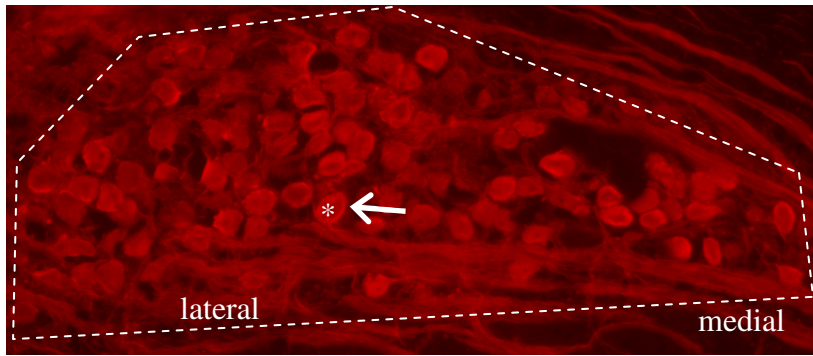
**A.**

**B.**
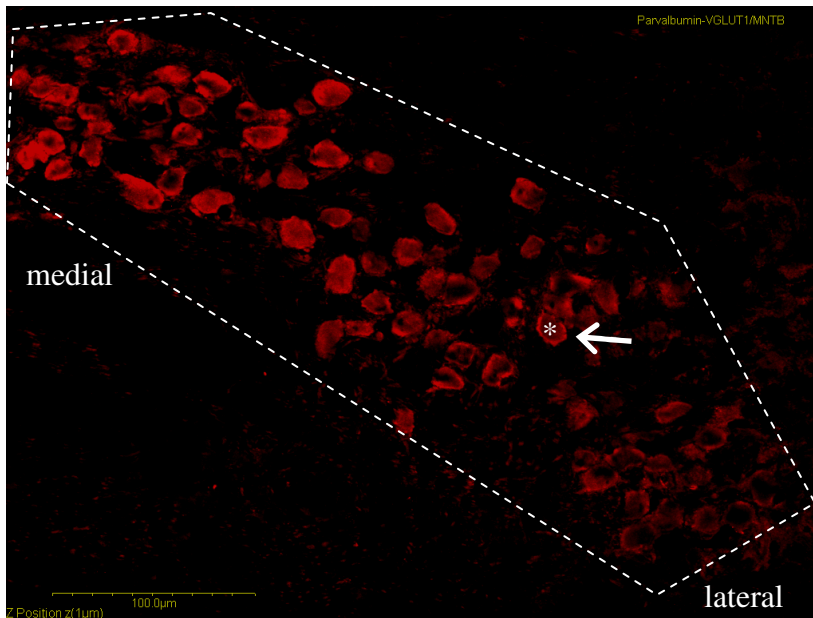


**Figure 66. Parvalbumin expression at 13 days postnatal in normal mice in the MNTB**

At 13 days postnatal in normal mice, PV staining intensity is still stronger in the calyces of Held (arrow), but PV staining intensity in the principal cell somata (*) is beginning to increase. Dashed line indicates area of MNTB. **A.** Fluorescence image taken at 20X magnification. **B.** Confocal image obtained with 20X dry objective.
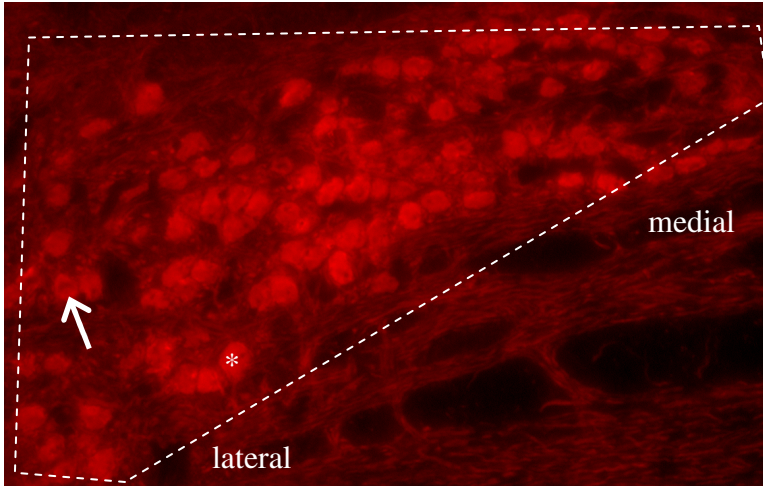
**Figure 67. Parvalbumin expression at 20 days postnatal in normal mice in the MNTB**

At 20 days postnatal in normal mice, PV staining intensity is still stronger in calyces of Held (arrow), but PV staining intensity continues increasing in the principal cell somata (*). Dashed line indicates area of MNTB. Fluorescence image at 20X magnification.
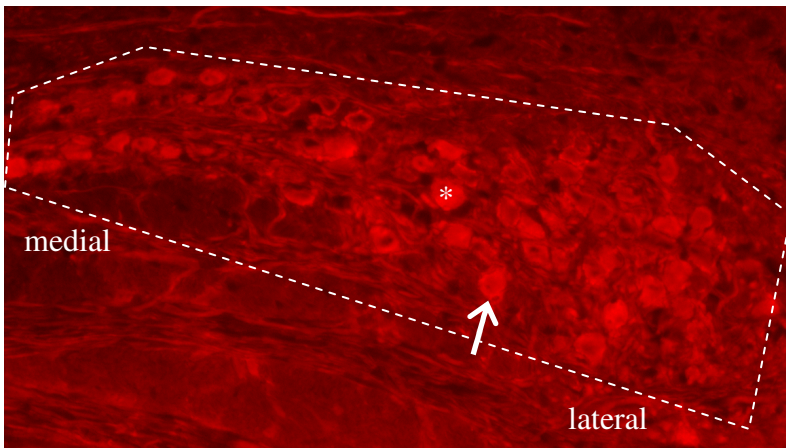


**Figure 68. Parvalbumin expression at 30 days postnatal in normal mice in the MNTB**

At 30 days postnatal in normal mice, PV staining intensity in most postsynaptic principal cell somata (*) has increased so that it is difficult to distinguish the postsynaptic element from the staining in the presynaptic calyces of Held (arrow). Dashed line indicates area of MNTB. Fluorescence image taken at 20X magnification

possible that the level of PV expression did not change in the calyces of Held. Alternatively, PV expression could have increased or decreased, but due to the close opposition of the pre- and postsynaptic elements which were both expressing PV, this could not be determined in these experiments. Thus, the large increase in PV staining intensity in the postsynaptic principal cell somata masked whatever changes (if any) may have occurred in PV expression in the presynaptic calyces of Held.

At 9 days postnatal in congenitally deaf mice, PV was expressed in nerve fibers and presynaptic calyces of Held, and postsynaptically in principal cell somata (Fig. 69). At this stage the intensity of PV staining in the calyces of Held was far greater than in the principal cell somata. As development proceeded in *dn/dn* mice, no changes in PV expression occurred in the MNTB (Fig. 70-71). Thus, *dn/dn* mice of all ages exhibited the same pattern of PV expression as was observed in 9 days postnatal *dn/dn* mice, with PV staining stronger in the presynaptic calyces of Held than in the postsynaptic principal cell somata.

Thus, significant differences were observed in the developmental expression of PV in the MNTB of normal hearing and congenitally deaf mice. At 9 days postnatal in both normal and *dn/dn* mice, PV staining was stronger in the presynaptic calyces of Held than in the postsynaptic principal cell somata (Fig. 65, 69). In *dn/dn* mice, no developmental changes in PV expression were observed, resulting in all ages of *dn/dn* mice resembling the 9 days postnatal normal hearing and congenitally deaf mice (Fig. 65, 69-71). Normal hearing mice, however, did exhibit developmental changes in PV expression in the MNTB. As development proceeded, the PV staining intensity in the postsynaptic principal cell somata increased progressively (Fig. 65-68). It was not clear
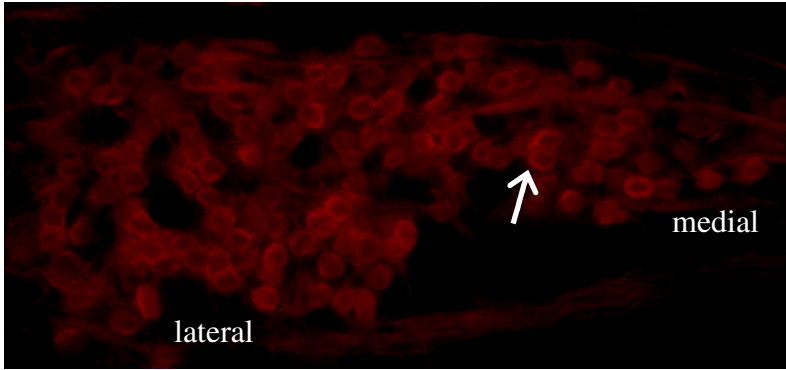
**Figure 69. Parvalbumin expression at 9 days postnatal in *dn/dn* mice in the MNTB**
At 9 days postnatal in *dn/dn* mice, PV staining intensity is much stronger in the calyces of Held (arrow) than in the principal cell somata.  This pattern closely resembles that observed in 9 day postnatal normal mice.  Fluorescence image taken at 20X magnification.
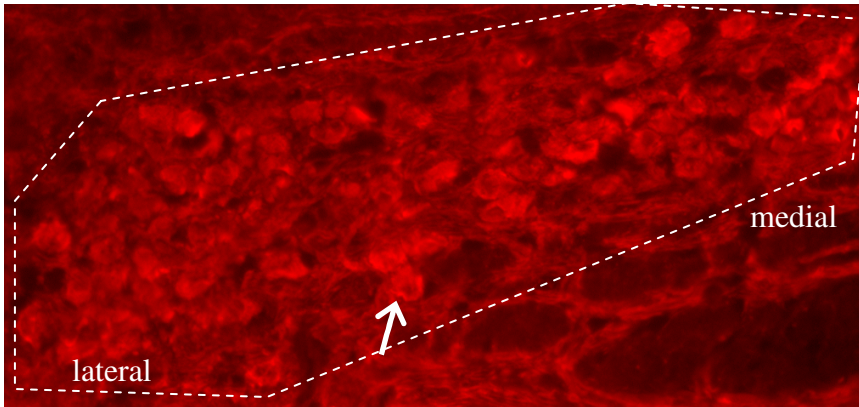
**Figure 70. Parvalbumin expression at 20 days postnatal in *dn/dn* mice in the MNTB**
At 20 days postnatal in *dn/dn* mice, PV staining intensity is still much stronger in the calyces of Held (arrow) than in the principal cell somata. This pattern closely resembles that observed in 9 and 13 day postnatal *dn/dn* and 9 day postnatal normal mice. Dashed line indicates area of MNTB. Fluorescence image taken at 20X magnification.



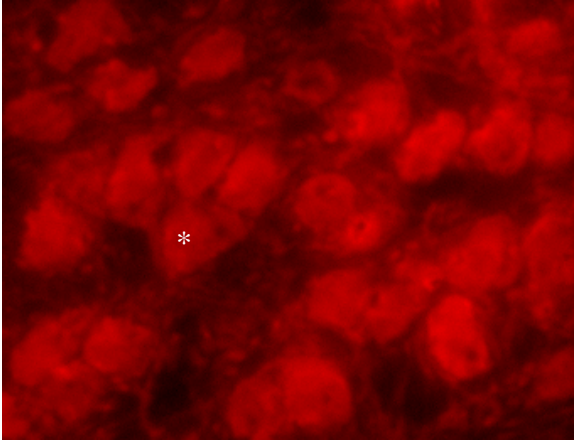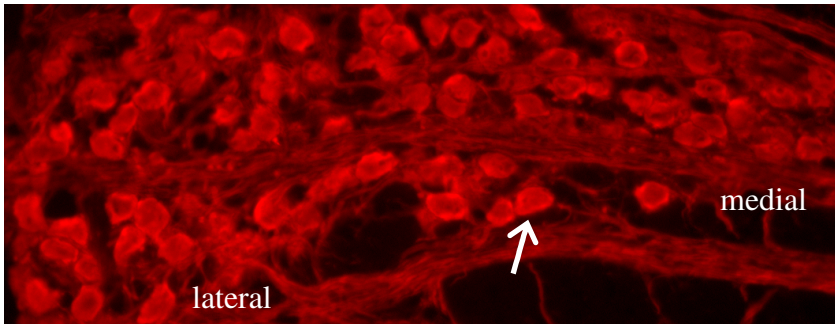**Figure 71. Parvalbumin expression at 30 days postnatal in *dn/dn* mice in the MNTB**
At 30 days postnatal in *dn/dn* mice, PV staining intensity is still much stronger in the calyces of Held (arrow) than in the principal cell somata. This pattern closely resembles that observed in 9, 13, and 20 day postnatal *dn/dn* and 9 day postnatal normal mice. Fluorescence image taken at 20X magnification.

if the level of PV expression in the presynaptic calyces of Held changed during development, because the increase in PV staining in the principal cell somata masked any changes that may have occurred in the calyces of Held due to their close opposition to one another.

# VI.  DISCUSSION

## Developmental Expression of Ca$^{2+}$-binding Proteins in Normal Hearing Mice

In normal hearing mice, patterns of Ca$^{2+}$-binding protein expression in the endbulb of Held synapse in the AVCN and in the calyx of Held synapse in the MNTB appeared to be developmentally regulated (Fig. 72, 73), which validated the first proposed hypothesis (see Introduction).  For each of the Ca$^{2+}$-binding proteins, a distinct pattern of expression was present at 9 days postnatal, before opening of the ear canal. The pattern of expression for each of these proteins was changed at 13 days postnatal, after opening of the ear canal, and then continued to change as the normal mice progressed through development thereafter.

In addition, the location and developmental pattern of expression for each individual protein (Calretinin, Calbindin D-28k, and Parvalbumin) varied with respect to one another in the AVCN and MNTB of normal mice.  CR (Fig. 10-15, 44-47) was expressed mainly in presynaptic terminals in the AVCN and MNTB, but also in a few postsynaptic somata in the MNTB of normal mice early in development.  CR appeared to be expressed in all presynaptic terminals in the AVCN, but was not expressed in all presynaptic terminals in the MNTB.  In addition, CR was expressed in a topographic pattern in the MNTB, and this topographic pattern changed during development.  CB (Fig. 25-28, 55-58) was expressed only in postsynaptic somata in the AVCN and

# Figure 72. Trends in the AVCN



**Relative Intensity of Calretinin Staining in Endbulb of Held terminals in the AVCN**

Normal          *dn/dn*

Greater

Less

Development →          Development →

**Relative Size of Endbulb Terminals in the AVCN (Visualized by Calretinin and/or VGLUT1 staining)**

Normal          *dn/dn*

Large

Small

Development →          Development →

**Relative Amount of Bushy Cell Somata Expressing Calbindin D-28k in the AVCN**

Normal          *dn/dn*

More

Less

Development →          Development →

**Relative Intensity of Calbindin D-28k Staining in Bushy Cell Somata in the AVCN**

Normal          *dn/dn*

Greater

Less

Development →          Development →

**Relative Intensity of Parvalbumin Staining in Bushy Cell Somata in the AVCN**

Normal          *dn/dn*

Greater

Less

Development →          Development →

# Figure 73. Trends in the MNTB

**Relative Expression of Calretinin in Principal Cell Somata in Medial MNTB**

Normal            *dn/dn*

More

Less

Development →        Development →

**Relative Expression of Calretinin in Calyces of Held in Lateral MNTB**

Normal            *dn/dn*

More

Less

Development →        Development →

**Relative Intensity of Calbindin D-28k Staining in Principal Cell Somata in Throughout Medio-Lateral MNTB**

Normal            *dn/dn*

Greater

Less

Development →        Development →

**Relative Intensity of Calbindin D-28k Staining in Principal Cell Somata in Lateral MNTB**

Normal            *dn/dn*

Greater

Less

Development →        Development →

**Relative Intensity of Parvalbumin Staining in Principal Cell Somata in Throughout Medio-Lateral MNTB**

Normal            *dn/dn*

Greater

Less

Development →        Development →

MNTB. CB was expressed in all postsynaptic somata in the MNTB, but was not expressed in all of the postsynaptic somata in the AVCN. There was also a topographic pattern of CB expression in the MNTB during development. PV (Fig. 34-36, 65-68) was expressed in both presynaptic terminals and postsynaptic somata in the AVCN and MNTB. It appeared that PV was present in all presynaptic terminals and all postsynaptic terminals in both the AVCN and MNTB. There was no apparent topographic pattern of PV expression in the MNTB during development.

The localization and developmental patterns of expression of CR, CB and PV in the MNTB (in normal mice) had been studied previously by Felmy and Schneggenburger (2004). They reported that CR was present in many, but not all, presynaptic calyces of Held, and that the number of CR-positive calyces and the intensity of their staining increased from 6 to 31 days postnatal. In addition, they reported that CR was expressed by calyces that were preferentially located in the lateral MNTB. The results of this experiment (Fig. 44-47) verified all of these findings for CR in the MNTB by Felmy and Schneggenburger. In addition, however, it was discovered that CR is expressed mainly in a few postsynaptic principal cells in the medial MNTB of 9 day postnatal normal mice. As development proceeded, CR began being expressed in more calyces of Held laterally, and less principal cell somata medially. Thus, a topographic pattern of CR expression in the MNTB was observed, and this topographic pattern changed during development. Felmy and Schneggenburger also reported that CB was expressed in all postsynaptic principal cell somata, but not in presynaptic calyces of Held. The results of this experiment (Fig. 55-58) verified their finding, but in addition, a topographic pattern of CB expression was observed. As development proceeded, CB staining intensity in

principal cells in the lateral MNTB appeared to increase, while the staining intensity in the medial MNTB appeared to remain the same. Felmy and Schneggenburger reported that PV was expressed in both presynaptic calyces of Held and postsynaptic principal cell somata, and that PV staining intensity in both calyces and principal cells increased during development. This series of experiments (Fig. 65-68) verified that PV is present both pre- and postsynaptically in the MNTB of normal mice. In addition, PV expression during development appeared to increase in the postsynaptic principal cells, which agreed with their results. This experiment, however, could not determine what changes, if any, had taken place in PV expression in the presynaptic calyces of Held. Any changes that took place for PV expression in the calyces of Held were masked due to the increase in PV expression in postsynaptic principal cells and the close opposition of pre- and postsynaptic elements. Thus, many of the results from Felmy and Schneggenburger (2004) were validated, but this experiment added some potentially important details to the patterns of developmental expression and localization of CR, CB and PV in the MNTB of normal hearing mice (Fig. 73).

**Developmental Expression of $Ca^{2+}$-binding Proteins in Congenitally Deaf Mice**

In congenitally deaf mice, developmental regulation of $Ca^{2+}$-binding protein expression in the AVCN and MNTB was altered, as specific patterns and changes seen during development in normal mice were not observed in *dn/dn* mice (Fig. 72, 73). These results supported the second proposed hypothesis (see Introduction). For each of the $Ca^{2+}$-binding proteins, a distinct pattern of expression was present at 9 days postnatal,

before opening of the ear canal. The pattern of expression for each of these proteins was unchanged, however, at 13 days postnatal, after opening of the ear canal, and then appeared to remain the same as the *dn/dn* mice progressed through development thereafter.

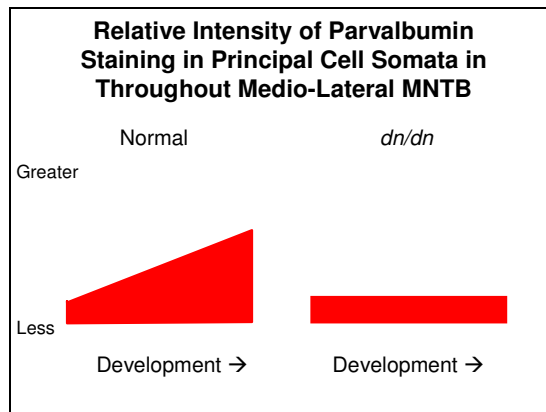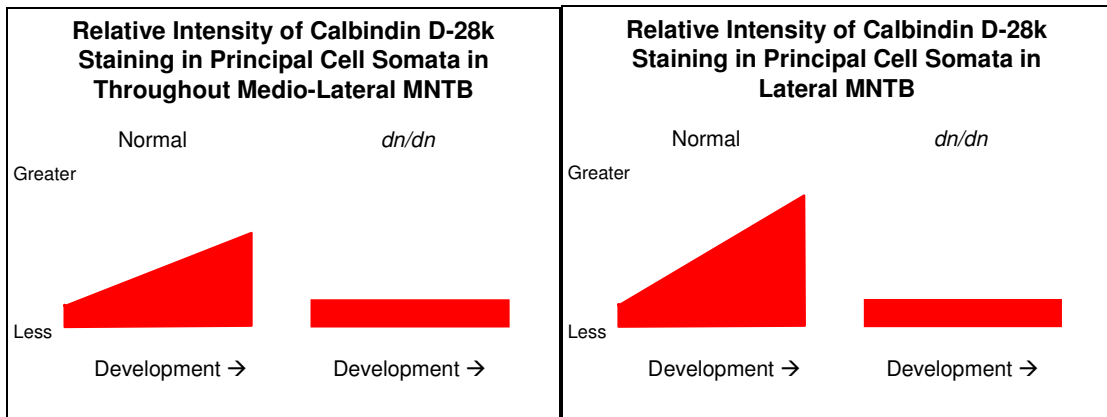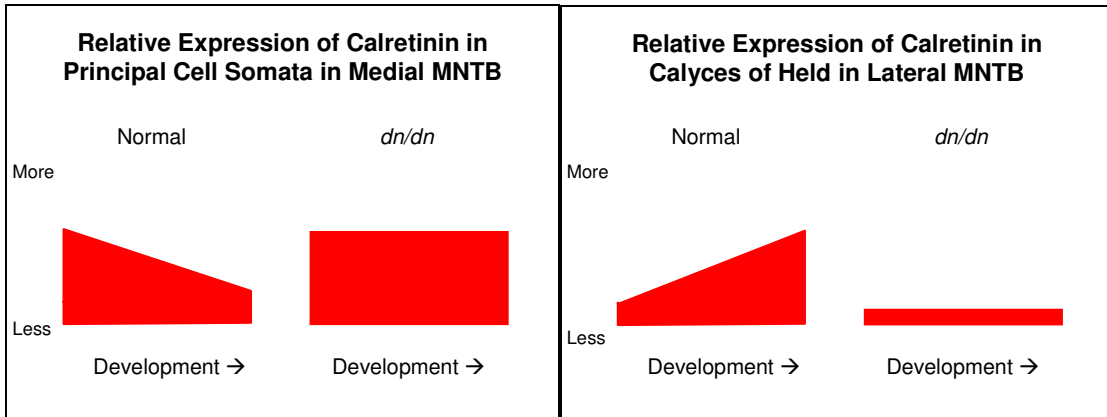The location and developmental pattern of expression of each individual protein (Calretinin, Calbindin D-28k, and Parvalbumin) did, however, vary with respect to one another in the AVCN and MNTB in *dn/dn* mice. CR in *dn/dn* mice (Fig. 16-21, 48-51) was expressed in presynaptic endbulbs of Held in the AVCN, and in postsynaptic principal cell somata in the MNTB. CR appeared to be expressed in all presynaptic endbulb terminals in AVCN, but in only a few postsynaptic somata in the medial portion of the MNTB (a topographic gradient). CB (Fig. 29-32, 59-62) was expressed only in postsynaptic somata in both the AVCN and MNTB of *dn/dn* mice. CB appeared to be present in all postsynaptic principal cell somata in the MNTB, but no topographic gradient was observed at any stage of development. CB was expressed only in postsynaptic bushy cell somata in the AVCN, but was present in only a few of the bushy cells. PV (Fig. 37-40, 69-71) was expressed simultaneously in both presynaptic terminals and postsynaptic somata in the AVCN and MNTB, with the presynaptic elements staining more intensely throughout the development of *dn/dn* mice. It appeared that PV was present in all presynaptic terminals and all postsynaptic terminals in both the AVCN and MNTB. There was no apparent topographic pattern of PV expression in the MNTB during development of *dn/dn* mice.

**Developmental Expression of Ca²⁺-binding Proteins in Normal vs. *dn/dn* Mice**

The results of this experiment revealed differences between normal hearing and congenitally deaf mice in the developmental expression of $Ca^{2+}$-binding proteins in the AVCN and MNTB (Fig. 72, 73). In both the AVCN and MNTB, normal and *dn/dn* mice at 9 days postnatal showed the same pattern of expression for each individual $Ca^{2+}$-binding protein. For example, CR was expressed mainly in postsynaptic principal cell somata in the medial MNTB at 9 days postnatal in normal and *dn/dn* mice (Fig. 44, 48), and CB was expressed in only a few postsynaptic bushy cell somata in the AVCN in both normal and *dn/dn* mice at 9 days (Fig. 25, 29). After opening of the ear canal, however, the pattern of $Ca^{2+}$-binding protein expression in normal mice began to change, while the pattern of $Ca^{2+}$-binding protein expression in *dn/dn* mice remained the same. These patterns continued throughout the course of development, so that normal mice at 49 days postnatal showed much difference in the pattern of $Ca^{2+}$-binding protein expression as compared to normal mice at 9 days, and the pattern of $Ca^{2+}$-binding protein expression in *dn/dn* mice at 49 days postnatal closely resembled that in both normal and *dn/dn* mice at 9 days.

The patterns of expression for each individual $Ca^{2+}$-binding protein began the same in normal hearing and congenitally deaf mice at 9 days postnatal, which was prior to opening of the ear canal and the onset of hearing. The patterns began to change in normal mice at 13 days postnatal, which was just after opening of the ear canal, and continued to change throughout the rest of development. The patterns of $Ca^{2+}$-binding protein expression in *dn/dn* mice, however, remained the same even after opening of the

ear canal. It is tempting, therefore, to suggest that the differences in $Ca^{2+}$-binding protein expression during the development of normal hearing and congenitally deaf mice were a result of differences in auditory nerve activity. Because the patterns of expression were the same in normal and *dn/dn* mice at 9 days, it would appear that spontaneous nerve activity plays little role in expression before opening of the ear canal. If spontaneous nerve activity was involved, it would likely result in different patterns of $Ca^{2+}$-binding protein expression in normal and *dn/dn* mice at 9 days postnatal. Instead, it would appear that differences in evoked auditory nerve activity are responsible, because the patterns of $Ca^{2+}$-binding protein expression only began to differ after opening of the ear canal, which corresponds to the onset of hearing. Normal hearing mice, therefore, experience changes in $Ca^{2+}$-binding protein expression during development because of evoked auditory nerve activity, while *dn/dn* mice, which lack evoked auditory nerve activity, experience no changes in $Ca^{2+}$-binding protein expression during development.

## Impaired $Ca^{2+}$ Buffering in the AVCN of *dn/dn* Mice

Oleskevich & Walmsley (2002) found enhanced synaptic strength in the endbulb of Held synapse in the AVCN of *dn/dn* mice (aged 11-16 days postnatal) when compared with normal mice. Their results were based on the finding that transmitter release probability at this synapse was greater in *dn/dn* mice. They theorized that auditory nerve activity in normal hearing mice may act to depress release probability, thus decreasing synaptic depression and improving high-fidelity transmission. In addition, they found that administration of the membrane permeable calcium buffer EGTA-AM diminished all

observed differences between deaf and normal mice.  As a result, they suggested

impaired calcium buffering in the endbulb terminals of deaf mice may be responsible for

the synaptic differences found between the deaf and normal mice (Oleskevich &

Walmsley 2002).

The differences observed in $Ca^{2+}$-binding protein expression in the AVCN

between normal and *dn/dn* mice in this experiment (Fig. 72) support the hypothesis

proposed by Oleskevich and Walmsley (2002).  CR and PV (Fig. 8-21, 33-40), which

were heavily expressed in the AVCN, appeared to be the main $Ca^{2+}$-binding proteins

involved in the endbulb of Held synapse, as CB (Fig. 22-32) was only observed in a few

postsynaptic bushy cell somata (at any given age).  CR was expressed in presynaptic

endbulb terminals at moderate levels in both normal and *dn/dn* mice at 9 days postnatal

(Fig. 10, 16).  CR expression increased dramatically throughout the rest of development

in normal mice (Fig. 11-15).  In *dn/dn* mice, however, CR expression remained the same

throughout the rest of development (Fig. 17-21), with all subsequent ages resembling the

9 day postnatal *dn/dn* (and 9 day normal) mice.  Thus, the patterns of CR expression

showed that presynaptic $Ca^{2+}$ buffering progressively increased after opening of the ear

canal in normal mice, but remained the same in *dn/dn* mice.  At 9 days postnatal in both

normal and *dn/dn* mice, PV was expressed in presynaptic endbulb terminals and

postsynaptic bushy cell somata, with the presynaptic terminals staining much stronger

than the postsynaptic somata (Fig. 34, 37).  During development it was unclear if the

expression of PV in the presynaptic terminals had changed in both normal and *dn/dn*

mice (see Results).  In normal mice, PV expression progressively increased in the

postsynaptic bushy cell somata throughout the rest of development (Fig. 34-36).  PV

expression in the bushy cells of *dn/dn* mice, however, remained the same throughout development (Fig. 37-40), with all subsequent ages resembling the 9 day postnatal *dn/dn* (and normal) mice. Thus, the patterns of PV expression showed that postsynaptic $Ca^{2+}$ buffering progressively increased after opening of the ear canal in normal mice, but remained the same in *dn/dn* mice. Patterns of CB expression also showed a developmental increase in postsynaptic $Ca^{2+}$ buffering in normal mice, and absence of this developmental increase in *dn/dn* mice (Fig. 25-32). The result showing impaired $Ca^{2+}$ buffering in the postsynaptic bushy cells is surprising, because Walmsley et al. (2006) reported that postsynaptic bushy cells in the AVCN show no difference in the membrane properties between normal and *dn/dn* mice, even though the bushy cells in *dn/dn* mice have lost their excitatory input.

It is important to note that CR and CB exhibit rapid $Ca^{2+}$-binding kinetics (Nägerl et al. 2000; see Felmy & Schneggenburger 2004) and that PV exhibits slow $Ca^{2+}$-binding kinetics (Lee, Schwaller & Neher 2000; see Felmy & Schneggenburger 2004). Thus, in the AVCN of normal mice, there is a developmental increase in a presynaptic $Ca^{2+}$-binding protein that exhibits rapid binding kinetics (CR) and a developmental increase in a postsynaptic $Ca^{2+}$-binding protein that exhibits rapid binding kinetics (CB) as well as one that exhibits slow binding kinetics (PV). CR and CB should act to decrease transmitter release probability during basal synaptic transmission (Felmy & Schneggenburger 2004), and PV should suppress the amount of transmitter release facilitation (Calliard et al. 2000; Vreugdenhil et al. 2003; see Felmy & Schneggenburger 2004). A developmental increase in CR, CB and PV would presumably ensure the fidelity of synaptic transmission at the endbulb of Held synapse in normal mice. In the

AVCN of *dn/dn* mice, however, neither the presynaptic CR nor the postsynaptic CB/PV increased. The results of this experiment, therefore, support the hypothesis that impaired calcium buffering in the AVCN of deaf mice may be responsible for the synaptic differences found between the deaf and normal mice (Oleskevich & Walmsley 2002), and show that this impaired calcium buffering is present both pre- and postsynaptically, and involves both rapidly and slowly acting $Ca^{2+}$-binding proteins.


**Altered Endbulb Morphology in the AVCN of Normal Mice**


Research by Ryugo et al. (1996; 1997; 1998) on endbulb structure in the AVCN during development of normal and deaf white cats suggests a correlation between amount of auditory activity and endbulb morphology. They found that in normal cats (with normal developmental auditory nerve fiber activity), there are smaller and more numerous synaptic specializations than in deaf white cats (with altered developmental auditory nerve activity) (Ryugo, Wu & Pongstaporn 1996; Ryugo et al. 1997; Ryugo et al. 1998; see Walmsley et al. 2006). Walmsley et al. (2006) suggest that these results support a theory that during normal development, spontaneous auditory nerve activity causes endbulbs to grow and become specialized, perhaps by a mechanism involving the splitting into many smaller specializations. The present experiment appeared to support this theory, as endbulbs in mature normal mice (Fig. 12-13, 15, 72), which were visualized by CR staining and VGLUT1 staining, appeared to be smaller and have more numerous specializations than endbulbs in younger normal mice (Fig. 10-11, 14, 72) and *dn/dn* mice at all ages (Fig. 16-21, 72). It can be inferred, therefore, if these observations

are accurate, that auditory nerve activity in mice causes endbulb morphology to change during development, with mature endbulbs in normal mice being smaller with more numerous specializations than endbulbs in younger normal mice and *dn/dn* mice at all ages.  It is important to note that this experiment did not quantify this result, and that more detailed analysis of endbulb size and morphology during development in normal hearing and congenitally deaf mice, perhaps through a detailed confocal microscopic experiment, needs to be studied.

**Topographic Gradients of Ca$^{2+}$-binding Proteins in the MNTB – Normal vs. *dn/dn* Mice**

The results of the current experiment indicated that CR and CB were expressed in topographic patterns in the MNTB during the development of normal hearing mice, and that these gradients were altered (absent) in congenitally deaf mice (Fig. 73).  (The developmental expression of PV in the MNTB did not appear to involve any topographic patterns in normal or *dn/dn* mice.)  Furthermore, these topographic gradients (or lack thereof) of Ca$^{2+}$-binding expression appeared to correspond with the established topographic gradients of channel and current expression that underlie the tonotopic organization (or lack thereof) of the MNTB of normal hearing (or congenitally deaf) mice (see Background & Significance; Fig. 3).

In both normal and *dn/dn* mice at 9 days postnatal, CR was expressed mainly in postsynaptic principal cell somata in the medial part of the MNTB (Fig. 44, 48).  This pattern of CR expression remained consistent throughout development in *dn/dn* mice

(Fig. 49-51). During the development of normal mice, however, CR was expressed in progressively fewer medially-located postsynaptic principal cell somata, and progressively more laterally-located presynaptic calyces of Held (Fig. 45-47). CR, therefore, was expressed, in normal mice before opening of the ear canal and *dn/dn* mice at all ages, in principal cell somata in the medial MNTB. These cells have been shown to respond well to high frequency stimulation, and to preferentially express Kv3.1 channels and their high threshold potassium currents (Leao et al. 2006) (Fig. 3). As development proceeded following opening of the ear canal in normal mice, CR was expressed in progressively fewer principal cell somata medially, and in progressively more calyces of Held in the lateral MNTB. These lateral calyces synapse with cells that have been shown to respond well to low frequency stimulation, and to preferentially express Kv1.1 channels and their low threshold potassium currents (Leao et al. 2006) (Fig. 3). It can be inferred, therefore, that during normal development, a greater level of presynaptic $Ca^{2+}$ buffering is required in the lateral MNTB in order to ensure the fidelity of low frequency signal transmission. As stated previously, the results of this experiment have indicated that the topographic pattern of CR expression changes in normal mice in response to evoked auditory nerve activity. As a result, the need for an increased level of presynaptic $Ca^{2+}$ buffering in the lateral MNTB of normal mice is satisfied as CR expression in the calyces of Held is increased in response to evoked auditory nerve activity. Auditory nerve activity is absent in *dn/dn* mice, and as a result, no change in the topographic gradient of CR expression occurs in the MNTB after opening of the ear canal. Thus, in *dn/dn* mice the need for an increased level of presynaptic $Ca^{2+}$ buffering in the lateral MNTB is not satisfied. In other words, there is no need for an increased level of

89

presynaptic $Ca^{2+}$ buffering in the lateral MNTB of *dn/dn* mice because evoked auditory nerve activity is absent.

In both normal and *dn/dn* mice at 9 days postnatal, CB was expressed at a consistent level in all postsynaptic principal cell somata throughout the medio-lateral extent of the MNTB (Fig. 55, 59). This pattern of CB expression remained consistent throughout development in *dn/dn* mice (Fig. 60-62). During the development of normal mice, however, the level of CB expression increased progressively in laterally-located postsynaptic principal cell somata (Fig. 56-58). These cells have been shown to respond well to low frequency stimulation, and to preferentially express Kv1.1 channels and their low threshold potassium currents (Leao et al. 2006) (Fig. 3). As stated previously, the results of this experiment have indicated that the topographic pattern of CB expression changes in normal mice in response to evoked auditory nerve activity. As a result, an increased level of postsynaptic $Ca^{2+}$ buffering in the lateral MNTB of normal mice occurs as CB expression in the principal cell somata is increased in response to evoked auditory nerve activity. Auditory nerve activity is absent in *dn/dn* mice, and as a result, no topographic gradient of CB expression occurs in the MNTB after opening of the ear canal. Thus, a developmental increase in CB expression does not occur in postsynaptic principal cell somata in the lateral MNTB of *dn/dn* mice.

Thus, the levels of expression of two separate $Ca^{2+}$-binding proteins, CR presynaptically and CB postsynaptically, are increased during development in normal mice in the lateral MNTB. The topographic gradients of CR and CB expression that develop in the MNTB of normal mice appear in the lateral MNTB, which have been shown to possess cells that respond best to low frequency stimulation (Leao et al. 2006).

These cells preferentially express Kv1.1 channels and their low frequency potassium currents (Leao et al. 2006) (Fig. 3), and thus the topographic gradient of CR and CB expression that occurs in the development of normal mice corresponds to these topographic gradients of Kv1.1 channels and low frequency potassium currents. In contrast, lack of evoked auditory activity in *dn/dn* mice resulted in the absence of topographic gradients of CR and CB expression in the MNTB during development, and as such, increased $Ca^{2+}$ buffering in the lateral MNTB was not achieved. The lack of topographic gradients of CR and CB expression in *dn/dn* mice corresponds with the lack of topographic gradients of channel and current expression, which presumably underlie that altered tonotopic organization of the MNTB in *dn/dn* mice (Leao et al. 2005, 2006) (Fig. 3).

**Kinetics of $Ca^{2+}$-binding Proteins in the MNTB of Normal vs. *dn/dn* Mice**

When analyzing the developmental expression of $Ca^{2+}$-binding proteins in relation to tonotopic organization of the MNTB in normal hearing and congenitally deaf mice, it is important to take into account the binding kinetics of the specific $Ca^{2+}$-binding proteins. As a $Ca^{2+}$-binding protein that exhibits fast binding kinetics (Nägerl et al. 2000; see Felmy & Schneggenburger 2004), CR should act to decrease transmitter release probability during basal synaptic transmission (Felmy & Schneggenburger 2004). It would seem, therefore, that CR would be a $Ca^{2+}$-binding protein that would be especially well-suited to ensure the fidelity of high frequency transmission. Such a pattern of CR expression was not observed, however, in the MNTB of normal mice. Although CR was

expressed in young normal mice mainly in principal cell somata in the medial MNTB (Fig. 44), which is the high frequency end of the tonotopic map (Leao et al. 2006) (Fig. 3), increased levels of CR expression in the MNTB of more mature normal mice were found in calyces of Held in the lateral MNTB (Fig. 45-47), which is the low frequency end of the tonotopic map (Leao et al. 2006) (Fig. 3). Thus, it appears that in the MNTB, CR is a $Ca^{2+}$-binding protein that is expressed in an effort to ensure the fidelity of low frequency synaptic transmission. Congenitally deaf mice at all ages of development, on the other hand, retain the pattern of CR expression seen in young normal mice (Fig. 44, 48-51). As a result, CR expression is not shifted to the lateral MNTB, and the fidelity of low frequency synaptic transmission is not ensured.

As another $Ca^{2+}$-binding protein that exhibits fast binding kinetics (Nägerl et al. 2000; see Felmy & Schneggenburger 2004), the presynaptic function of CB would be to decrease transmitter release probability during basal synaptic transmission (Felmy & Schneggenburger 2004). CB, however, was only observed in the postsynaptic principal cell somata in the MNTB (Fig. 52-62). The specific postsynaptic function of CB in the principal cell somata is not known. Presumably, CB would still maintain low cytosolic $Ca^{2+}$ levels through fast binding kinetics, but postsynaptically it would not affect neurotransmitter release.

PV is a $Ca^{2+}$-binding protein that exhibits slow $Ca^{2+}$-binding kinetics (Lee, Schwaller & Neher 2000; see Felmy & Schneggenburger 2004), in which the delayed $Ca^{2+}$ binding will accelerate the decay of residual $Ca^{2+}$ ions (Atluri & Regehr 1996; Lee, Schwaller & Neher 2000; see Felmy & Schneggenburger 2004), and presynaptically results in suppression of the amount of transmitter release facilitation (Calliard et al.

2000; Vreugdenhil et al. 2003; see Felmy & Schneggenburger 2004). In this experiment, expression of PV in the MNTB was observed in both the presynaptic calyces of Held and the postsynaptic principal cell somata (Fig. 63-64), and no topographic gradients of PV expression were observed in normal or *dn/dn* mice. In young normal mice, PV expression in the calyces of Held is far greater than in the principal cell somata (Fig. 65). This pattern was observed as well in *dn/dn* mice at all ages of development (Fig. 69-71). It was unclear if PV expression in the presynaptic calyces changed during normal mice development (see Results and Discussion above). As a result, no statement can be made in regard to the role that developmental changes in presynaptic PV expression may play in synaptic transmission at the calyx of Held synapse. During development of the normal mice, PV expression increased dramatically in the postsynaptic principal cell somata (Fig. 66-68). The specific postsynaptic function of PV in the principal cell somata is not known. Presumably, PV would still maintain low cytosolic $Ca^{2+}$ levels through slow binding kinetics, but postsynaptically it would not affect neurotransmitter release. Since no topographic gradients of PV expression were observed presynaptically or postsynaptically in the MNTB of normal or *dn/dn* mice (Fig. 65-71), it appears that PV is a $Ca^{2+}$-binding protein that is equally important in the high and low frequency ends of the tonotopic map in the MTNB.

# VII.  CONCLUSIONS


The expression of the $Ca^{2+}$-binding proteins Calretinin (CR), Calbindin D-28k (CB) and Parvalbumin (PV) in the Anteroventral Cochlear Nucleus (AVCN) and Medial Nucleus of the Trapezoid Body (MNTB) of normal hearing mice varies during development (Fig. 72, 73).  The expression of each $Ca^{2+}$-binding protein is at a certain level in specific locations in the AVCN and MNTB at 9 days postnatal, before opening of the ear canal, and begins to change at 13 days postnatal, after opening of the ear canal. The patterns of $Ca^{2+}$-binding protein expression in normal mice continue to change from 13 days postnatal through the duration of development.  In addition, the pattern of expression for each individual $Ca^{2+}$-binding protein in the AVCN and MNTB of normal mice is unique when compared to the patterns of expression for the other $Ca^{2+}$-binding proteins.

In congenitally deaf mice (*dn/dn*), the patterns of expression for CR, CB and PV in the AVCN and MNTB do not vary during development (Fig. 72, 73).  The expression of each $Ca^{2+}$-binding protein is at a certain level in specific locations in the AVCN and MNTB at 9 days postnatal, before opening of the ear canal, and remains the same in all ages of *dn/dn* mice after opening of the ear canal.  Thus, the pattern of expression for each $Ca^{2+}$-binding protein in the AVCN and MNTB of *dn/dn* mice remains the same throughout development.  The pattern of expression for each individual $Ca^{2+}$-binding

protein in the AVCN and MNTB of *dn/dn* mice, however, is unique when compared to the patterns of expression for the other $Ca^{2+}$-binding proteins.

Differences occur in the developmental expression of CR, CB and PV in the AVCN and MNTB between normal and *dn/dn* mice (Fig. 72, 73). These differences occur as a result of the presence (in normal mice) or absence (in *dn/dn* mice) of evoked auditory nerve activity. Expression of each individual $Ca^{2+}$-binding protein in the AVCN and MNTB appears to be the same at 9 days postnatal, before opening of the ear canal, in both normal and *dn/dn* mice. Expression of each individual $Ca^{2+}$-binding protein in the AVCN and MNTB remains the same at all ages of development after opening of the ear canal in *dn/dn* mice. In normal mice, however, the pattern of expression for each individual $Ca^{2+}$-binding protein in the AVCN and MNTB begins to change at 13 days postnatal, after opening of the ear canal, and continues to change throughout the duration of development. Because the patterns of expression for each individual $Ca^{2+}$-binding protein is the same before opening of the ear canal, it appears that the presence or absence of spontaneous auditory nerve activity plays little role in expression patterns before the onset of hearing. The differences in $Ca^{2+}$-binding protein expression in the AVCN and MNTB between normal and *dn/dn* mice do occur, on the other hand, as a result of the presence (in normal mice) or absence (in *dn/dn* mice) of evoked auditory nerve activity. This is because *dn/dn* mice, which lack evoked auditory nerve activity, retain the same patterns of $Ca^{2+}$-binding protein expression before and after the opening of the ear canal, and normal mice, which experience evoked auditory nerve activity, exhibit changed patterns of $Ca^{2+}$-binding protein expression after opening of the ear canal.

This experiment shows that there is impaired $Ca^{2+}$ buffering in the AVCN of

*dn/dn* mice (Fig. 72). In normal mice, there is a developmental increase in presynaptic

(CR) $Ca^{2+}$-binding protein expression in the endbulb of Held terminals, and in

postsynaptic (CB and PV) $Ca^{2+}$-binding protein expression in the bushy cell somata. In

*dn/dn* mice, on the other hand, developmental expression of $Ca^{2+}$-binding proteins does

not increase presynaptically or postsynaptically. This result supports the hypothesis by

Oleskevich and Walmsley (2002) that the enhanced synaptic strength they observed at the

endbulb of Held synapse of *dn/dn* mice when compared with normal mice may be a result

of impaired $Ca^{2+}$ buffering in the endbulb terminals in *dn/dn* mice.

Finally, there are topographic gradients of CR and CB expression in the MNTB

(Fig. 73). In normal mice, these gradients change during development, with expression

of CR (presynaptically) in calyces of Held and CB (postsynaptically) in principal cell

somata increasing progressively in the lateral MNTB. The lateral MNTB is the low

frequency end of the tonotopic map, and preferentially expresses Kv1.1 channels and

their low frequency potassium currents (Leao et al. 2006) (See Fig. 3). Thus, in normal

mice the topographic patterns of CR and CB expression in the MNTB correspond with

the topographic patterns of Kv1.1 channels and low frequency potassium currents, which

underlie part of the tonotopic organization of the MNTB. The lateral part of the MNTB,

it seems, requires an increased level of presynaptic $Ca^{2+}$ buffering (CR) as development

proceeds in order to ensure the fidelity of low frequency synaptic transmission. In *dn/dn*

mice, on the other hand, topographic gradients of CR and CB expression in the MNTB do

not change during development. The MNTB in *dn/dn* mice lacks topographic gradients

of channel and current expression, and lacks a tonotopic organization (Leao et al. 2005,

2006) (See Fig. 3). Thus, the lack of changes in $Ca^{2+}$-binding protein expression gradients in the MNTB of *dn/dn* mice corresponds with the lack of topographic gradients of channel and current expression and the overall lack of tonotopic organization in the MNTB of *dn/dn* mice. Because CR expression in *dn/dn* mice does not increase during development in the lateral MNTB, the fidelity of low frequency transmission cannot be ensured.

In summary, the results of this experiment demonstrate that patterns of $Ca^{2+}$-binding protein expression in the AVCN and MNTB change during the development of normal hearing mice in response to evoked auditory nerve activity. It appears that the developmental changes that occur in expression of these $Ca^{2+}$-binding proteins are important for ensuring the fidelity of synaptic transmission in the central auditory pathway, and that patterns of expression correlate with the established tonotopic organization of the MNTB in normal mice (Fig. 3). In addition, the results demonstrate that patterns of $Ca^{2+}$-binding protein expression are altered in congenitally deaf mice, as they do not change during development due to the absence of evoked auditory nerve activity. The altered patterns of $Ca^{2+}$-binding protein expression in *dn/dn* mice correspond with the altered tonotopic organization of the MNTB in *dn/dn* mice (Fig. 3). Thus, $Ca^{2+}$ buffering is impaired at synapses in the central auditory pathways of *dn/dn* mice. This is especially important in the AVCN, as it supports the hypothesis by Oleskevich and Walmsley (2002) that impaired $Ca^{2+}$ buffering at the endbulb of Held synapse may be responsible for the enhanced synaptic strength observed at this synapse in *dn/dn* mice when compared with normal mice. In order to develop an accurate quantitative analysis of the developmental expression of these $Ca^{2+}$-binding proteins in

the AVCN and MNTB of normal and *dn/dn* mice, a DAB experiment followed by optical density analysis is needed. In addition, this experiment will be repeated utilizing confocal microscopy so that the developmental expression of $Ca^{2+}$-binding proteins normal and *dn/dn* can be examined in greater detail. Confocal microscopy will enable the results of the current experiment to be verified, and will provide greater insight into presynaptic changes in PV expression (which were unclear in this experiment) and into the differences in endbulb of Held morphology observed in the AVCN during the development of normal hearing and congenitally deaf mice.

# REFERENCES

**Adams JC & Mugnaini E** (1990) Immunocytochemical evidence for inhibitory and disinhibitory circuits in the superior olive. Hearing Research 49: 281-298.

**Arai R, Winsky L, Arai M & Jacobowitz DM** (1991) Immunohistochemical localization of Calretinin in the rat hindbrain. Journal of Comparative Neurology 310: 21-44.

**Atluri PP & Regehr WG** (1996) Determinants of the time course of facilitation at the granule cell to purkinje cell synapse. Journal of Neuroscience 16: 5661-5671.

**Bellingham MC, Lim R & Walmsley B** (1998) Developmental changes in EPSC quantal size and quantal content at a central glutamatergic synapse in rat. Journal of Physiology 511: 861-869.

**Bock GR, Frank MP & Steel KP** (1982) Preservation of central auditory function in the deafness mouse. Brain Research 239: 608-612.

**Caicedo A, d'Aldin C, Puel J-L & Eybalin M** (1996) Distribution of calcium-binding protein immunoreactivities in the guinea pig auditory brainstem. Anatomy and Embryology 194: 465-487.

**Caillard O, Moreno H, Schwaller B, Llano I, Celio MR & Marty A** (2000) Role of the calcium-binding protein parvalbumin in short-term synaptic plasticity. Proceedings of the National Academy of Sciences of the United States of America 97: 13372-13377.

**Carafoli E** (1987) Intracellular calcium homeostasis. Annual Review of Biochemistry 56: 395-433.

**Carafoli E, Santella L, Branca D & Brini M** (2001) Generation, control, and processing of cellular calcium signals. Critical Reviews in Biochemistry and Molecular Biology 36(2): 107-260.

**Celio MR** (1990) Calbindin D-28k and parvalbumin in the rat nervous system. Neuroscience 35: 375-475.

**Chuhma N & Ohmori H** (1998) Postnatal development of phase-locked high-fidelity synaptic transmission in the medial nucleus of the trapezoid body of the rat. Journal of Neuroscience 18: 512-520.

**Dodson PD, Barker MC & Forsythe ID** (2002) Two heteromeric Kv1 potassium channels differentially regulate action potential firing. Journal of Neuroscience 22: 6953-6961.

**Edmonds B, Reyes R, Schwaller B & Roberts WM** (2000) Calretinin modifies presynaptic calcium signaling in frog saccular hair cells. Nature Neuroscience 3: 786-790.

**Felmy F, Neher E & Schneggenburger R** (2003) The timing of phasic transmitter release is $Ca^{2+}$-dependent and lacks a direct influence of presynaptic membrane potential. Proceedings of the National Academy of Sciences of the United States of America 100(25): 15200-15205.

**Felmy F & Schneggenburger R** (2004) Developmental expression of the $Ca^{2+}$-binding proteins calretinin and parvalbumin at the calyx of held of rats and mice. European Journal of Neuroscience 20(6): 1473-1482.

**Friauf E & Lohmann C** (1999) Development of auditory brainstem circuitry. Activity-dependent and activity-independent processes. Cell and Tissue Research 297(2): 187-195.

**Futai K, Okada M, Matsuyama K, Kobayashi K & Takahashi T** (2001) High-fidelity transmission acquired by developmental loss of NMDA receptors in the medial nucleus of the trapezoid body in mice. Journal of Neuroscience 21: 2234-2239.

**Garcia ML & Strehler EE** (1999) Plasma membrane ATPases as critical regulators of calcium homeostasis during neuronal cell function. Frontiers in Bioscience: A Journal and Virtual Library 4: D869-882.

**Joris PX, Carney LH, Smith PH & Yin TC** (1994) Enhancement of neural synchronization in the anteroventral cochlear nucleus. I. Responses to tones at the characteristic frequency. Journal of Neurophysiology 71: 1022-1036.

**Joshi I & Wang LY** (2002) Developmental profiles of glutamate receptors and synaptic transmission at a single synapse in the mouse auditory brainstem. Journal of Physiology 540: 861-873.

**Kandler K & Friauf E** (1993) Pre- and postnatal development of efferent connections of the cochlear nucleus in the rat. Journal of Comparative Neurology 328: 161-184.

**Katz B & Miledi R** (1965) The effect of Calcium on Acetylcholine release from motor nerve terminals. Proceedings of the Royal Society of London. Series B, Containing Papers of a Biological Character 161: 496-503.

**Katz B & Miledi R** (1967) The timing of calcium action during neuromuscular transmission. Journal of Physiology 189(3): 535-544.

**Katz B & Miledi R** (1968) The role of calcium in neuromuscular facilitation. Journal of Physiology 195(2): 481-492.

**Katz B & Miledi R** (1970) Further study of the role of calcium in synaptic transmission. Journal of Physiology 207(3): 789-801.

**Keats BJ & Berlin CI** (1999) Genomics and hearing impairment. Genome Research 9: 7-16.

**Kip SN, Gray NW, Burette A, Canbay A, Weinberg RJ & Strehler EE** (2006) Changes in the expression of plasma membrane calcium extrusion systems during the maturations of hippocampal neurons. Hippocampus 16(1): 20-34.

**Kuwabara N, DiCaprio RA & Zook JM** (1991) Afferents to the medial nucleus of the trapezoid body and their collateral projections. Journal of Comparative Neurology 314: 684-706.

**Leao RN, Berntston A, Forsythe ID & Walmsley B** (2004a) Reduced low-voltage activated $K^+$ conductances and enhanced central excitability in a congenitally deaf (dn/dn) mouse. Journal of Physiology 559(Pt 1): 25-33.

**Leao RN, Oleskevich S, Sun H, Bautista M, Fyffe RE & Walmsley B** (2004b) Differences in glycinergic mIPSCs in the auditory brain stem of normal and congenitally deaf neonatal mice. Journal of Neurophysiology 91(2): 1006-1012.

**Leao RN, Svahn K, Berntson A & Walmsley B** (2005) Hyperpolarization-activated (I) currents in auditory brainstem neurons of normal and congenitally deaf mice. European Journal of Neuroscience 22(1): 147-157.

**Leao RN, Sun H, Svahn K, Berntson A, Youssoufian M, Paolini AG, Fyffe RE & Walmsley B** (2006) Topographic organization in the auditory brainstem of juvenile mice is disrupted in congenital deafness. Journal of Physiology 571(Pt 3): 563-578.

**Lee DJ, Cahill HB & Ryugo DK** (2003) Effects of congenital deafness in the cochlear nuclei of Shaker-2 mice: an ultrastructural analysis of synapse morphology in the endbulbs of Held. Journal of Neurocytology 32: 229-243.

**Lee SH, Schwaller B & Neher E** (2000) Kinetics of $Ca^{2+}$ binding to parvalbumin in bovine chromafin cells: implications for $[Ca^{2+}]$ transients of neuronal dendrites. Journal of Physiology (London) 525: 419-432.

**Liberman MC** (1991) Central projections of auditory-nerve fibers of differing spontaneous rate. I. Anteroventral cochlear nucleus. Journal of Comparative Neurology 313(2): 240-258.

**Lohmann C & Friauf E** (1996) Distribution of the calcium-binding proteins in the auditory brainstem of adult and developing rats. Journal of Comparative Neurology 367: 90-109.

**McAlpine D, Jiang D & Palmer AR** (2001) A neural code for low-frequency sound localization in mammals. Nature Neuroscience 4: 396-401.

**Mauk MD & Buonomano DV** (2004) The neural basis of temporal processing. Annual Review of Neuroscience 27: 307-340.

**Meinrenken CJ, Borst JG & Sakmann B** (2002) Calcium secretion coupling at calyx of held governed by nonuniform channel-vesicle topography. Journal of Neuroscience 22(5): 1648-1667.

**Miller RJ** (1991) The control of neuronal $Ca^{2+}$ homeostasis. Progress in Neurobiology 37(3): 255-285.

**Nägerl UV, Novo D, Mody I & Vergara JL** (2000) Binding kinetics of calbindin D-28k determined by flash photolysis of caged $Ca^{2+}$. Biophysical Journal 79: 3009-3018.

**Neises GR, Mattox DE & Gulley RL** (1982) The maturation of the end bulb of Held in the rat anteroventral cochlear nucleus. The Anatomical Record 204: 271-279.

**Nicol MJ & Walmsley B** (2002) Ultrastructural basis of synaptic transmission between endbulbs of Held and bushy cells in the rat cochlear nucleus. Journal of Physiology 539(3): 713-723.

**Oleskevich S & Walmsley B** (2002) Synaptic transmission in the auditory brainstem of normal and congenitally deaf mice. Journal of Physiology 540(2): 447-455.

**Oleskevich S, Youssoufian M & Walmsley B** (2004) Presynaptic plasticity at two giant auditory synapses in normal and deaf mice. Journal of Physiology 560(Pt 3): 709-719.

**Paolini AG, FitzGerald JV, Burkitt AN & Clark GM** (2001) Temporal processing from the auditory nerve to the medial nucleus of the trapezoid body in the rat. Hearing Research 159: 101-116.

**Penniston JT** (1982) Plasma membrane $Ca^{2+}$-pumping ATPases. Annals of the New York Academy of Sciences 402: 296-303.

**Resibois A & Rogers JH** (1992) Calretinin in the rat brain: an immunohistochemical study. Neuroscience 46: 101-134.

**Rowland KC, Irby NK & Spirou GA** (2000) Specialized synapse-associated structures within the calyx of Held. Journal of Neuroscience 20: 9135-9144.

**Rubel EW & Fritzsch B** (2002) Auditory system development: primary auditory neurons and their targets. Annual Review of Neuroscience 25: 51-101.

**Ryugo DK & Fekete DM** (1982) Morphology of primary axosomatic endings in the anteroventral cochlear nucleus of the cat: a study of the endbulbs of Held. Journal of Comparative Neurology 210: 239-257.

**Ryugo DK, Pongstaporn T, Huchton DM & Niparko JK** (1997) Ultrastructural analysis of primary endings in deaf white cats: morphologic alterations in endbulbs of Held. Journal of Comparative Neurology 385(2): 230-244.

**Ryugo DK, Rosenbaum BT, Kim PJ, Niparko JK & Saada AA** (1998) Single unit recordings in the auditory nerve of congenitally deaf white cats: morphological correlates in the cochlea and cochlear nucleus. Journal of Comparative Neurology 397(4): 532-548.

**Ryugo DK, Wu M & Pongstaporn T** (1996) Activity-related features of synapse morphology: a study of endbulbs of Held. Journal of Comparative Neurology 365(1): 141-158.

**Sätzler K, Söhl LF, Bollmann JH, Borst JG, Frotscher M, Sakmann B & Lübke JHR** (2002) Three-dimensional reconstruction of a calyx of held and its postsynaptic principal neuron in the medial nucleus of the trapezoid body. The Journal of Neuroscience 22(24): 10567-10579.

**Schneggenburger R, Sakaba T & Neher E** (2002) Vesicle pools and short-term synaptic depression: lessons from a large synapse. Trends in Neurosciences 25: 206-212.

**Smith AJ, Owens S & Forsythe ID** (2000) Charaterisation of inhibitory and excitatory postsynaptic currents of the rat medial superior olive. Journal of Physiology 529(Pt 3): 681-698.

**Smith PH, Joris PX & Yin TC** (1998) Anatomy and physiology of principal cells of the medial nucleus of the trapezoid body (MNTB) of the cat. Journal of Neurophysiology 79: 3127-3142.

**Spangler KM, Warr WB & Henkel CK** (1985) The projections of principal cells of the medial nucleus of the trapezoid body in the cat. Journal of Comparative Neurology 238(3): 249-262.

**Strehler EE** (1990) Plasma membrane $Ca^{2+}$ pumps and $Na^+/Ca^{2+}$ exchangers. Seminars in Cell Biology 1(4): 283-295.

**Taschenberger H, Leao RM, Rowland KC, Spirou GA & von Gersdorff H** (2002) Optimizing synaptic architecture and efficiency for high-frequency transmission. Neuron 36: 1127-1143.

**Taschenberger H & von Gersdorff H** (2000) Fine-tuning an auditory synapse for speed and fidelity: developmental changes in presynaptic waveform, EPSC kinetics, and synaptic plasticity. Journal of Neuroscience 20: 9162-9173.

**Vreugdenhill M, Jefferys JG, Celio MR & Schwaller B** (2003) Parvalbumin-deficiency facilitates repetitive IPSCs and gamma oscillations in the hippocampus. Journal of Neurophysiology 89: 1414-1422.

**Walmsley B, Alvarez FJ & Fyffe RE** (1998) Diversity of structure and function at mammalian central synapses. Trends in Neurosciences 21(2): 81-88.

**Walmsley B, Berntson A, Leao RN & Fyffe RE** (2006) Activity-dependent regulation of synaptic strength and neuronal excitability in central auditory pathways. Journal of Physiology (Epub ahead of print).

**Wu SH & Kelly JB** (1993) Response of neurons in the lateral superior olive and medial nucleus of the trapezoid body to repetitive stimulation: intracellular and extracellular recordings from mouse brain slice. Hearing Research 68: 189-201.

**Youssoufian M, Oleskevich S & Walmsley B** (2005) Development of a robust central auditory synapse in congenital deafness. Journal of Neurophysiology 94(5): 3168-3180.